STUDIES ON SELECTIVE ADSORPTION OF AQUEOUS GLUCOSE OR FRUCTOSE ON VARIOUS CATIONIC FORMS OF ZEOLITE Y

SUAT BORA YEŞİLTEPE

JULY 2006

STUDIES ON SELECTIVE ADSORPTION OF AQUEOUS GLUCOSE OR FRUCTOSE ON VARIOUS CATIONIC FORMS OF ZEOLITE Y

A THESIS SUBMITTED TO
THE GRADUATE SCHOOL OF NATURAL AND APPLIED SCIENCES
OF
MIDDLE EAST TECHNICAL UNIVERSITY

BY

SUAT BORA YEŞİLTEPE

IN PARTIAL FULFILLMENT OF THE REQUIREMENTS
FOR
THE DEGREE OF MASTER OF SCIENCE
IN
BIOTECHNOLOGY

JULY 2006

Approval of the Graduate School of Natural and Applied Sciences

Prof.Dr. Canan ÖZGEN
Director

I certify that this thesis satisfies all the requirements as a thesis for the degree of Master of Science.

Prof.Dr. Fatih YILDIZ
Head of Department

This is to certify that we have read this thesis and that in our opinion it is fully adequate, in scope and quality, as a thesis for the degree of Master of Science.

Prof.Dr. Lemi TÜRKER Co-Supervisor	Prof.Dr. N. Suzan KINCAL Supervisor

Examining Committee Members

Prof.Dr. Hayrettin YÜCEL	(METU, CHE)	_____
Prof.Dr. N. Suzan KINCAL	(METU, CHE)	_____
Prof.Dr. İnci EROĞLU	(METU, CHE)	_____
Asst. Prof. Tünay DİK	(METU, TVSHE)	_____
Asst. Prof. Füsun YÖNDEM MAKASCIOĞLU	(METU, TVSHE)	_____

I hereby declare that all the information in this document has been obtained and presented in accordance with academic rules and ethical conduct. I also declare that, as required by these rules and conduct, I have fully cited and referenced all material and results that are not original to this work.

Name, Last name:

Signature :

ABSTRACT

STUDIES ON SELECTIVE ADSORPTION OF
AQUEOUS GLUCOSE OR FRUCTOSE ON VARIOUS CATIONIC FORMS OF
ZEOLITE Y

YEŞİLTEPE, Suat Bora

M.Sc., Department of Biotechnology

Supervisor: Prof. Dr. N. Suzan Kıncal

Co-Supervisor: Prof. Dr. Lemi Türker

July 2006, 136 Pages

The equilibria of adsorption on calcium and hydrogen forms of zeolite Y by equimolar solutions of 12.5 %, 20%, 25%, 30% and 35% w/v of mixtures of glucose, G and fructose, F; also the non-equimolar mixtures of 20% w/v glucose - 30% w/v fructose, 30% w/v glucose - 20% w/v fructose, 25% w/v glucose – 35% w/v fructose, and 35% w/v glucose-25% w/v fructose solutions, which were prepared 24 hours in advance at the experimental temperature, have been studied batch wise at 50ºC.

Glucose adsorption, in solutions that had adsorption differences, was fast on both zeolites, on the contrary of slow adsorption of fructose with the stable dynamics. Both adsorptions had small amounts of adsorption changes after minute 30. The

treatments made under the same conditions with the same mixtures showed Ca-Y zeolite had better separation capacity compared to H-Y zeolite.

Some trials were repeated with $CaCl_2$ added to the solutions. The slowed down affection of fructose adsorption in spite of the small change of glucose adsorption led to better separation. Samples were analyzed by classical methods, not HPLC.

All the data were considered with various models and their convergence numbers were tested for their closeness to reality. The models were analyzed by response surface methodology and some of those models had correlation factors as high as 88% at the equilibrium points at 30^{th} minutes. Besides, time dependent models have been considering the lag times with a time dependent variable included all the data of all treated solutions with correlation as high as 79.5%.

Keywords: Zeolites, Adsorption, Separation, Glucose, Fructose

ÖZ

GLİKOZ VE FRUKTOZUN SULU ÇÖZELTİLERİNİN ZEOLİT Y'NİN FARKLI KATYONİK FORMLARI ÜZERİNDE SEÇİCİ OLARAK ADSORPLANMALARI ÜZERİNE ÇALIŞMALAR

YEŞİLTEPE, Suat Bora

Yüksek Lisans, Biyoteknoloji Bölümü

Tez Yöneticisi: Prof. Dr. N. Suzan Kıncal

Ortak Tez Yöneticisi: Prof. Dr. Lemi Türker

Temmuz 2006, 136 sayfa

Kalsiyum ve hidrojen formlarındaki Y tipi zeolitlerin % 12.5 (w/v) luk, % 20 (w/v) lik, % 25 (w/v) lik, % 30 (w/v) luk, ve % 35 (w/v) lik glikoz ve fruktozun eşit ağırlıktaki karışımları ile % 20 (w/v) glikoz - %30 (w/v) fruktoz, % 30 (w/v) glikoz - % 20 fruktoz, % 25 (w/v) glikoz - % 35 (w/v) fruktoz, % 35 (w/v) glikoz - % 25 (w/v) fruktoz farklı ağırlıkta olan ve 24 saat önceden hazırlanıp deney sıcaklığında bekletilen karışımlarının adsorpsiyon hızları ve denge değerleri 50ºC'de kesikli sistemde araştırılmıştır.

Glikoz adsorplanması, tüm zeolitlerde daha durağan bir dinamik gösteren fruktoz adsorplanmasına gore hızlıdır. Tüm adsorplanma değerleri, 30. dakika sonrası küçük

farklar göstermişlerdir. Aynı şartlar altında ve aynı karışımlarla yapılan çalışmalar, kalsiyum-Y zeolitin, hidrojen-Y zeolit ile karşılaştırıldığında daha çok ayırma kapasıtesi olduğunu göstermektedirler. Bazı denemeler, karışımlara kalsiyum klorür eklenerek tekrarlanmışlardır. Glikoz adsorplanmasındaki küçük değişimlerine rağmen, fruktozun, yavaşlayan adsorplanması sonucunda daha iyi bir ayrım elde edilmiştir. Alınan örnekler, HPLC yerine klasik metodlarla analiz edilmişlerdir.

Sonuçlar, çeşitli modellere uygulanmaya çalışılmış, modellere yaklaşma değerleri ile incelenmişlerdir. Modeller, Cevap Yüzey Yöntemi ile incelenmiş, 30. dakika denge noktalarında, modellere %88'e varan yaklaşım göstermişlerdir. Ayrıca zamana bağımlı olan ve deney başlarındaki bekleme zamanını da içine katan modeller de, uygulamalarda % 79.5'a varan yakınlık göstermişlerdir.

Anahtar kelimeler: Zeolitler, Adsorpsiyon, Separasyon, Glikoz, Fruktoz

To My Parents

ACKNOWLEDGEMENTS

I would like to express my sincere gratitude to my supervisor Prof. Dr. N. Suzan Kıncal and co-supervisor Prof. Dr. Lemi Türker for the opportunity they have given me to explore the amazing field of sugar industry by offering me this subject. Their guidance, advice, criticism, encouragements and sharing their deep knowledge with me throughout the research were invaluable.

TABLE OF CONTENTS

LIST OF FIGURES

FIGURES

LIST OF TABLES

TABLES

CHAPTER 1

INTRODUCTION

Carbohydrates, sugars and starches, are major foods for humans that are synthesized by plants using carbon dioxide and water from atmosphere. They are used as the principal foodstuffs for animals and humans, and they all have potential as major chemical raw materials. Human also desire for sweetness in their diet and nature provides it from natural sources.

As a brief history for sugar, humankind knew it many centuries before Christ, and it probably traveled from New Guinea to India and from east to Europe by the trade between Asia and Europe. For centuries, sugar was one of the commercial items.

Sugar was first extracted in North America in 1689, using sugarcane (*Saccharum officinarum*) from West Indies, and in 1751 cane was grown on the continent. From that time on, the industry increased; steam-driven crushing and grinding roller mills in eighteenth century, later; vacuum pan, bone-char decolorization and then multieffect evaporation and first suspended centrifuge were developed in the nineteenth century.

In 1747 beet sugar (*Beta vulgaris*) was discovered, and it was not introduced to United States, used in the Europe.

The first preparation of dextrose in 1811, by the German chemist Gottlied Sigismund Kirchoff who claimed that by boiling starch with dilute sulfuric acid, a sweet solution was produced from which a sugar could be crystallized, led to the

development of the corn-sugar industry. The first manufacturing began about 1872, the product being liquid glucose. In 1918, appreciable quantities of pure, crystalline dextrose were produced.

The most recent major change in the industry was the introduction of high-fructose corn-derived sweetener (HFCS), which became commercial around 1970. This made a high quality sweetening material available, which made corn competitive with cane and sugar beets as a major source of sweetener [1].

Regardless of botanical source, all starches are polymers consisting of α-linked anhydroglucopyranose units. Hydrolysis products made from various starch sources are virtually identical in terms of chemical, physical, and organoleptic properties. As a result, starch hydrolysis products are manufactured from a wide variety of raw materials throughout the world.

In Asia, it is not uncommon for a factory to use sago, tapioca, or maize (corn) starch for glucose production, depending on availability and price.

In Thailand, for example, a syrup called “Chinese maltose” is produced from wheat and glutinous rice. In Pakistan, broken rice is used to produce 42% fructose and enzyme-enzyme glucose syrups having qualities comparable to products made from maize starch. Starches from barley, sago, sorghum, wheat, rice, potato, tapioca, and other grains and roots serve as raw materials for making of hydrolysis products around the world. But, the unsurpassed productivity of the maize plant has made it the leading source of starch for conversion [2].

Bergius process for the production of sugar by saccharification, or hydrolysis of wood, was started to be investigated for a century. These acid hydrolysis processes

seem to be promising due to the low price and abundance of cellulose. Studies with cellulase enzyme conversions to convert wood wastes to be fermented to give alcohol for use as motor fuel are also promising [1].

Nowadays, natural sweeteners produced from starch are more involved in food industry; glucose and fructose syrups are the most common examples. The fact that fructose is sweeter than glucose and also more soluble than sucrose, made the fructose syrups more involved in various industrial applications, like canned foods, carbonated beverages, baked foods, processed and semi-processed foods and also dairy industries.

Later, more advantages of using fructose in food industry have been recognized, like relatively high sweetness values with the same amount of competitor sugars and also its ease of metabolization in the body without the use of insulin. People with diabetes can healthily consume fructose. For the production of fructose syrups, corn, rice and wheat can be used which contain high levels of starch. One of the high fructose syrups is high fructose corn syrup. It is produced and consumed in large quantities in the United States, Eastern Europe and Asia, which are major growth areas for high fructose corn syrup production [3].

Production of high fructose corn syrup is based on several steps. First, the starch is hydrolyzed to obtain a solution, which contains high glucose concentrations. Then, this glucose is enzymatically isomerized to fructose. In the final step, fructose is separated from the glucose-fructose mixtures by using different techniques.

This separation step is very important, as the high fructose content of the syrup is important for the syrup quality. Today, there are various technologies involving

adsorption processes by using resins or zeolites to separate the fructose from the mixture.

1.1 Sugars

Sugar term applied loosely to any of a number of chemical compounds in the carbohydrate group that are readily soluble in water; are colorless, odorless, and usually crystallizable; and are more or less sweet in taste. In general, all monosaccharide, disaccharides, and trisaccharides are termed sugars, as distinct from polysaccharides such as starch, cellulose, and glycogen.

1.1.1 Sucrose

Sucrose (β-D-fructofuranosyl-α-D-glucopyranoside), $C_{12}H_{22}O_{11}$, is a disaccharide composed of glucose and fructose residues joined by an α,β-glycosidic bond. Figure 1.1 shows the structural representation of a sucrose molecule.

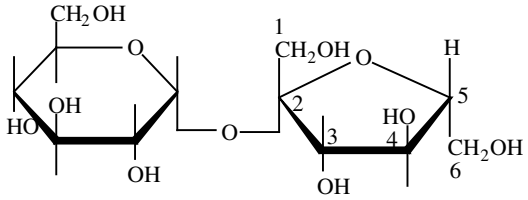

Figure 1.1 Structural representation of sucrose

Sucrose, also called saccharose is generally known as cane sugar even when its source is not the sugarcane. Sucrose is used as a sweetening agent for foods and in the manufacturing of candies, cakes, puddings, preserves, soft and alcoholic beverages, and many other foods. As a basic foodstuff, sucrose supplies

approximately 13 percent of all energy that is derived from foods.

The sweet taste of sucrose is regarded as the standard for other sweeteners. The relative sweetness is influenced by temperature, pH, sugar concentration, physical properties of the food system, etc. The sweetening powers of sucrose and other sweeteners are compared in Table 1.1 [4].

Table 1.1 Relative Sweetness of Sucrose and Other Sweet Substances [1]

Sweetener	Relative sweetness	Sweetener	Relative sweetness
Fructose	1.2 – 1.8	Saccharin	250-550
Sucrose	1.00	Aspartame	120-200
Glucose	0.60	Sucralose	550-750
Maltose	~0.5	Cyclamate	30-50
Lactose	0.15 – 0.30	Acesulfame K	~200
Galactose	0.32	Alitame	2000

1.1.2 Glucose and Fructose

Dextrose is the common name for the purified and crystalline commercial form of the common saccharide D-glucose [Chemical Abstracts Service Registry Number (CAS) 50-99-7]. Crystalline D-glucose is a sweet white powder that can be crystallized in both anhydrous and monohydrate forms. It is also known as grape sugar or blood sugar and was first isolated from the juice of grapes. It is readily soluble in water and easily metabolized by the body and fermented by yeasts and other microorganisms.

D-glucose (dextrose) is by far the most abundant sugar in nature. It occurs either in the monosaccharide form (free state) or in a polymeric form of anhydrodextrose units. As a monosaccharide, dextrose is present in substantial quantities in honey,

fruits, and berries. As a polymer, dextrose occurs in starch, cellulose and glycogen. Sucrose is a disaccharide of dextrose and fructose. Commercial dextrose products are produced in both dry and syrup forms. Dry products are prepared by crystallization to either an anhydrous, $C_6H_{12}O_6$, or hydrated, $C_6H_{12}O_6.H_2O$, form. The hydroxyl group on the C-1 carbon atom of D-glucose can take two possible positions. These are known as alpha and beta positions. The polymers of D-glucose that are α-linked are readily hydrolyzed by acid or enzymes into shorter chains and eventually to α-D-glucose or more precisely α-D-glucopyranose [Chemical Abstract Service Registry Number 492-62-6]. Oligosaccharides (maltodextrins) or maltose are good examples of such readily hydrolyzed D-glucose polymers. The β-linked polymers such as cellulose are not as readily hydrolyzed by mild acids or enzymes to the β-D-glucose (β-D-glucopyranose, CAS 492-61-5) form. These include dextrose hydrate, anhydrous α-D-glucose and anhydrous β-D-glucose. Syrup products contain from 95 to over 99% dextrose [5].

All glucose syrups are hydrolysis products of starch and they are mixtures of polymers of D-glucose. Glucose syrups are known in the United States as corn syrups. Glucose syrup is defined in food law as follows: “Glucose syrup is a purified concentrated aqueous solution of nutritive saccharides obtained from starch [Codes Stan. 9-1981. EEC council directive 73/437].

The glucose syrup industry developed rapidly in the United States in the latter half of the nineteenth century as a result of the plentiful supply of maize as a raw material.

Maize remains to this day the major source of starch for glucose syrup manufacture.

Fructose, also levulose or fruit sugar, is a monosaccharide with the formula $C_6H_{12}O_6$ that occurs with glucose in sweet fruits and fruit juices. It is formed along with glucose in the splitting of sucrose and is produced in the hydrolysis of various carbohydrates, and can also be prepared by hydrolyzing inulin with enzymes or dilute acid [6]. Fructose is crystallized with difficulty; the crystals melt in the range from 102° to 104° C. It is levorotatory; that is, solutions of fructose rotate the plane of polarized light to the left.

The production of fructose syrup from cornstarch was made possible by significant advances in industrial isomerization and chromatographic separation technologies in the 1960s and 1970s. The primary raw material used worldwide for the production of fructose syrup is corn. Fructose syrup derived specifically from corn starch is called high fructose corn syrup (HFCS). Fructose syrup from the starch sources like corn, rice, wheat, tapioca and potato, is called simply high fructose syrup (HFS) [6].

Figure 1.2 shows the process of high fructose syrup production from the starch. Starch follows liquefaction and saccharification steps sequentially and turns into dextrose. After refining steps, it is turned into a glucose-fructose mixture and passes through a fractionation column for the desired percentage of glucose and fructose in the syrup

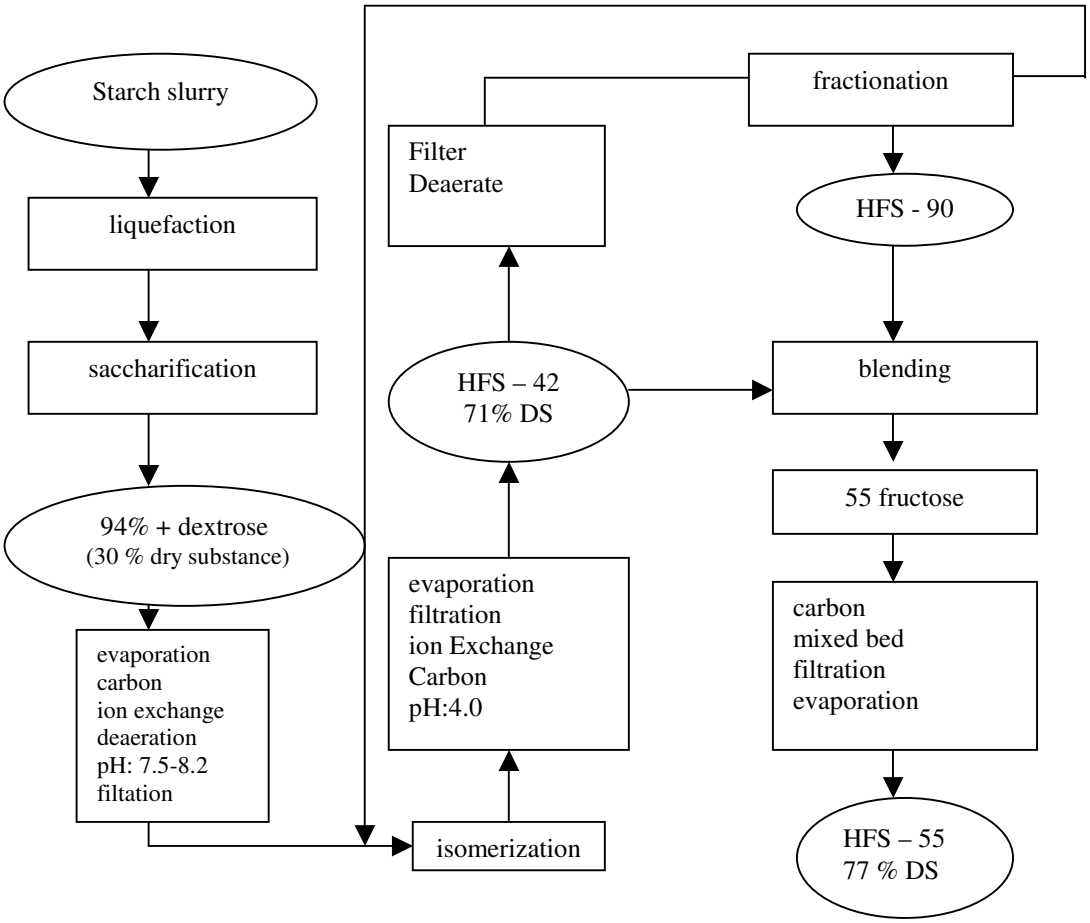

Figure 1.2 High fructose syrup manufacturing process diagram. [7] (DS: dry substance)

1.1.3 Tautomeric Forms of Glucose and Fructose

In a mixture of glucose and fructose, both of the sugars undergo a rapid mutarotation to a mixture of tautomers as shown in Figure 1.3 and 1.4 [8].

In contrast to glucose, which occurs only in two forms, α-D and β-D glucopyranose; five tautomers of fructose are present; namely the α-D and β-D fructofuranose, α-D and β-D fructopyranose and a small amount of open chain keto form. The relative amounts of the tautomeric forms present in solution are interrelated through equilibrium whose position depends on temperature, pH and the presence of electrolytes [9].

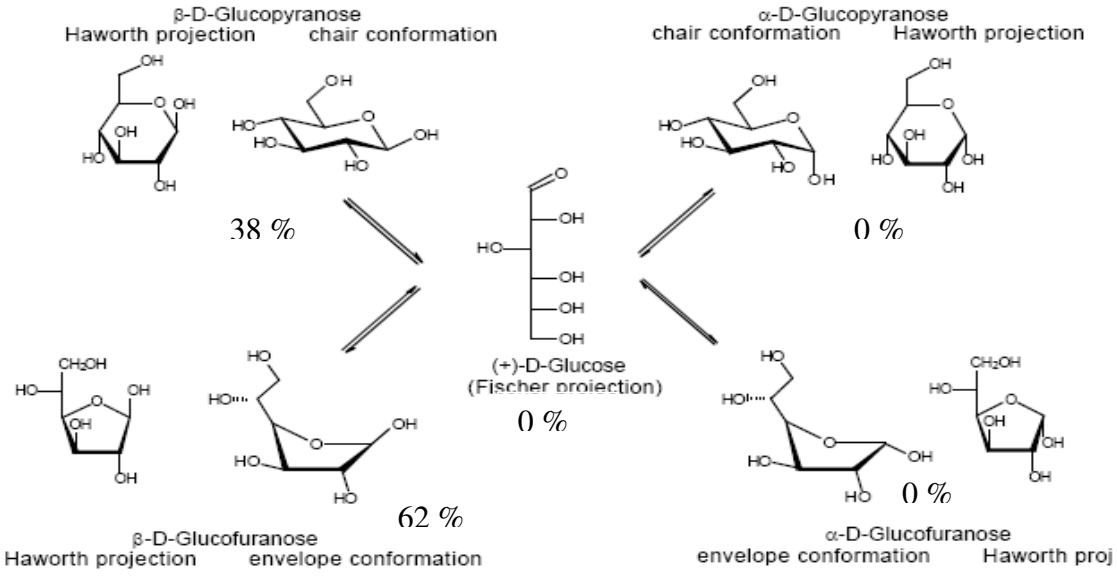

Figure 1.3 Glucose Tautomeric Distributions

While the major tautomer is β- D glucopyranose at all temperatures for glucose, the major tautomer for fructose at 20ºC is β-D fructopyranose, present to the extent of 72.5%. β-Fructofuranose constitutes 19% of the equilibrium mixture and the other forms are present in very small amounts: 5, 2.5 and 1% respectively [8].

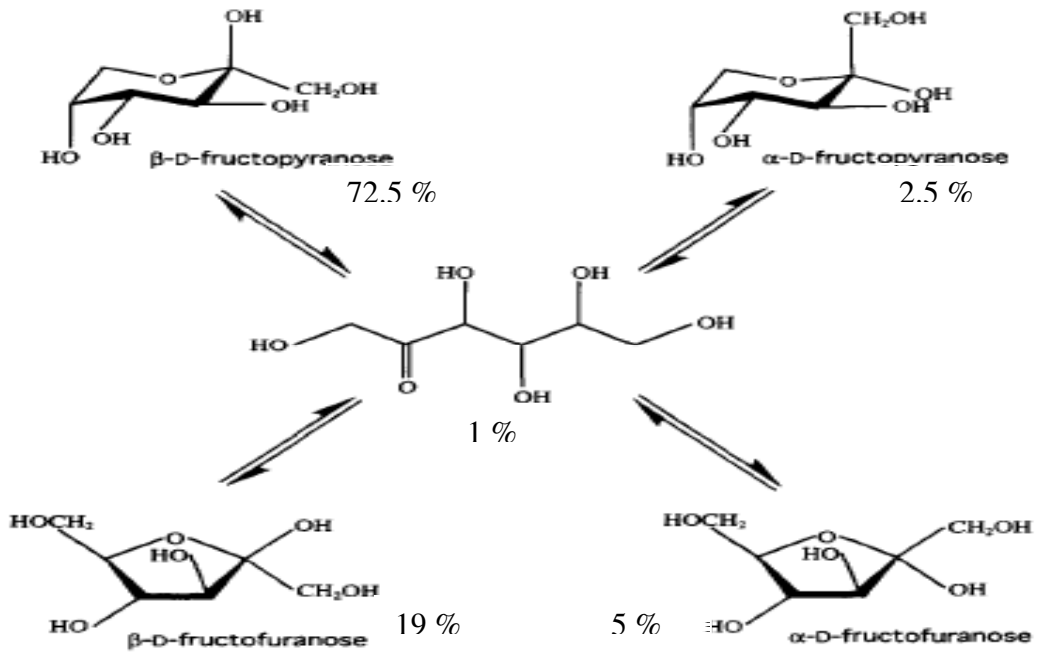

Figure 1.4 Fructose Tautomeric Distribution at 20^0C

Grabka [9] reported the interaction between calcium hydroxide and tautomeric distributions of D-glucose and D- fructose solutions. The effect of $Ca(OH)_2$ was examined with NMR spectrometer. It was seen that addition of $Ca(OH)_2$ to the glucose solution changes the proportions of α and β anomers. At 20ºC, in pure glucose solution, the ratio of α anomer to β anomer is 59:41. When $Ca(OH)_2$ is added to make $Ca(OH)_2$:glucose molar ratio 0.39, the anomeric distribution becomes 21:79.

Shallenberger and Birch [10] reported that, rate of mutarotation changes with temperature, pH and electrolytes. The rate rises 1.5-3 times as the temperature increases by 10ºC. Both acids and bases accelerate the mutarotation of sugars. The rate of mutarotation is at a minimum for pyranose-pyranose interconversion at a pH range from 2.5 to 6.5. The rate of mutarotation for pyronose-furanose

interconversion is at a minimum at a pH 4.0, but increases markedly with either an increase or decrease in the pH of the solution. Within a short period of time, alteration of pH does not seem to affect the position of the equilibrium. No general rule can be given for the effect of salts on mutarotation.

Cokman et al. [11] studied the mutarotation of fructose in water to determine equilibrium compositions as a function of temperature. The instruments, GLC and GLC/MS, which can detect even the small amounts of α-fructopyranose and the open chain keto form, were used for the studies. They found and presented a tautomeric distribution of fructose versus temperature.

1. 2 Adsorption

Adsorption is the accumulation of solute molecules at an interface (including gas-liquid interfaces, as in foam fractionation, and liquid-liquid interfaces, as in detergency). The accumulation per unit surface area is small; thus, highly porous solids with very large internal area per unit volume are preferred. Adsorbent surfaces are often physically and/or chemically heterogeneous, and bonding energies may vary widely from one site to another.

Adsorbents are natural or synthetic materials of amorphous or microcrystalline structure. Those used on a large scale, in order of sales volume, are activated carbon, molecular sieves, silica gel, and activated alumina. The working capacity of a sorbent depends on fluid concentrations and temperatures. Graphical depiction of sorption equilibrium for single component adsorption or binary ion exchange is usually in the form of isotherms or isosteres. Historically, isotherms have been classified as

favorable, concave downward, or unfavorable, concave upward. These terms refer to the spreading tendencies of transitions in fixed beds [12].

Table 1.2 classifies common adsorbents by structure, type and water adsorption characteristics. Structured adsorbents take advantage of their crystalline structure (zeolites and silicate) and/or their molecular sieving properties. The hydrophobic choice of (non-polar) or hydrophilic (polar surface) character may vary depending on the competing adsorbate. A large number of zeolites have been identified, which include both synthetic and naturally occurring (e.g. mordenite, chabazite) varieties [12].

Table 1.2 Classification of Common Adsorbents

	Amorphous	Structured
Hydrophobic	Activated carbon polymers	Carbon molecular sieves Silicate
Hydrophilic	Silica gel Activated alumina	Common zeolites: 3A (KA), 4A (NaA), 5A(CaA), 13X(NaX), Mordenite, Chabazite, etc

The inverse process (removal) is called desorption. In adsorption, the adsorbate accumulates on the adsorbent, which is then loaded with adsorbate. During desorption, the adsorbate present in the condensed phase passes from the surface of the adsorbent into the fluid phase.

1.2.1 Adsorption Rates

Simple models have been widely used to describe the relationship between adsorbed and soluble material. The Freundlich and Langmuir isotherms are used most often:

Freundlich, $q=K_d*C^{1/n}$ .....(1.1)

Langmuir, $q=k*Cb / (1+kC)$.....(1.2)

Or in linear form;

Freundlich $\log q = \log K_d + 1/n \log C$.....(1.3)

Langmuir $C/q = (1 / kb) + C/b$.....(1.4)

q=quantity of adsorption (adsorbate per mass of adsorbent)

C=equilibrium solution concentration of the adsorbate

K_d=distribution coefficient

k=binding strength constant

b= maximum amount of adsorbate that can be adsorbed

n=empirical parameter.

The linear forms (log q vs. Log C and C/q vs. q) may be plotted to obtain values of the various constants. However, these equations are empirical and are based on gas adsorption for a flat, solid surface.

Sometimes, it is desired to adsorb only molecules below a certain diameter. Molecular sieves or carbon are ideal for this aim as they have a very narrow distribution of micro-pores. Depending on their mechanism, only components with critical diameter smaller than the opening of the micro-pores will be adsorbed. In this way, mixtures can be separated by adsorption [12].

In adsorption from solutions, solute and solvent molecules compete for sites on the adsorbent. In order to get adsorbed, the solute molecule must first displace a solvent molecule. If the adsorbent is a polar material, non-polar molecules will have little affinity for the surface and will not be retained. Molecules with polar functional groups will have a strong affinity for the adsorbent surface and will be strongly retained [13].

The most important applications of adsorption depend on the selectivity, the difference in the affinity of the surface for different components. As a result of this selectivity, adsorption offers a relatively straightforward means of purification (removal of an undesirable trace component from a fluid mixture) and a potentially useful means of bulk separation, in case like glucose- fructose separation [14].

For bulk separation, highly selective adsorbents are needed; resins and zeolites are the mostly used ones. Resins are being used in industry since the middle of the last decade and in literature there is vast amount of information about them. Zeolites are the other important class of adsorbents and this research is focused on zeolites.

1.2.2 Chromatographic Separation Process

There were remarkable progresses in understanding the phenomenon of chromatographic separation. The separation media for saccharides employed in large-scale separation plants are shown in Table 1.3 [6].

Table 1.3 Commercial Separation Media for Saccharides [6]

Cation-exchange resin in calcium form
Fructose-dextrose
Mannose-dextrose
Cation-exchange resin in sodium form
Dextrose-higher saccharide
Maltose-higher saccharide
Isomaltose-Isomaltodextrin
Cation-exchange resin in potassium and/or sodium form
Sucrose-raffinose
Sucrose-fructose and dextrose
Sucrose recovery from molasses
Faujasite-type molecular sieve Y in calcium form
Fructose-dextrose

The separation media used to separate saccharides should be highly hydrophilic because water is the most cost-effective eluent. Adsorbents such as activated carbon do not meet this requirement.

Important physical characteristics of a separation medium are shape, particle size distributions, pore size distribution, crush strength, resistance to abrasion and ability to withstand osmotic shock. An economically optimum particle size exists in each case. Almost all reported applications use separation media with a particle diameter between 0.1 and 1.0 mm for both ion-exchange resins (IER) and molecular sieves.

In most cases, available resins provide adequate thermostability. The system operating temperature must be high enough to inhibit bacterial growth and at the same time, low enough to prevent significant decomposition of the saccharides. Operating temperature is usually between 55 and 90°C. This temperature range does not damage cation-exchange resins in the salt form, but resin life is highly dependent

on the composition of the feed stream and the quality of the eluent.

Anion-exchange resins are not used in commercial saccharide separation at present. This is because of their instability at the elevated temperatures needed for inhibition of bacterial growth.

Fructose-dextrose separation has formed the basis of the chromatographic separation technique for saccharides. There are alternative processes to obtain enriched fructose corn syrup from high fructose corn syrup: a single-column batch system, a semi-continuous system, and a continuous simulated moving-bed system [6].

In moving-bed chromatography, separation is carried out in independent vessels linked in series. Fructose has a greater affinity than dextrose for the calcium salt form of strong-acid, cation-exchange resin. This affinity slows its progress relative to dextrose as the saccharides move through the chromatography column accomplishing the separation [28].

The fractions of the fructose product and raffinate (dextrose and higher saccharides) by-product streams that are chromatographically distinct are withdrawn. Sophisticated valving continuously feeds substrate and withdraws product in successive chromatographic compartments [6]. The results of a plant (Table 1.4) illustrate the ability of moving-bed chromatography to efficiently separate fructose from other products of isomerization.

Table 1.4 Moving-Bed Chromatographic Separation of Dextrose Isomerization Products [6]

	Separation Stream (%)		
Component	**Substrate (Feed)**	**Fructose (Product)**	**Raffinate (By-product)**
Fructose	43-44.5%	80-90%	0-10%
Dextrose	50-55%	0-15%	80-90%
Higher saccharides	0-1%	0-1%	0-3%
Maltose	0-2%	0-2%	4-7%
Dry substance	59-61%	25-35%	25-35%

1.3 Zeolites

Zeolites are crystalline aluminosilicates. Zeolitic adsorbents have their water of hydration removed by calcinations to create a structure with well-defined openings into crystalline cages. The molecular sieving properties of zeolites are based on the size of these openings [12].

The term “molecular sieve” is used to describe a class of materials that exhibit selective sorption properties, i.e. that are able to separate components of a mixture on the basis of molecular size and shape [15].

Zeolites are hydrated aluminosilicates that are built from an infinitely extending three-dimensional network of AlO_4 and SiO_4 tetrahedra, linked to each other by the sharing of oxygen atoms [16].

Each AlO_4 tetrahedron in the framework bears a net negative charge, which is balanced by a cation, normally from the group IA and IIA. The framework contains channels and interconnected voids, which are occupied by the cation and water molecules. The cations are mobile and may usually be removed reversibly leaving intact a crystalline host structure permeated by microphores and voids which may amount to as much as 50% volume of the dehydrated crystals.

The Si/Al ratio is an important characteristic of zeolites. The charge imbalance due to the presence of aluminum in the zeolite framework determines the ion exchange properties of zeolites and induces potential acidic sites. As the Si/Al ratio increases, the cation content decreases, the thermal stability increases and the surface selectivity changes from hydrophilic to hydrophobic [15].

1.3.1 Application and practical utilization

There are three properties of zeolites that make them technologically important: they are selective and strong adsorbents, they are selective ion exchangers and they are catalytically active. Zeolites are widely used as drying agents, in separation processes (such as n-paraffin from branched paraffins and p-xylene from its isomers), in laundry detergents, as catalysts and catalyst supports (e.g. in petroleum refining), in wastewater treatment, nuclear effluent treatment, etc [17].

Synthetic zeolites and molecular sieves are generally produced as fine crystals. Often, this form is not useful for practical application and further processing is necessary. Agglomerates of molecular sieves are commonly prepared by the addition of an inorganic binder, usually a clay mineral, to produce a wet mixture [16].

The quantity of liquid adsorbed by a solid depends on temperature, the nature of the liquid and the nature of the solid. The adsorption isotherm is determined by measuring the amount of liquid adsorbed by weighing when equilibrium is attained. Then an isotherm equation is applied. In addition to standard isotherms equations, several trials have been made but no universal adsorption equation exists [16].

1.3.2 Zeolites as Adsorbents

Zeolites are being used in food industry for many years as adsorbent for glucose-fructose separation. As glucose and fructose are big molecules, the zeolites with largest pore sizes are preferred, such as Zeolite Y and Zeolite X. Si/Al ratio is another important factor for adsorption [17].

Hashimoto et al. [18] used simulated moving bed adsorber packed with zeolite Ca-Y in glucose fructose separation. The continuous separation of a glucose/fructose mixture was experimentally performed with the Ca^{+2} form of zeolite. Experimental runs were carried out to examine the validity of the models over a wide range of conditions and they presented mathematical models. It was found that the Ca^{+2} form of zeolite Y adsorbed fructose selectively and the adsorption isotherms of glucose and fructose on the adsorbent were linear and independent of each other.

Klatt et al. [19] used simulated bed for the preparation of fructose and glucose. They presented the design of a model-based optimization and propose a two-layer control architecture where the optimal operating trajectory is calculated off-line by dynamic optimization based on a rigorous process model.

In the study done by Zhang et al. [20], a model to verify the dynamic SMB model to maximize the net productivity of HFS 55 using a minimum solvent during the production of high fructose syrup by isomerization of glucose was observed.

They found a set of equally good solutions, which are known as Pareto optimal solutions. Finally, their results indicated that reducing fructose content in the feed is beneficial for the forward reaction further, thereby increasing the conversion of glucose.

Lee [21] modified the three-section SMB from the two-section model and applied it to the separation of an aqueous mixture of glucose and fructose at high concentration up to 500 kg/m^3. He used Dowex 50W-X12 resin of Ca^{2+} form as an adsorbent and water as an isocratic eluent. The equilibrium isotherms in terms of a quadratic expression and a plug flow model with mass transfer effect were used to predict both the products and on-concentrations in the two-section SMB process. The two-section SMB process suggested in this work was successful in obtaining high fructose corn syrup at the high concentration of 500 kg/m^3.

Ching et al. [22] studied and compared Ca-Y zeolite and Duolite resin adsorbents packed in a small column for the high concentration under conditions similar to the commercially employed processes. They found the overall performance of the system similar for both adsorbents, although the flow conditions required to achieve separation are significantly different. The resin adsorbents have higher equilibrium selectivity's than Ca-Y zeolites but the zeolite adsorbents have smaller mass transfer resistance.

In a study of Buttersack et al. [23], the adsorption of several sugars using Y zeolite and dealuminated Y zeolite in batch system was observed. Henry constants of glucose, fructose and other oligosaccharides were found on the zeolite Y in various forms Ca and Na, K, and St. They found that glucose was adsorbed only in case of the dealuminated Na-Y zeolite. In other cases, the concentration of glucose inside the zeolite pores was found to be lower than the concentration in the bulk solution. In dealuminated zeolite Na-Y, fructose was adsorbed more than the other forms of zeolites. A significant interaction for fructose was found to exist even the K^+ show weak interactions with monosaccharides. The interaction of glucose and fructose containing disaccharides with the Na-Y zeolite was low but the data for the Ca^{+2} containing zeolites show that the fructosyl residues cannot develop their intrinsic comlexation in the same extent compared with the monosaccharide [23].

In one of the studies of Buttersack et al. [24], the dealuminated Y zeolite was obtained by treatment with $SiCl_4$. It was seen that the zeolite becomes more and more hydrophobic as the Si/Al ratio increased by dealumination. It was also found that the high selectivity or molecular recognition was due to the ability of the carbohydrate molecule to change its tautomeric equilibrium and conformation, besides shape selectivity was found superimposed. The Henry's constant value of fructose is significantly greater for the Ca-Y. They found that fructose was enriched in the zeolite pores while the other sugars were more or less excluded from the pores. As the Si/Al ratio increased, all sugars were enriched in the zeolite pores.

In another study by Schöllner et al. [25], the adsorption of D–fructose-, D-glucose- and D-arabinose-water mixtures on K^+, St^{2+}, Ca^{2+}, Ba^{2+} and La^{3+} ion exchanged X and Y zeolites has been performed. From the adsorption excess isotherms, the separation factor and the equilibrium diagrams X_2^S vs. X_2^1 of the binary mixtures were calculated. Also, the possible triangles of O atoms of monosaccharide, their interactions with cations, the influence of crystallographic cation positions and the Si: Al ratio of zeolites on formation of adsorption complexes was analyzed. They found that higher contents of Ca^{+2} adsorbs greater amounts of fructose, the triangles of two OH groups and the O atom of the acetal group of the pyranose and furanose ring are able to interact strongly with Ca^{2+} ions in position SII in Y zeolites and K^+ ions in position SII in X and Y zeolites.

Atalay [26] studied the adsorption of fructose and glucose on zeolites Na-X, and Na-Y, Ca-Y and decationated forms of Y, batch wise. The effect of temperature and concentration on adsorption was examined and adsorption isotherms were determined. In the experiments, the mixtures were not studied due to the limits of the analysis methods and used low concentrations for the experiments.

Heper [27] studied the kinetics and equilibria of adsorption by Na-, Ca-, NH_4-, Mg- and H- forms of Zeolite Y from aqueous solutions containing 25 % (w/v) of either one or an equimolar mixture of glucose, G and fructose, F at 50ºC. It was found that Na-, Mg- and H- forms did not exhibit rate-based selectivity, while the Ca- an NH_4- forms adsorbed G faster than F. Addition of $CaCl_2$ improved the difference between the amounts of G and F.

1.2 Color Reactions of Hexoses

In some group specific color reactions of carbohydrates, the sensitivity of various classes of carbohydrates, for example, mono- and polysaccharides, is of the same order of magnitude, and the absorption maxima are very nearly identical for more than one class of carbohydrate. This group of reactions is particularly useful for identification of a substance as a carbohydrate and for estimation of total amounts of carbohydrate.

The only reaction in which the reactivity of various classes of ketoses have been investigated systematically is the reaction with L-cysteine and carbazole in sulfuric acid, which can be used for detection of various ketoses as well as for their quantitative determination. In this reaction, however, aldoses also react, although much more slowly and with extinction coefficients very much smaller so that, in general, an accurate determination of ketoses with this reaction is possible [29].

1.5 Response Surface Method

Global optimization is the process of finding set of parameters in the feasible design space for which the objective function will have its optimum value (maximum/minimum) where the objective function can have several local optima. For these problems, local optimization methods are likely to terminate prematurely before the global optimum is reached. Example of local optimization methods is Powell's method of conjugate directions, Hooke and Jeeve's pattern search method and Cyclic coordinate search. Global optimization methods include Response

Surface Methods (RSM), Simulated Annealing (SA) and Genetic Algorithms (GA). For this study, the focus will be on the use of Response Surface Methodology as a global optimization method [30].

RSM comprises a group of statistical techniques for empirical model building and model exploitation [30]. A response or output function is related to a number of input variables that affect it. The variables studied will depend on the specific field of application. If there is only one input variable then the output can be revealed by a curve. If there are two inputs then we have a three-dimensional space in which the coordinates axes represent the output and the two input variables. In this case we get a response surface. When there are N input variables (*N >>2),* we have a response surface in the N+1 dimensional space of the variables [31].

RSM is used when only a small number of computational or physical experiments can be conducted due to the high costs (monetary or computational) involved. Response surfaces are fit to the limited data collected and are used to estimate the location of the optimum. The RSM gives a fast approximation to the model, which can be used to identify important variables, visualize the relationship of the input to the output and quantify tradeoffs between multiple objectives. Statistical methods including Statistical Process Control (SPC) and the Design of Experiments (DOE) play a key role in quality improvement that is most effective when it occurs early in the product and process development cycle. RSM is an important branch of experimental design in this regard. RSM is critical in developing new processes, optimizing their performance and improving the design and formulation of new products [31]

1.5.1 Origin of Response Surface Methodology

Response Surface Methodology's first published account occurred in 1951 in the journal of the Royal Statistical Society by Box and Wilson [32]. The investigated characteristic of the product or the process is called the response or the response variable. The factors or the input variables that influence the response are called the independent variables. The analytical function used to approximate the response is called a response function.

Wilson and Box's [32] paper uses RSM for optimizing a single response variable by adjusting the settings of a set of factors when the functional relationship among the variables is unknown. RSM was not considered for optimizing multiple response variables until 1959. In 1959, Hoerl [33] used RSM to optimize multiple response variables. Hoerl suggested two different ways to optimize multiple response variables. The first method was to combine the different response functions into a single function using a weighted average of the response functions. The second method was to consider one of the response variables as primary and to optimize it subject to the limits placed on the remaining response variables. Hoerl does not mention how the different weights for the first method are calculated and he does not give an application of the first method. He does describe about the application of the second method where a primary response variable is identified and the limits for the remaining variables are identified. Then each response function is optimized individually and contour plots are developed the latter are superimposed on each other to find the region where the solution lies. The optimal location is identified visually. This approach can be used only for a small number of factors and response variables.

1.5.2 Applications of Response Surface Methodology

There are broad three categories of problems where Response Surface Methodology (RSM) is useful:

1. Mapping a response surface (RS) over a particular region of interest. A suitable response surface is mapped over a region of interest for the experimenter to get a good idea of how the response would change with the change in the factors on which the response depends.
2. Optimization of the response. Response Surface Methodology can be used to find the conditions that optimize the design process under consideration.
3. Selection of operating conditions to achieve specifications or customer requirements. In most RSM problems, there are several responses that must be considered simultaneously.

RSM is often an important engineering tool as the objectives such as quality improvement can be enhanced. In some industrial problems, the response variables of interest in the product are a function of the proportions of the different ingredients used in its formulation. This is a special type of RS problem called the mixture problem.

1.5.3 Sequential nature of Response Surface Method (RSM)

Myers and Montgomery [31] described RSM as 'a collection of statistical and mathematical techniques useful for developing, improving and optimizing process'. These techniques include Design of Experiments, least-squares regression analysis, determining optimum factor settings, response surface model building and 'model exploitation'.

Screening experiments are done initially to find those set of factors, which are the most influential to the response(s) being studied. Then the experimenter conducts experiments at different levels of the factors and the corresponding responses(s) are recorded. The experimenter assumes the response to be a particular model. The model is fit to the data recorded. Then the model is tested to see if it is adequate. If the model is found to be inadequate, then the design is augmented with additional points and a new model is used. Once the model is found to be adequate, it is then analyzed to get the optimum conditions.

CHAPTER 2

EXPERIMENTAL

2.1 Materials

Materials used in this study, α-D (+) glucose and β-D (-) fructose were obtained from Sigma. The catalog numbers are G-5767 and F-0127, respectively. They are analytical grade materials with the purity of 99%.

Sodium Y and Ammonium Y zeolites were purchased from Aldrich. Catalog numbers were 33.444-8 and 33.444-3, respectively.

2.1.1 Pretreatment of samples for preparation of zeolites

Zeolite Ca-Y was prepared by exchanging the cations of Na-Y as outlined below:

25g Na-Y was brought into contact with successive 500 mL portions of 2N $CaCl_2$ solution in a shaker for 24 h. The zeolite was allowed to settle down and a sample of decantate was analyzed for Na^+ by flame photometer (Jenway PFP). This procedure was repeated several times until no more Na^+ ions were detectable. The sample was washed with deionised water, filtered and dried. The dried sample obtained was Ca-Y zeolite [16].

Decationated zeolite Y was obtained from dacationation of zeolite NH_4-Y according to the method reported by Breck [16]. 25g of NH_4-Y were calcined at 540ºC for 3h.

2.2 Methods

2.2.1 Batch Adsorption Experiments

In this study, the kinetics and equilibria of adsorption by calcium and hydrogen forms of zeolite Y was investigated batch wise at 50ºC. The aqueous solutions containing glucose, fructose and their admixtures were used as solutions. Zeolites were kept at 30% relative humidity in a desiccator containing glycerol solution at 98% by weight. As fructose was known to be highly hygroscopic, it was kept in a desiccator containing regenerated silica gel as desiccant. Sugar solutions were prepared with deionised water. The samples were prepared 24 hours before the experiments so as to minimize the effect of differences due to tautomeric distribution over adsorption profiles. The increase in temperature favors the formation of α-D-pyranose anomer in glucose and favors the formation of furanose forms in fructose [10].

1.0 g zeolite (0.75 g dry zeolite) and 6 mL of sugar solution were brought into contact in test tubes. The sugar samples detected were, (% w/v) glucose+ (% w/v) fructose basis, 12.5+12.5, 25+25, 35+35, 20+20, 30+30, 25+35, 35+25, 20+30, and 30+20 sugar solutions, in which there was only glucose or fructose. Glass beads were added to test tubes in order to prevent the settling of zeolites and help them to suspend in the solution. Samples were placed in a shaking water bath filled with ethylene glycol and shaken at 50°C for 60 minutes. The suspended solution was centrifuged at 3500 rpm for 10 min. The decantate was filtered with 45μm filter paper and analyzed. The determination of the amount adsorbed for g dry zeolite, was based on the

amounts of sugar disappearing from solutions. The data and calculations are given in Appendix B and C.

12.5 % w/v glucose+12.5 % w/v fructose and 25 % w/v glucose +25 (% w/v) fructose solutions were detected to see the effect of Ca^{2+} ions on distribution in the tautomeric forms of glucose and fructose by additions $CaCl_2$. There was 1 mol of Ca^{2+} ion interacting with 1 mol of fructose to form a complex.

In order to design better experiments and make sense of the results, some models were fit by nonlinear regression method. By LAB, curve fitting software, surface responses were found and analyzed.

2.2.2 Assay Methods

2.2.2.1 Determination of Fructose

Fructose was assayed by the method of Dishe and Borenfreund [29]. Ryu, Chung and Katoh [34] modified and formed "cystein-carbazole" assay procedure. The analyses were done with spectrophotometer, which is an absorption measurement with an underlying principle of that; the intensity of color is a measure of the amount of a material in the solution.

The idea was to detect the amount of fructose of 5.0 to 60μg in 1.0 ml. of sample. 2% L-cystein hydrochloride solution was added in an amount of 0.1 ml. Then, 5.0 ml of 75 % sulfuric acid solution was added and sequentially 0.15 ml of 0.12% carbazole solution was poured. Test tube was vortexed, and then kept in 40°C water bath for 30 minutes, where the color forming reaction occurred. To end the reaction, the sample was hold in ice bath for 2 minutes and while keeping at room temperature

at 560nm wavelength, the spectrophotometric analyses were done. D-fructose gave pink color. The advantage of this method seemed to be its allowance to the detection and estimation of fructose in the presence of glucose.

First the suitable wavelength was selected with one of the samples of fructose in cystein-carbazole solution. The absorbance values were detected from 280 to 560 nm. Besides, the blank solution was observed with the same absorbencies, and 560 nm was found as the maximum absorbance for the sample and minimum absorbance for the blank solution.

Then, with the samples of fructose, fructose and glucose in equal amounts, fructose and double amount of glucose, fructose and triple amount of glucose, fructose and ten fold amount of glucose; also fructose and double amount of glucose in which all the samples were measured fresh and in which all the samples were hold for a night outside and also hold in a freezer were detected to obtain a calibration curve. Finally, the test was repeated with glucose then its effect on glucose only solutions was shown. With the average of all data, a calibration graph was obtained.

2.2.2.2 Determination of Total Reducing Sugar

The total reducing sugar amount was detected by the volumetric procedure of Lane and Eynon [35] as their procedure has largely replaced other copper reduction methods for studies on foods. This procedure involves the determination of the volume of sugar solution required to reduce either 10 ml or 25 ml of mixed Fehling's solution, using methylene blue as the internal indicator. Air is excluded from the reaction mixture by keeping the liquid boiling throughout the titration.

First the Fehling's solution was prepared by mixing equal volumes of 69.278 g. of copper sulphate per liter of water and 346 g. of Rochelle salt and 100 g of sodium hydroxide per liter of water. Also, methylene blue indicator was prepared as 1 % aqueous solution.

The solution to be analyzed was put in a 50-mL burette, which was fitted with a pinchcock instead of a tap and a bent piece of glass tubing, so that the burette was not directly over the conical flask, during titrations. 10 mL of Fehling's solution; to analyze 0.1-to 0.3 g. of sugar in 100 mL of solution (25 ml of Fehling's solution was used to analyze 0.25 to 0.80 g of sugar in 100 mL of solution), was pipetted into the flask and 15 mL of solution of solution was added from the burette. The flask was heated on plain gauze supported on a tripod stand so that the liquid boils briskly. 4 drops of 1% methylene blue was added and sugar solution was added in 1 mL amounts every 15 seconds. Keeping the liquid boiling, the additions continued until the blue color was discharged and the titer amount was recorded. Then, this amount was checked by accurate titration.

Again 10 mL (or 25 mL) of mixed Fehling's solution was pipetted into the flask and an amount of solution, which is 1 mL less than the titer amount was added from the burette. The liquid was boiled for 1.5 to 2 minutes and 4 drops of methylene blue solution was added again. This time, 0.25 mL of sugar solution was added every 15 seconds and the titration was completed within 3 minutes from the time boiling starts. The blue color should have been disappeared, which shows complete reduction of the copper and the new color should have been orange-red in color. The amount of the titrate was then found on the table of "Factors for Lane and Eynon

Process" as seen on Appendix A. There are 2 tables, one is suitable for titrations with 10 mL of Fehling's solution and the other is for titrations with 25 mL of Fehling's solution. There is a factor depending on the type of reducing sugar and amount titrated. This factor is multiplied by 100 and divided to the titrate amount. The result gave us the amount of sugar in milligrams in 100 mL solution. The result of Lane-Eynon procedure was used in calculating total reducing sugar calculations. Then, the same sample was checked for fructose amount, by cystein-carbazole method.

2.2.2.3 Determination of Glucose

Glucose concentrations were calculated by the difference between two results. Detection of the glucose amount by Roche's Accu-Check® was also under consideration. Various concentrations of samples were prepared for calibration curve as seen in Appendix A. The resulting calibration curve was not meaningful for analysis.

CHAPTER 3

RESULTS AND DISCUSSIONS

3.1 Adsorption Results

In the previous study by Heper [27], the adsorption behaviors of Na-, Ca-, NH_4-Mg- and H- forms of Zeolite Y from aqueous solutions containing 25% w/v of either one or an equimolar mixture of glucose and fructose were studied batch-wise at 50^{o}C. In all experiments, constant amounts of 0.5 g zeolite and 3 mL solutions were used. In the present study, the samples were prepared from 1 g zeolite and 6 mL of solution, also the solutions were not taken out of the test tubes; test tubes were kept in the water bath during shaking.

The results of the present study were based on the amount of sugar disappearing from the solution and those values were calculated by using the % sugar values and then the results were converted into the amount adsorbed per 100 g dry zeolite values. The equation, sample calculation and the tabulated results were presented in Appendix C. The reproducibility graph was created and shown in Appendix E so as to check the reliability of the results and to show the agreement between independent results of the experiment.

The experiments were done with solutions, which were kept at the desired temperatures, 50ºC, for 24 hours. The analyses were done on various concentrations of solutions for the Ca-Y and H-Y zeolites.

Heper [27] found adsorption of pure glucose fast, with no change after minute 30 and adsorption of pure fructose was depending on the cationic form of zeolite, slowing down in the sequence $H^+ > Mg^{+2} > NH_4^+ > Ca^{+2} > Na^+$ of the cations. Comparing adsorption behaviors from solutions containing both glucose and fructose; the Ca- an NH_4- forms adsorbed glucose faster than fructose.

H-Y zeolites had no cations, which made the adsorption profiles observed as expected. Ca-Y zeolites showed vast differences on the adsorption profiles and that made the zeolite a very suitable adsorbent for separation purposes.

Normally, first 5 minutes, or around, was considered to be a time lag and adsorptions started following that time lag. Glucose started to be adsorbed immediately, until it reached the equilibrium at the 30^{th} minutes of the experiments. But fructose had a slow adsorption till the 20^{th} minutes and then adsorption increased to 30^{th} minutes. The results were similar for all the mixtures. Nonetheless, total sugar level of 70% in total, which resembled a saturation point for the zeolites showed no separation at all.

Besides, 35% w/v G + 25% w/v F solutions showed very poor separation curves for both zeolites, though 25% w/v G + 35% F w/v solutions showed rather better results.

Figure 3.1 shows the adsorption profile of 12.5% w/v G + F solutions, on Ca-Y zeolite. Glucose was adsorbed very low, up to 10^{th} minutes, with 3.7 g / 100 g DZ, but started to be adsorbed incrementally when it reached an equilibrium at 30^{th} minute with 16.5 g / 100 g DZ. Fructose adsorption was only 4.3 g / 100 g DZ at 20^{th} minute, but it reached an equilibrium value at 30^{th} minute with 16 g / 100 g DZ.

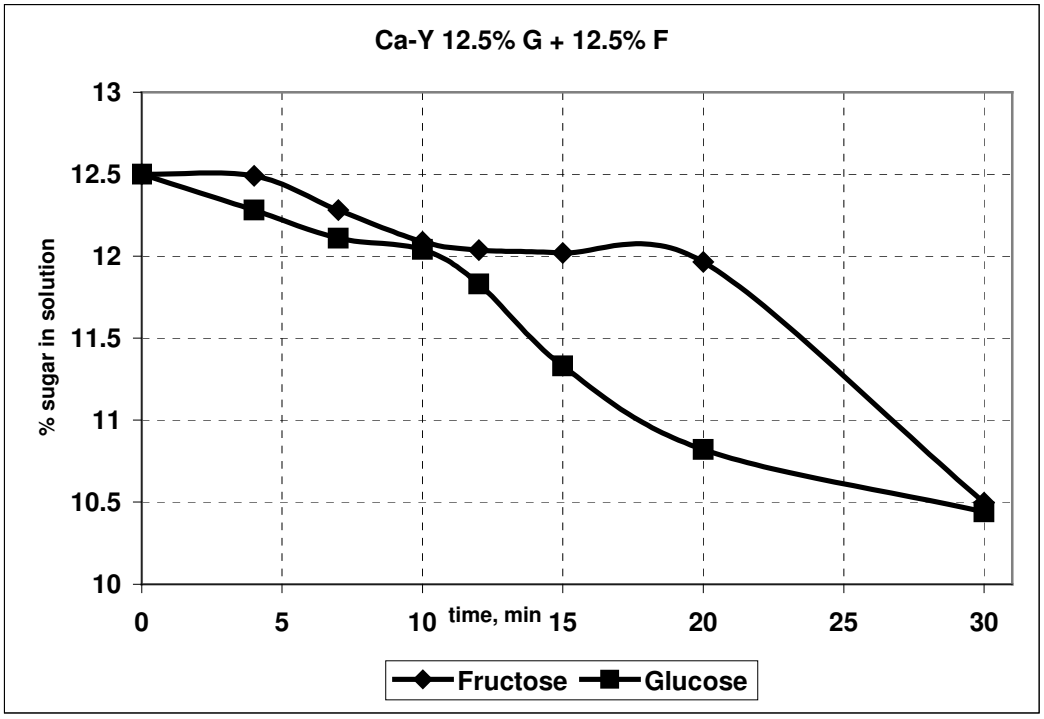

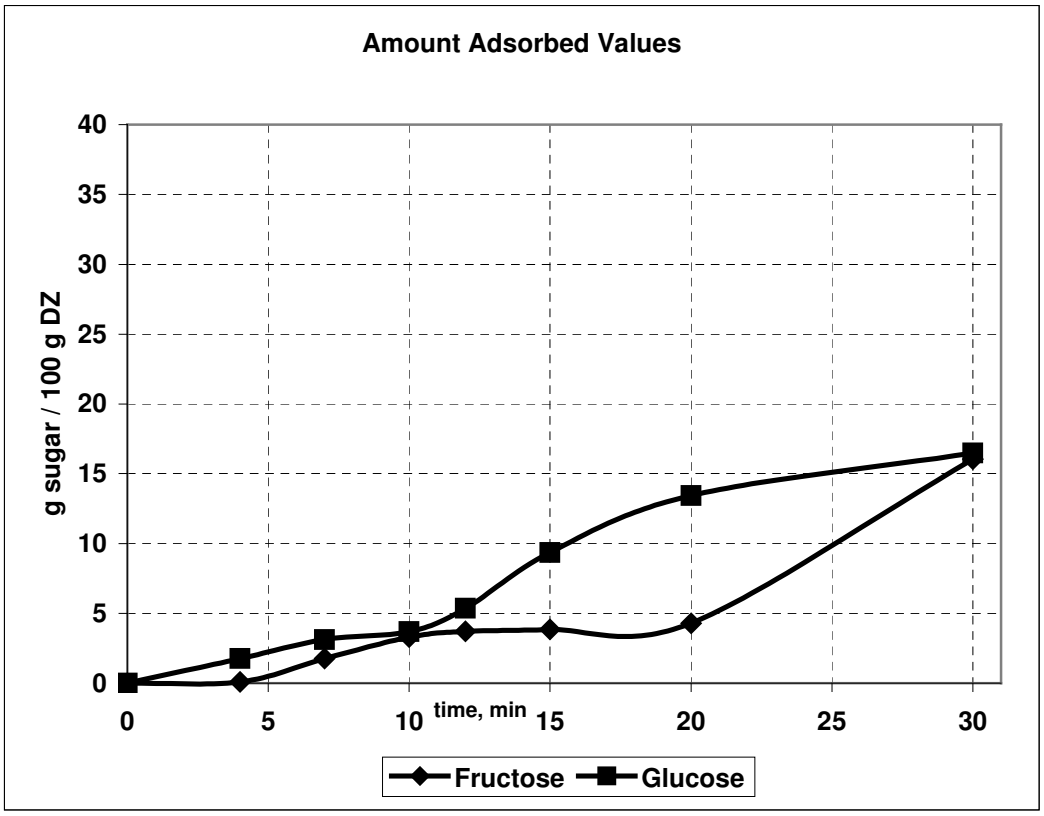

Figure 3.1 Adsorption Kinetics of Sugar Solutions (12.5 % w/v G + F) on Ca-Y zeolite

12.5% w/v G + F solution was treated on H-Y zeolites and the adsorption profile of 12.5 % w/v G+F solutions on H-Y zeolite was shown on Figure 3.2. The separations were not better than Ca-Y zeolite, instead glucose started to be adsorbed faster until 10^{th} minute though it started with a less adsorption value than Ca-Y zeolite. Fructose adsorption was not that much affected, and as the adsorption differences were low at 20^{th} minute, i.e. 11,9 g / 100 g DZ for glucose and 6 g per 100 g. dry zeolite for fructose, it could not be mentioned about an ideal separation.

Next experiment was processed with double amounts of the previous experiment. Figure 3.3 shows the results on Ca-Y zeolite. It was obvious that, when the trials were completed, doubling the amount of concentrations had doubled the amount-adsorbed values, up to 32 g. per 100 g dry zeolite, both for glucose and fructose. Besides, there was a very sudden increase in glucose adsorption between 10^{th} and 20^{th} minutes, where the rate of fructose adsorption was not changing.

The results were quite different for H-Y zeolites, as seen on Figure 3.4. The increase in the adsorption of glucose was turned into a decline after 15^{th} minute of the experiment, so was fructose. Though, both glucose and fructose showed increases till 32 g. per 100 g. dry zeolite value, the process did not mean a good separation either.

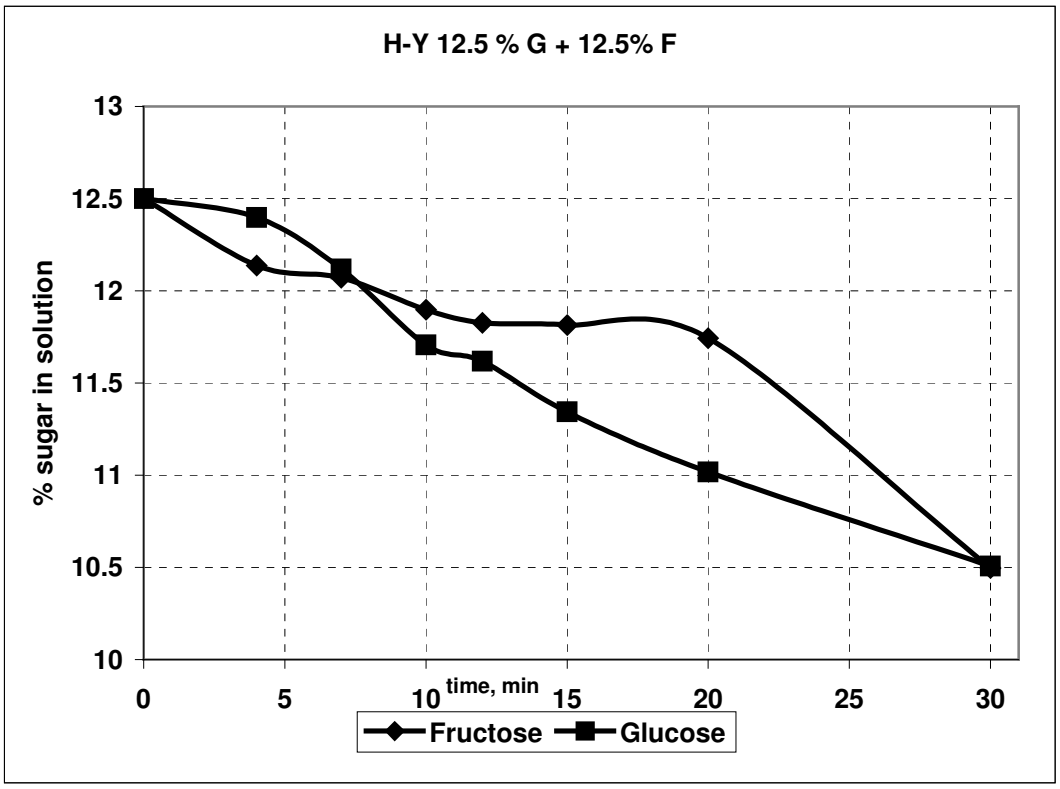

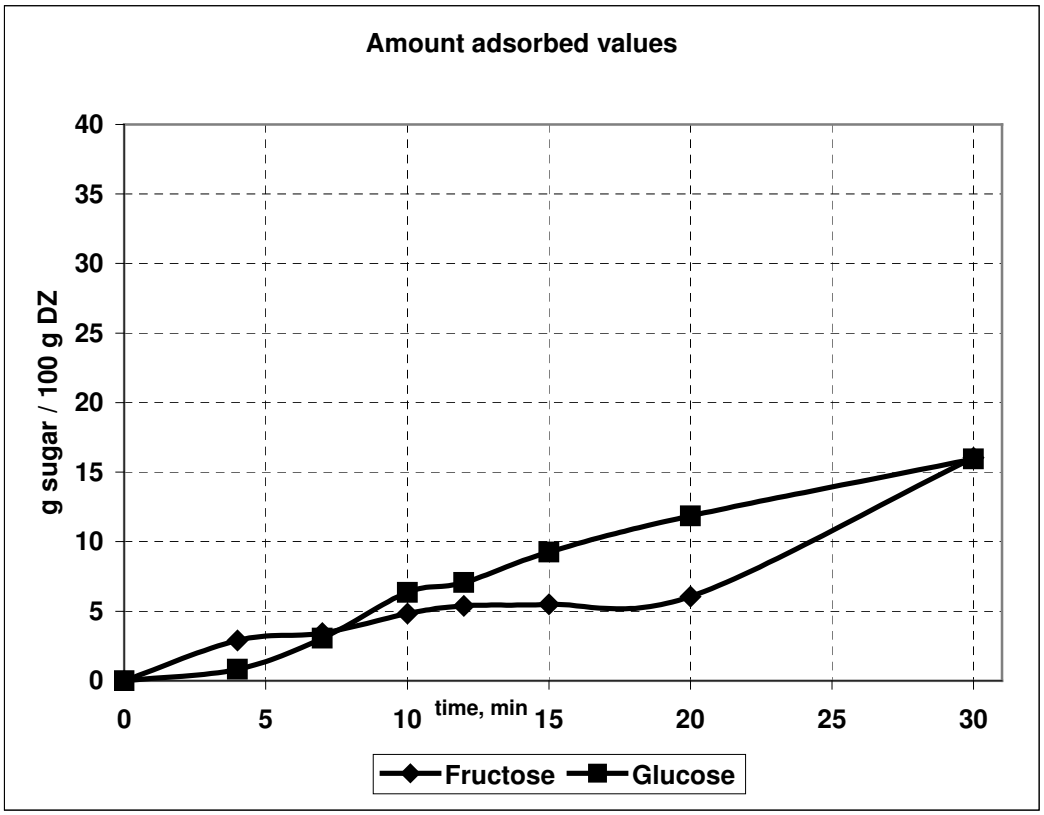

Figure 3.2 Adsorption Kinetics of Sugar Solutions (12.5 %w/v G + F) on H-Y zeolite

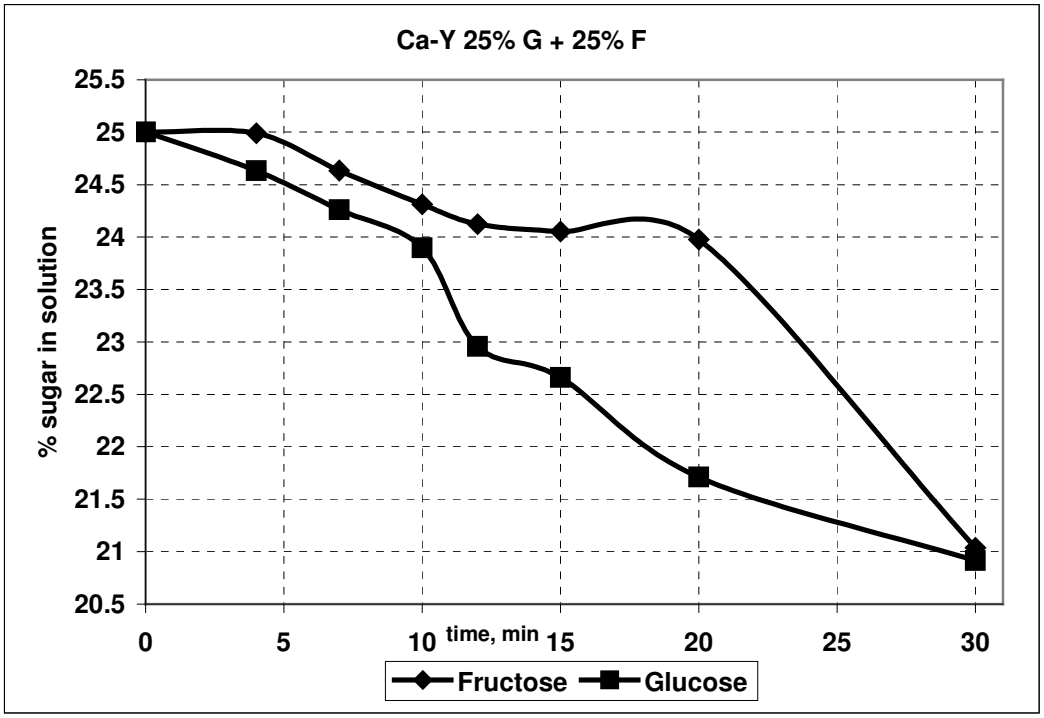

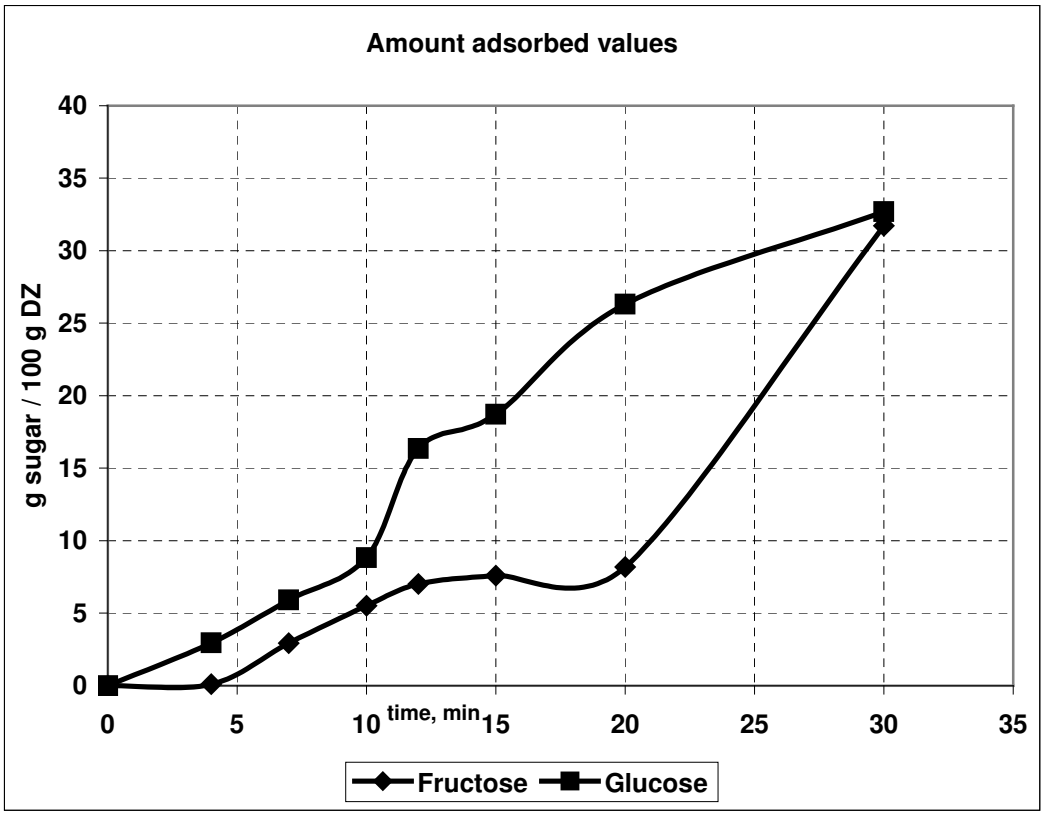

Figure 3.3 Adsorption Kinetics of Sugar Solutions (25 %w/v G + F) on Ca-Y zeolite

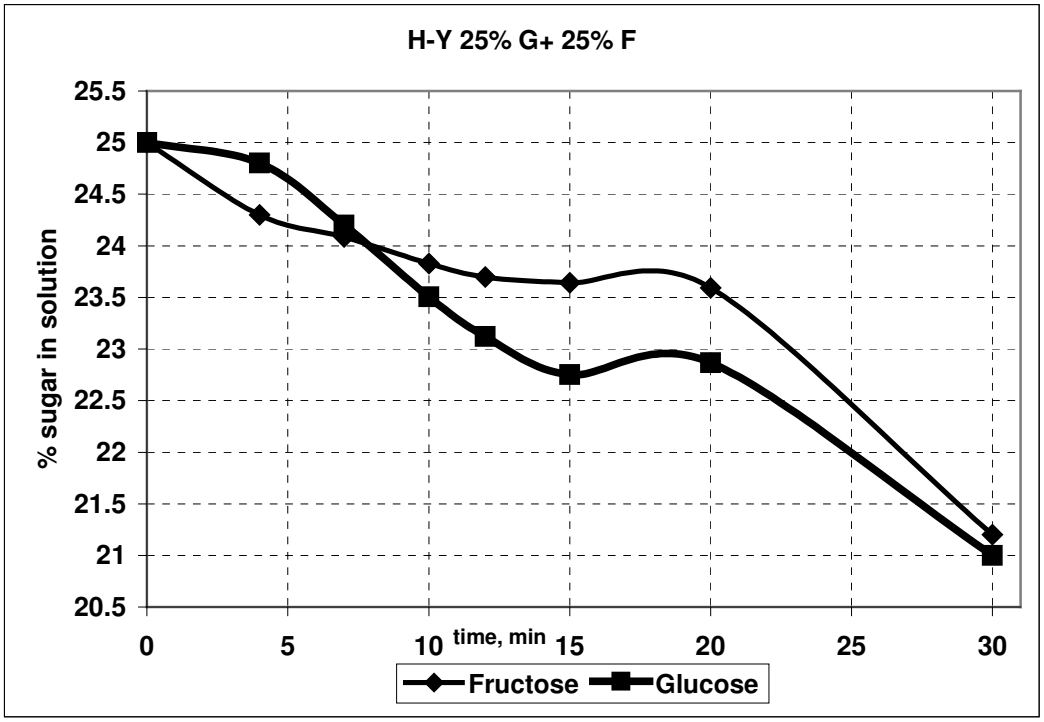

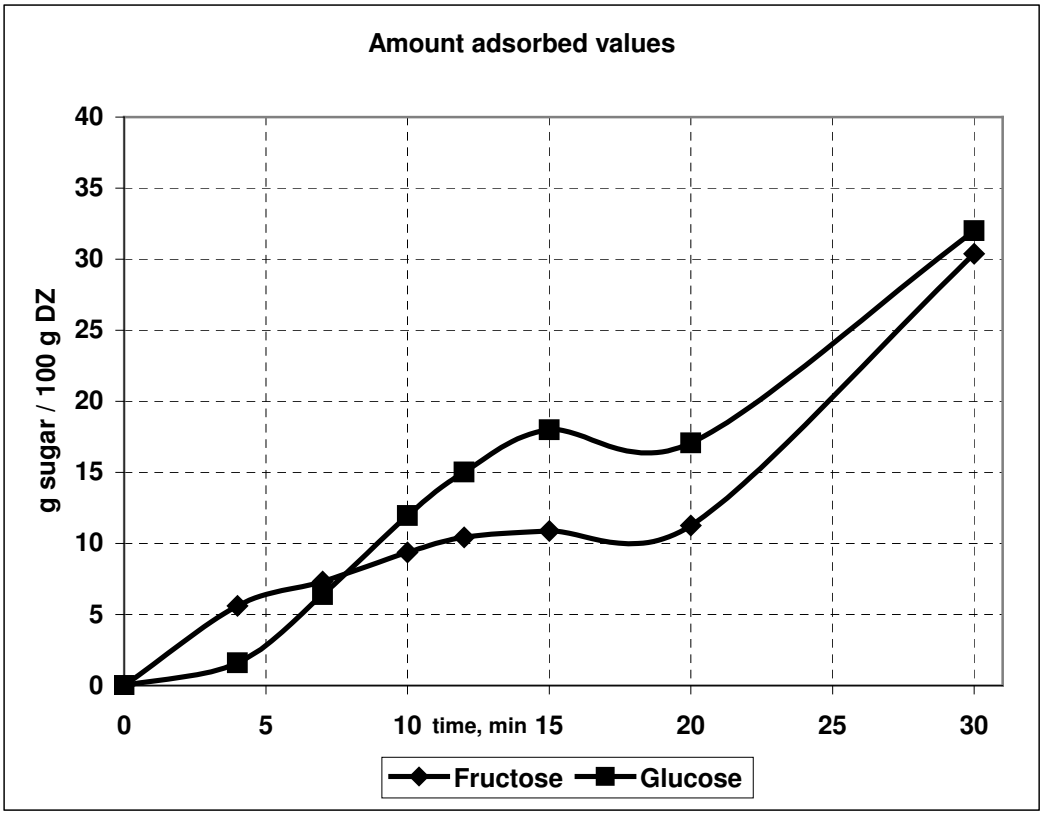

Figure 3.4 Adsorption Kinetics of Sugar Solutions (25 %w/v G + F) on H-Y zeolite

Concentrations of glucose and fructose in the mixtures were prepared as high as 35% w/v and it was seen that adsorptions and separation changed their behaviors. The separation was almost disappearing; even the adsorption amounts had reached up to 35 g. per 100 g dry zeolite amounts. Both glucose and fructose had the same tendencies at the same times towards the zeolite. The adsorbed amounts were about 3.5 g at 10^{th} minute and about 8. g at minute 20. This slow rate changed into a sudden fast adsorption rate between the minutes 20 and 30. The graph is outlined in Figure 3.5

In Figure 3.6, fructose was adsorbed rather slowly, which means a poor separation, which started from 10^{th} minute and increased until 20^{th} minute. But, comparing the previous studies, 14.3 g / 100 g DZ and 8.9 g / 100 g DZ does not mean a good separation.

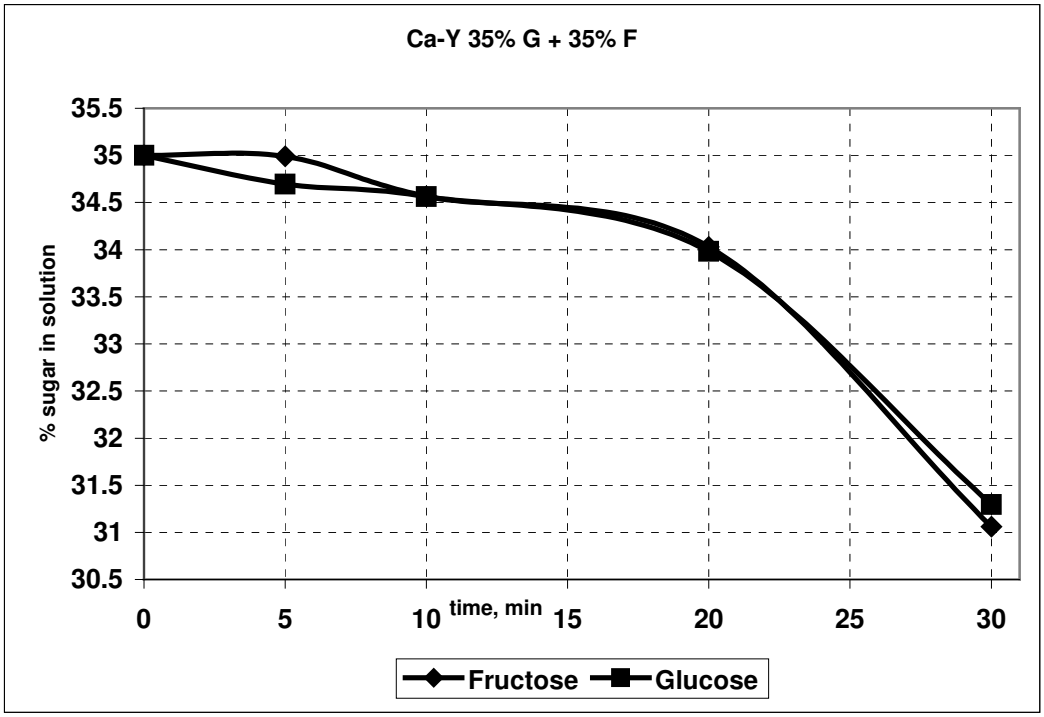

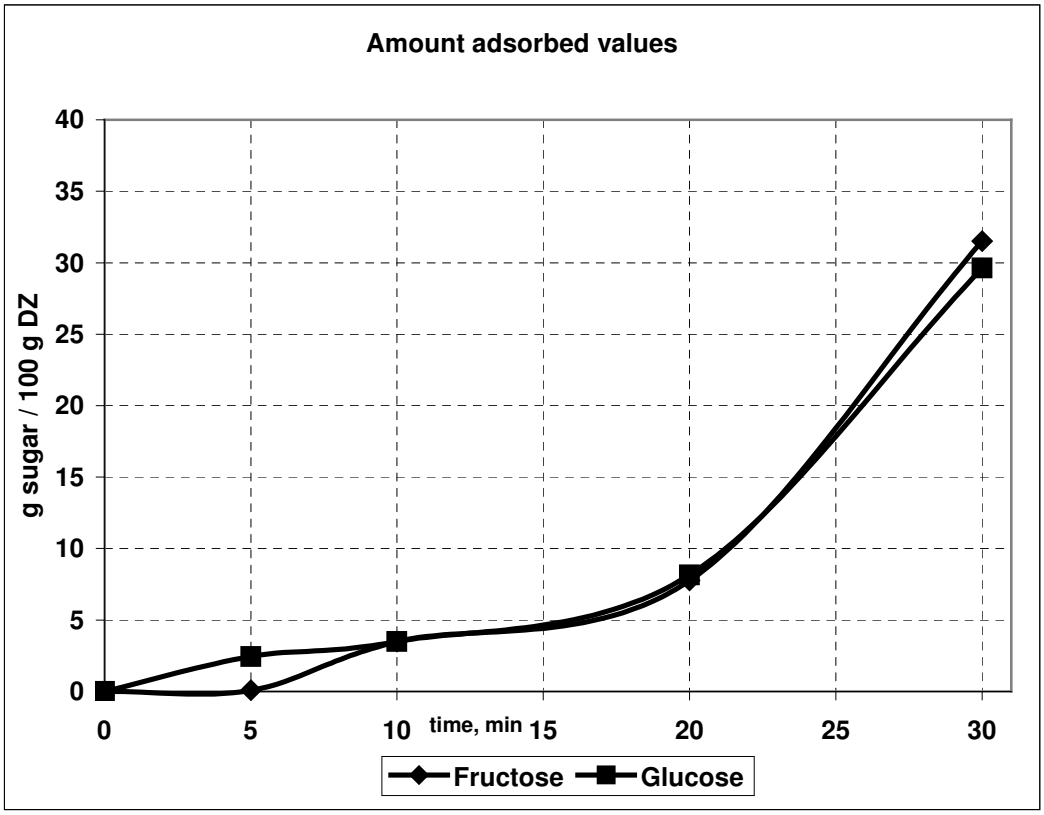

Figure 3.5 Adsorption Kinetics of Sugar Solutions (35 %w/v G + F) on Ca-Y zeolite

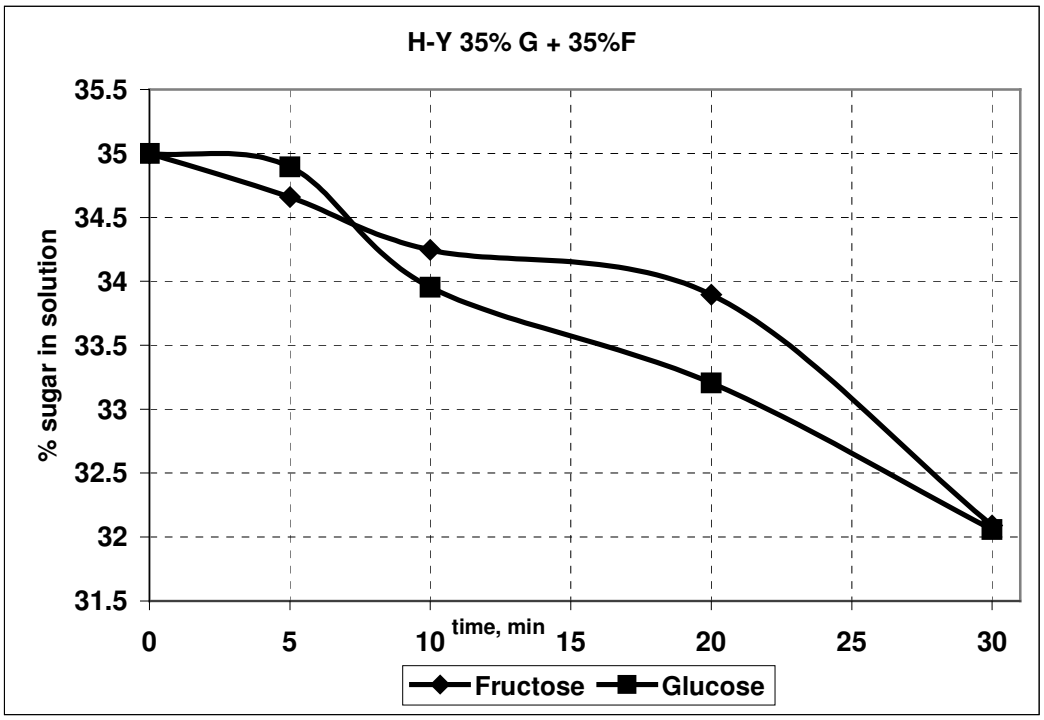

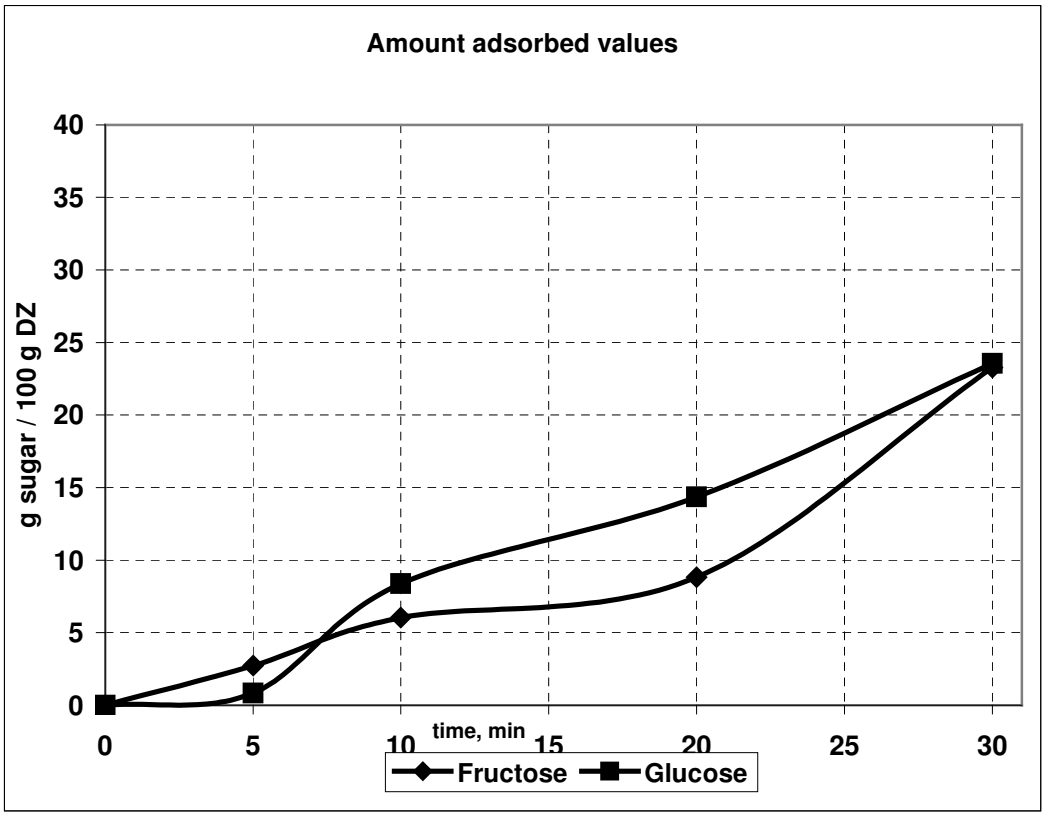

Figure 3.6 Adsorption Kinetics of Sugar Solutions (35 %w/v G + F) on H-Y zeolite

High total sugar amounts, i.e. 35% w/v glucose and 35% w/v fructose, did not show better results than 50% total, 25% w/v glucose and 25% w/v fructose solutions, and 40% total, 20% w/v glucose and 20% w/v fructose concentrations, with the zeolites.

Ca-Y zeolite had a good separation at minute 15, as fructose was adsorbed slowly around 6.7 g / 100 g DZ and glucose was adsorbed fast up to 17.6 g per 100 g dry zeolite levels, as seen on Figure 3.7. Though fructose was adsorbed about 28 g for 100 g dry zeolite, the difference between the amount adsorbed values got smaller and they ended up in equilibrium where glucose was adsorbed at 27 g per 100 g. dry zeolite.

Adsorption profiles on H-Y zeolite were not good. As seen on Figure 3.8, fructose adsorption rate did not change between 5^{th} and 20^{th} minutes and started to be adsorbed very fast between 20^{th} and 30^{th} minutes. But glucose again had a rather fast adsorption for the first 10 minutes and stayed at the constant adsorption rate between 10^{th} and 20^{th} minutes and then adsorbed very fast between 20^{th} and 30^{th} minutes.

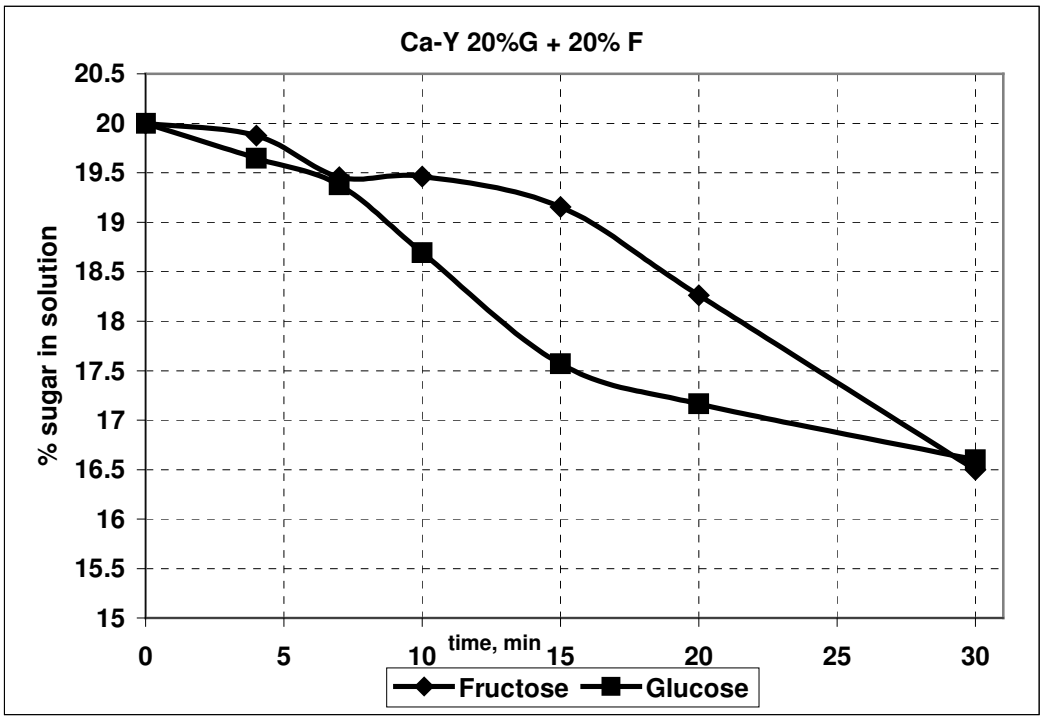

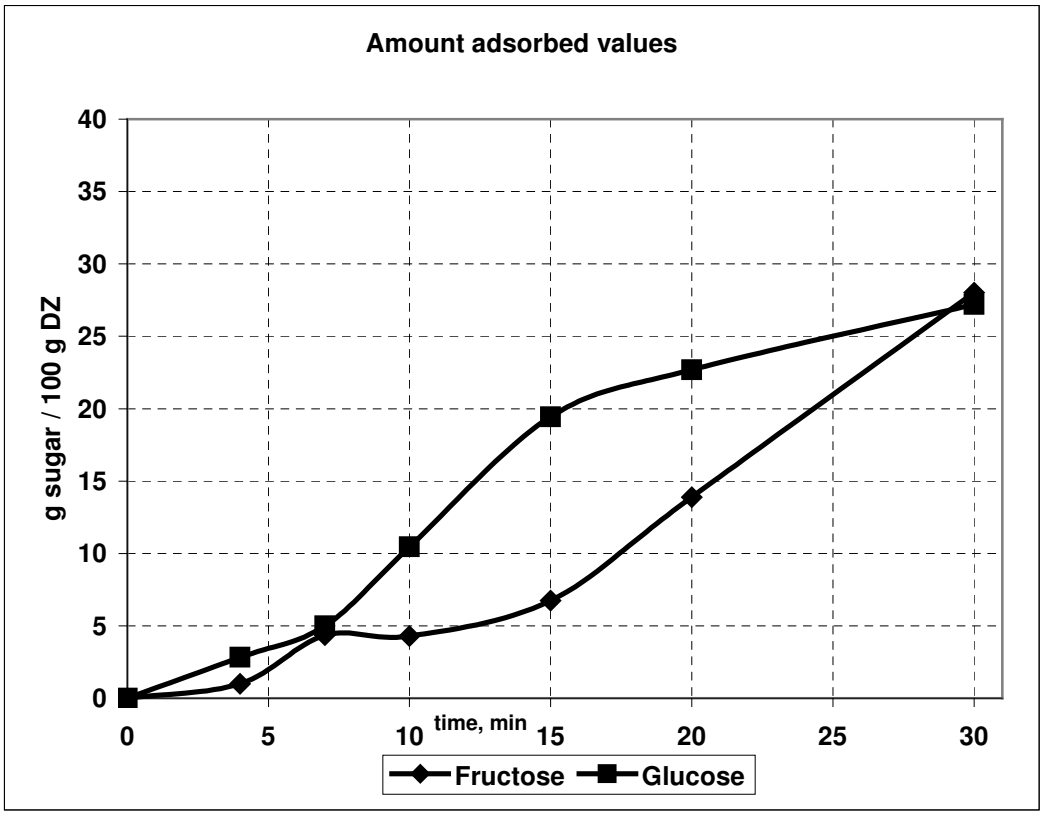

Figure 3.7 Adsorption Kinetics of Sugar Solutions (20 %w/v G + F) on Ca-Y zeolite

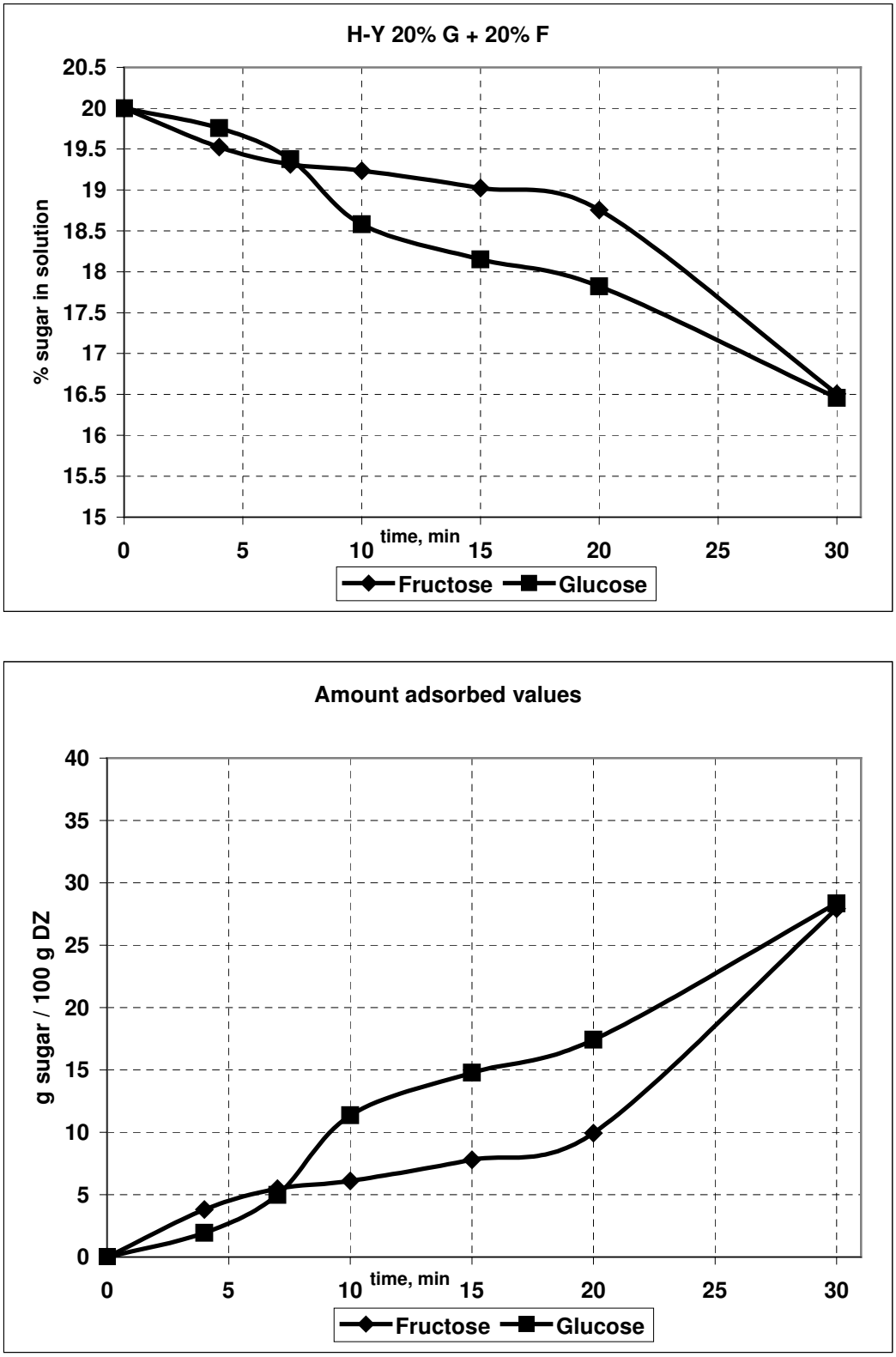

Figure 3.8 Adsorption Kinetics of Sugar Solutions (20 %w/v G + F) on H-Y zeolite

There was a great difference between the adsorption rates of 35 % w/v glucose-fructose mixtures and 20 % w/v mixtures. 30 % w/v mixtures were also observed, to understand the trend of the rates.

On Figure 3.9, the adsorption profile of 30% w/v glucose and fructose mixture solutions treated with Ca-Y zeolite was plotted. Until 10^{th} minute of the experiment, glucose and fructose adsorption profiles were increasing. Glucose started with a fast adsorption rate, which was followed by a slower rate. On the other hand, adsorption rate of fructose started slowly and increased from 9 g. / 100 g dry zeolite to 32.7 g. / 100 g dry zeolite at the 30^{th} minute.

As seen on Figure 3.10, glucose was adsorbed fast until it started a lag phase between 15^{th} and 20^{th} minutes on H-Y zeolite. Fructose was also adsorbed more than the previous studies. Ca-Y zeolite adsorbed fructose around 9 grams of fructose per 100 grams of dry zeolite when H-Y zeolite adsorbed fructose around 13 grams per 100 grams of dry zeolite.

At the end of experiments, glucose and fructose adsorptions were 32 grams of solution per 100 grams of dry zeolite for Ca-Y zeolite and 31 grams of solution per 100 grams of dry zeolite for H-Y zeolite. This showed us the separations between 15^{th} and 20^{th} minutes on Ca-Y zeolite and 15^{th} minute on H-Y zeolite.

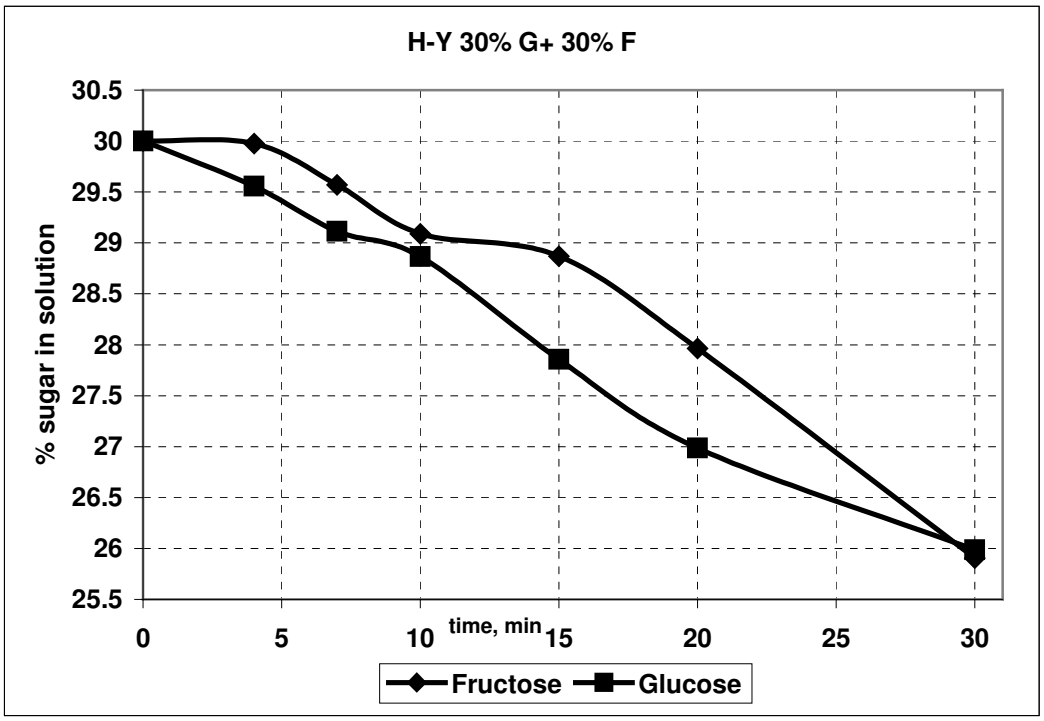

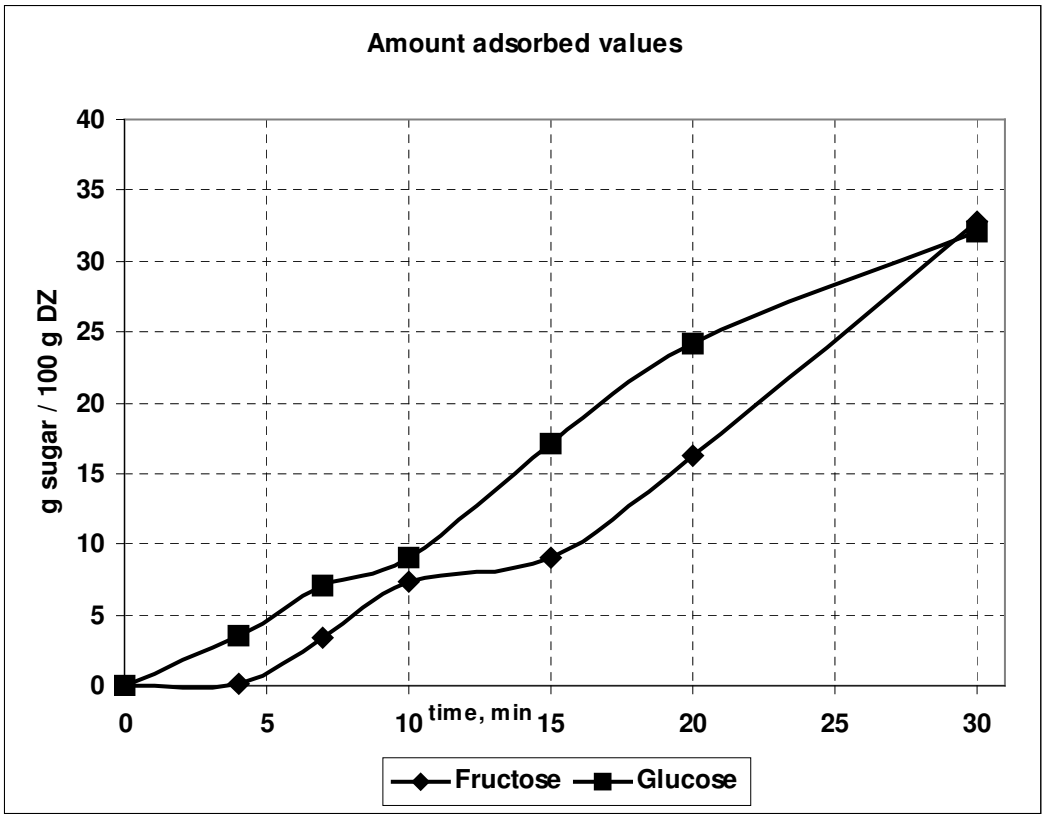

Figure 3.9 Adsorption Kinetics of Sugar Solutions (30 %w/v G + F) on Ca-Y zeolite

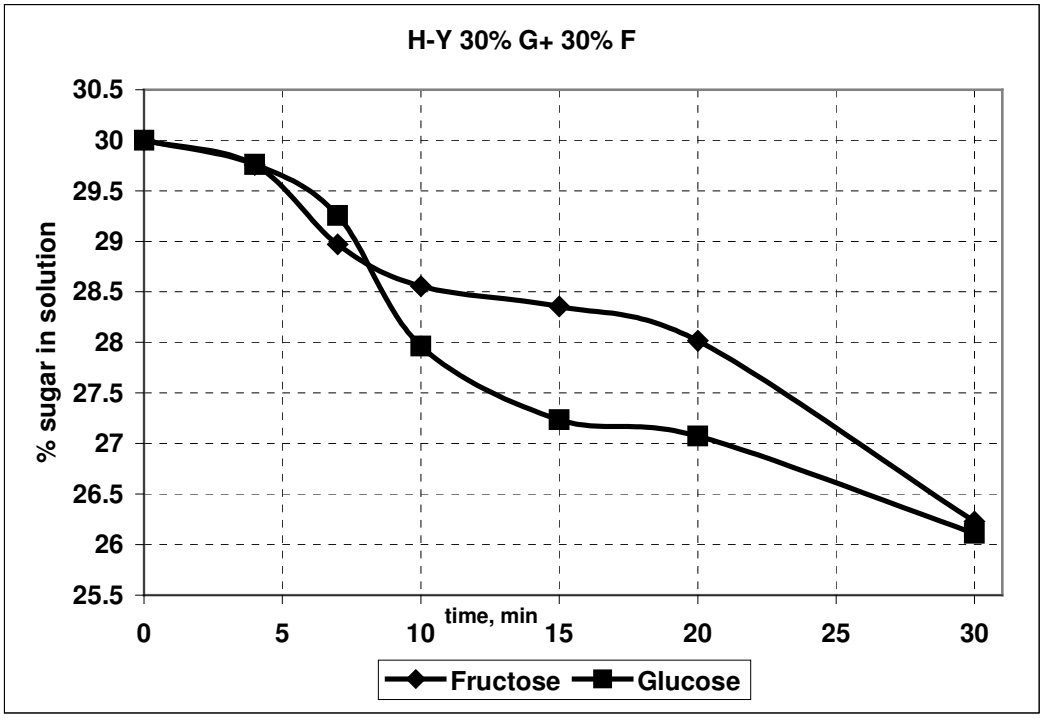

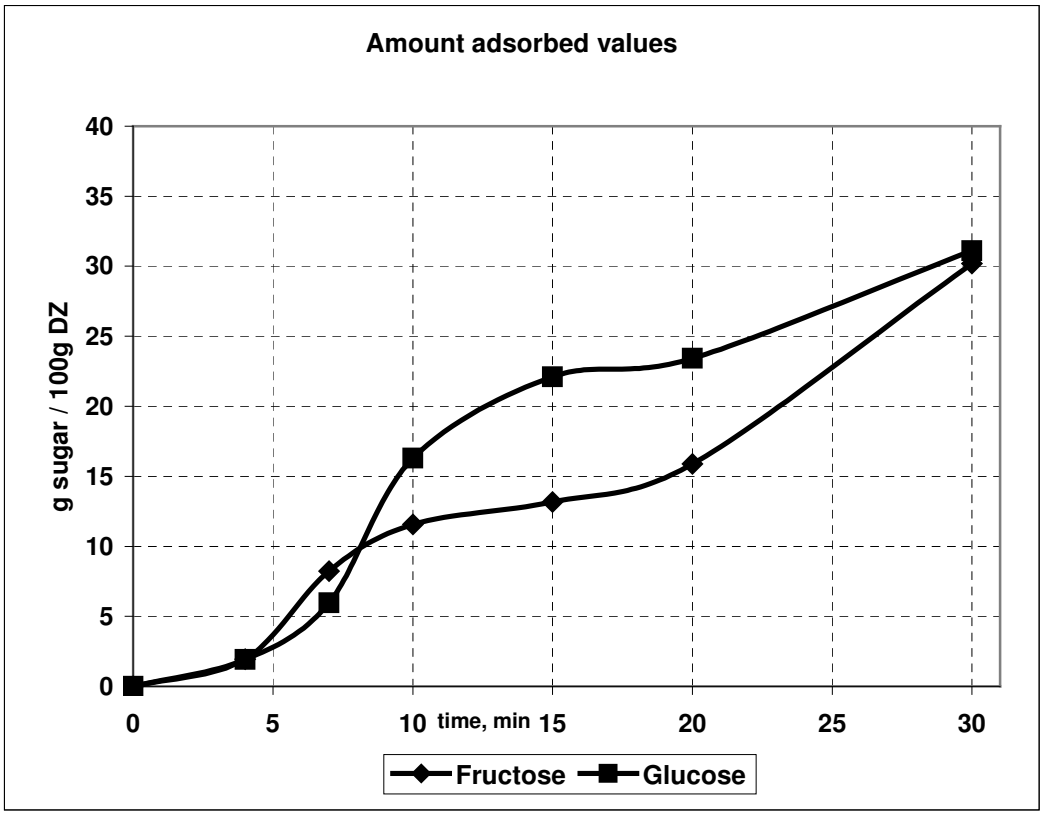

Figure 3.10 Adsorption Kinetics of Sugar Solutions (30 %w/v G + F) on H-Y zeolite

Non-equimolar mixtures of glucose and fructose were analyzed after equimolar solutions. 25 % w/v fructose - 35 % w/v glucose solutions, and 35 % w/v fructose - 25 % glucose solutions were prepared.

25 % w/v fructose and 35 % w/v glucose solution mixture on Ca-Y zeolite did not make a big adsorption difference so showed a poor separation. Both glucose and fructose were adsorbed at very close amounts. They were adsorbed up to 7.7 g / 100 g dry zeolite levels and adsorption rates increased until minute 30. Though they increased their rate of adsorptions, there was not a big difference, which led to a poor separation at the end. The adsorption curve was plotted on Figure 3.11

H-Y zeolite results different. Here, glucose was adsorbed nearly at a linear rate, increasing up to 22.7 g / 100 g dry zeolite levels. Fructose was adsorbed in the first 10 minutes and in the next ten minutes; there was almost no adsorption. The rate of adsorption increased from 9.8g /100 g dry zeolite to 29.6 g /100 g dry zeolite until 30^{th} minute, as seen on Figure 3.12. At the end of 30^{th} minute, the amount-adsorbed values were different; they did not reach the equilibrium.

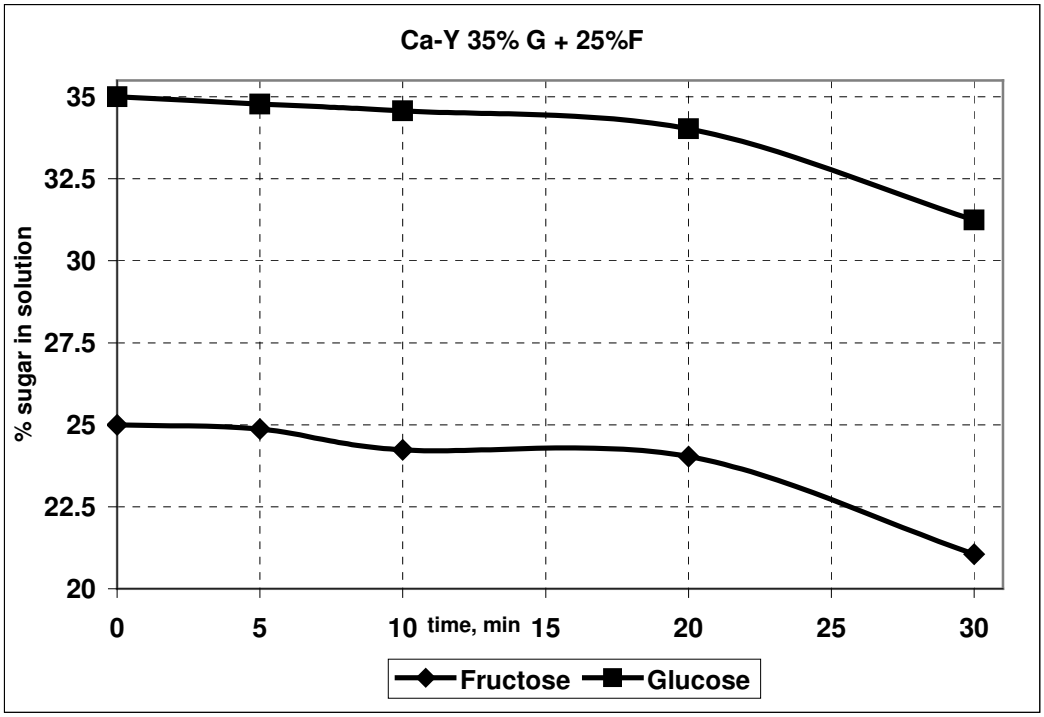

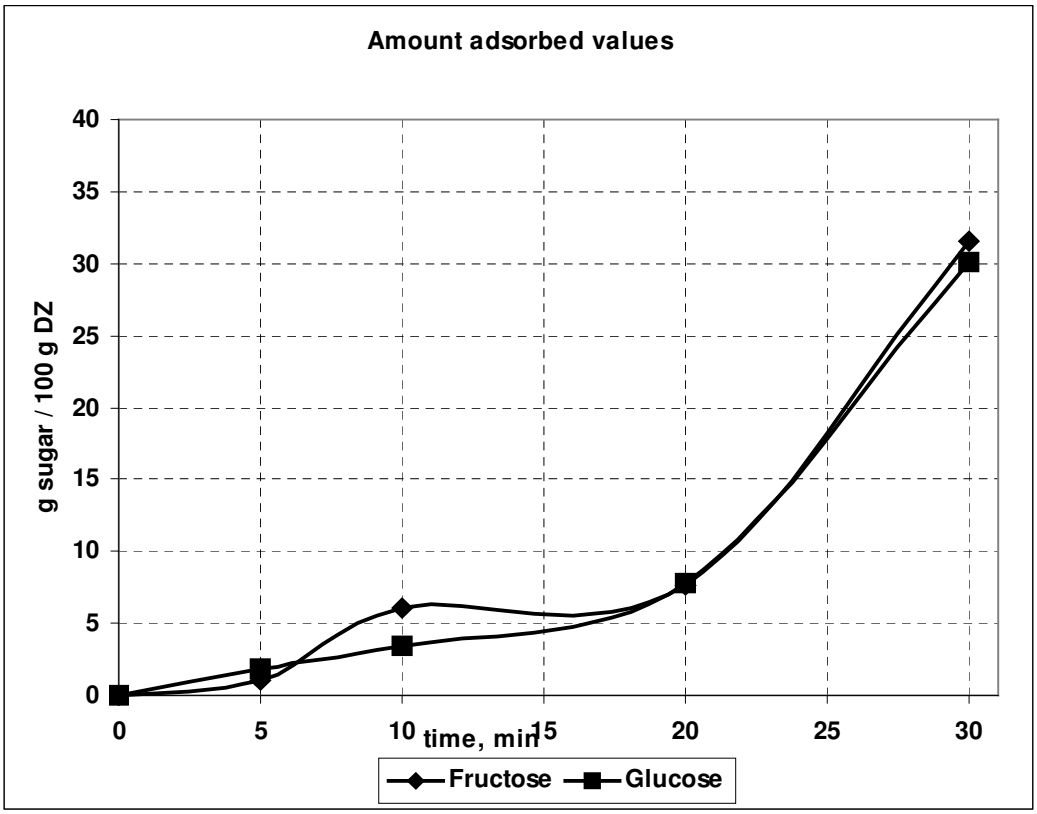

Figure 3.11 Adsorption Kinetics of Sugar Solutions (25% w/v F + 35% w/v G) on Ca-Y zeolite

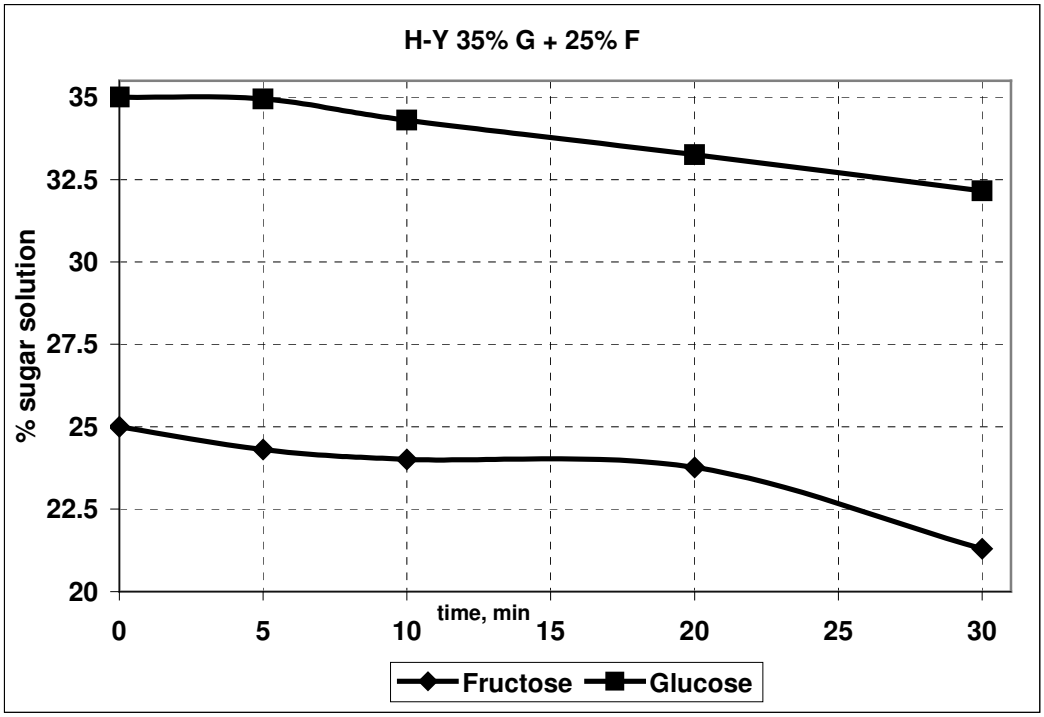

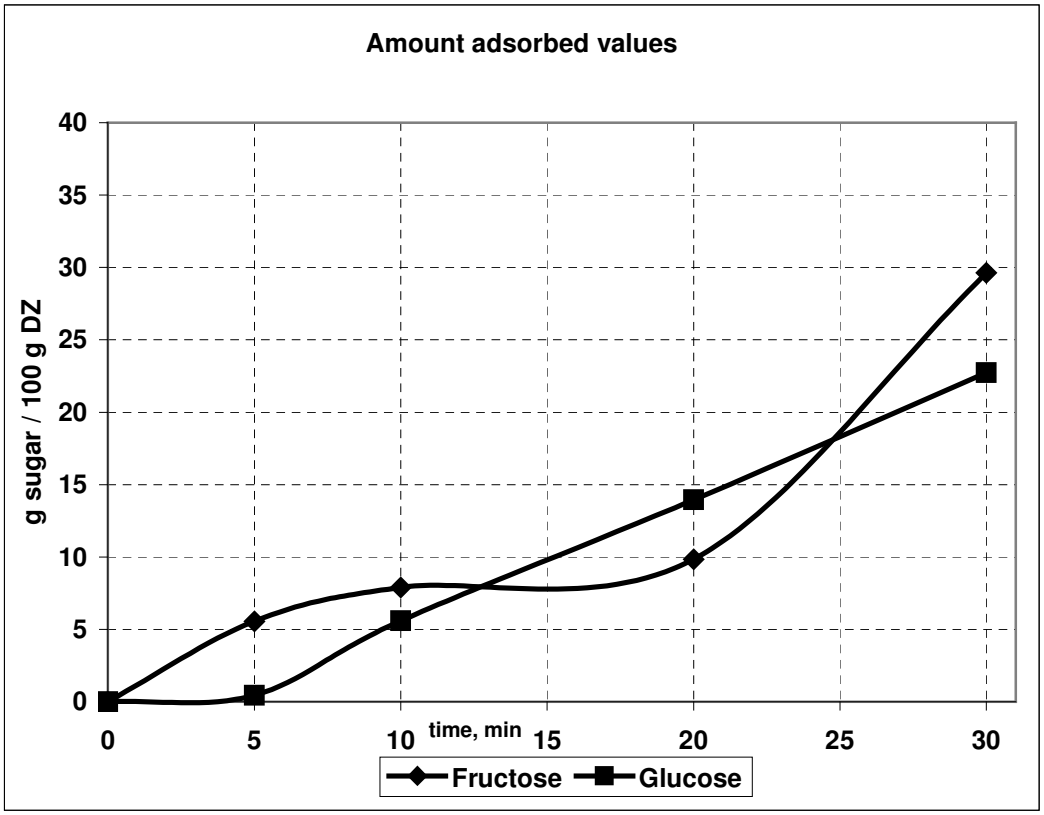

Figure 3.12 Adsorption Kinetics of Sugar Solutions (25% w/v F + 35% w/v G) on H-Y zeolite

Non-equimolar mixture of 25% w/v glucose and 35% w/v fructose concentrations had a good separation on Ca-Y zeolite with an adsorption difference as high as 17.6 g sugar per 100 g dry zeolite at minute 20. The rate of adsorption of fructose was very slow in the first 20 minutes when the glucose adsorption rate was increasing continuously.

H-Y zeolite showed, contrarily, increasing adsorption rates for both glucose and fructose, but this parallel behavior led to a poor separation at the end. Figure 3.13 shows the adsorption rates of the solutions on Ca-Y zeolite and Figure 3.14 on H-Y zeolite.

Next, 20 % w/v fructose - 30% w/v glucose concentration solution was observed on zeolites. There seemed a better separation compared to 25 % w/v fructose and 35 % w/v glucose concentration solutions. On Ca-Y treatments, the adsorption profiles were parallel, keeping the difference from the beginning, and the best separation could be mentioned at minute 20, where glucose was adsorbed about 22.1 g / 100 g DZ, and fructose was adsorbed about 13.3 g / 100 g DZ, as seen on Figure 3.15

H-Y zeolite treated samples showed again a different profile, i.e. fructose was adsorbed more and then started declining where the glucose adsorption was increasing. The separation zone was between 10^{th} and 20^{th} minutes; where the difference between the adsorption rates was about 10 g / 100 g DZ for the 10^{th} minute and 13.5 g / 100 g DZ for the 20^{th} minute. Their adsorptions at minute 30 were 30.4 g / 100 g dry zeolite and 25.18 g /100 g dry zeolite for glucose and fructose respectively, as seen on Figure 3.16.

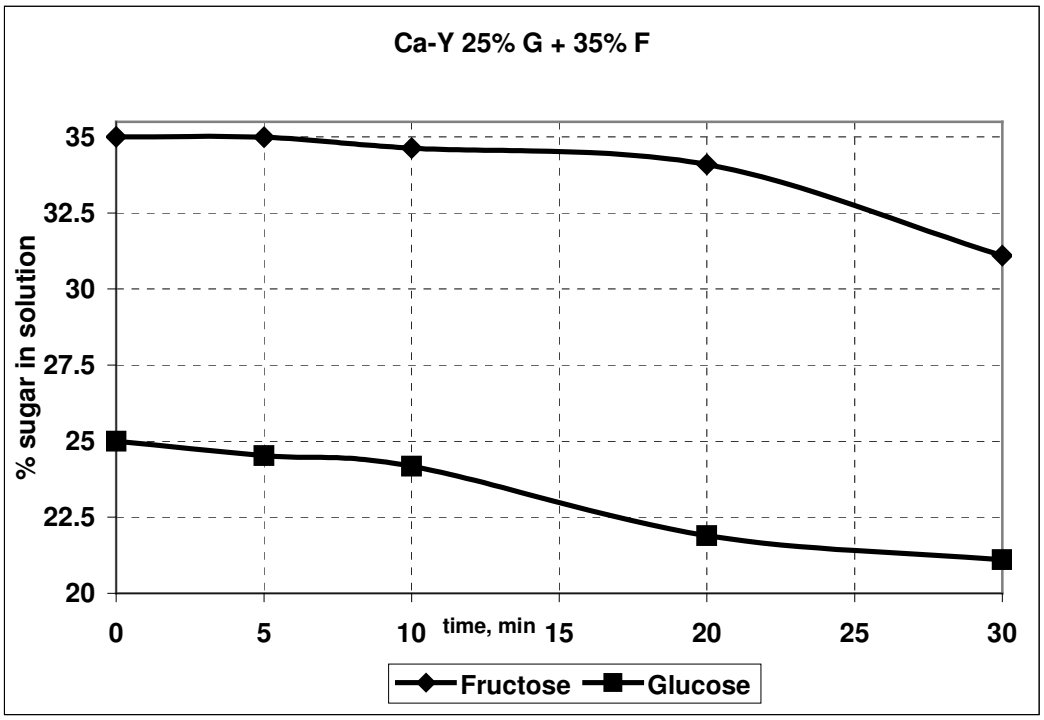

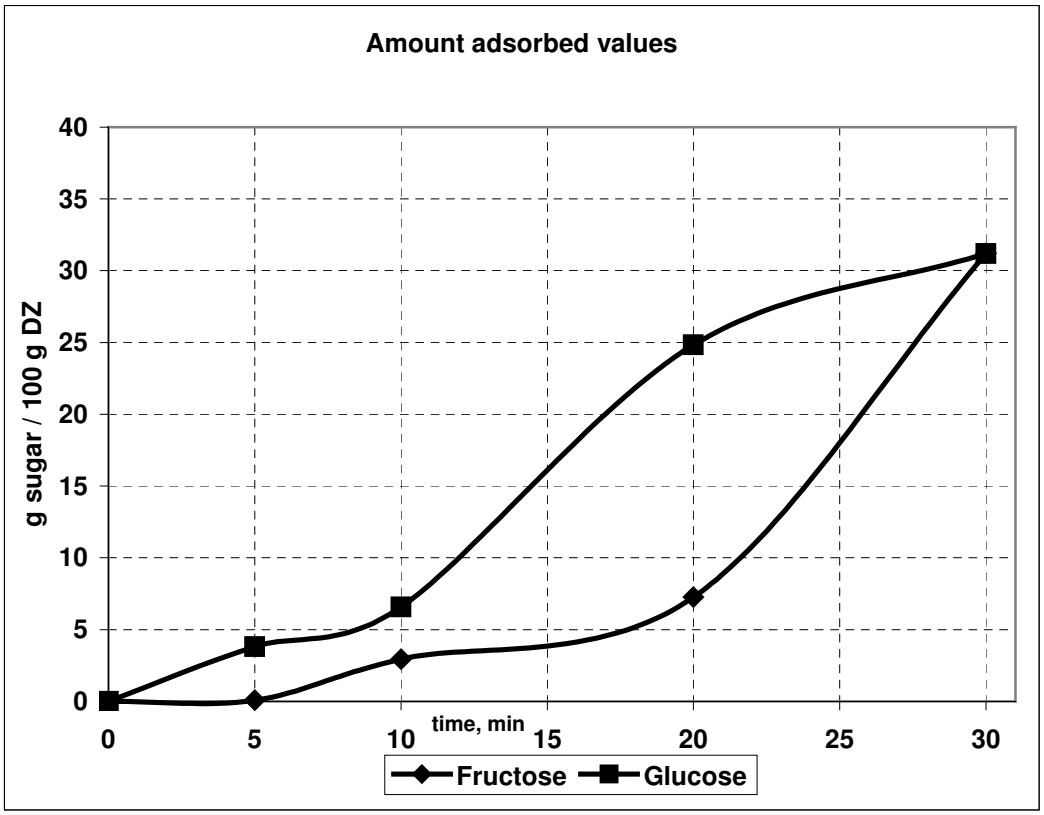

Figure 3.13 Adsorption Kinetics of Sugar Solutions (35% w/v F + 25% w/v G) on H-Y zeolite

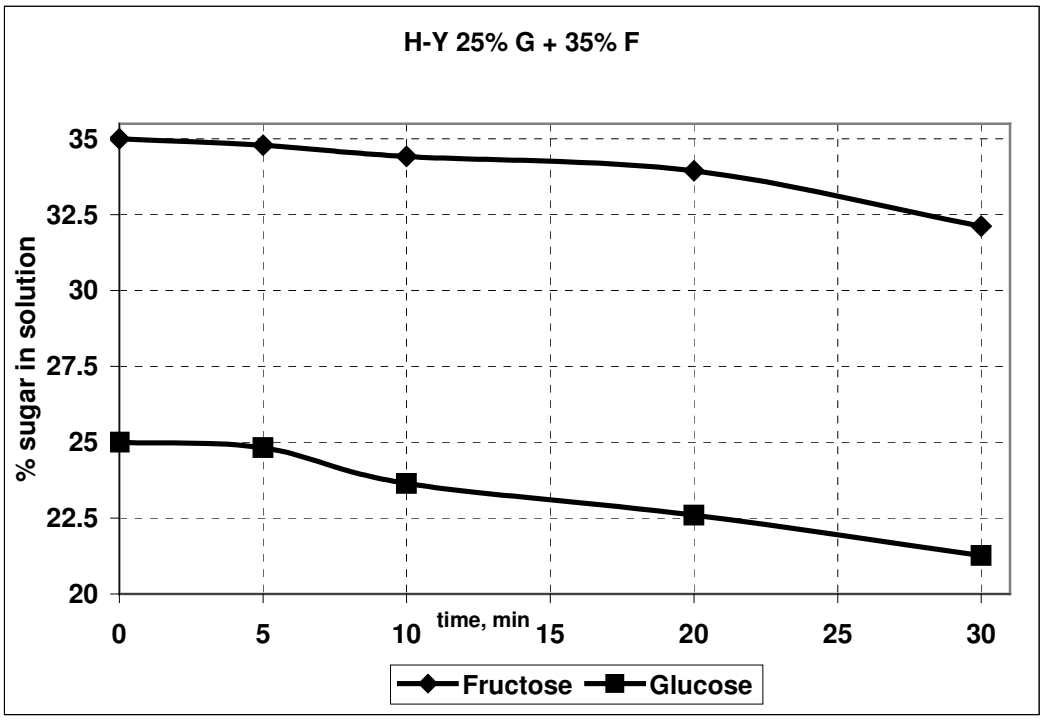

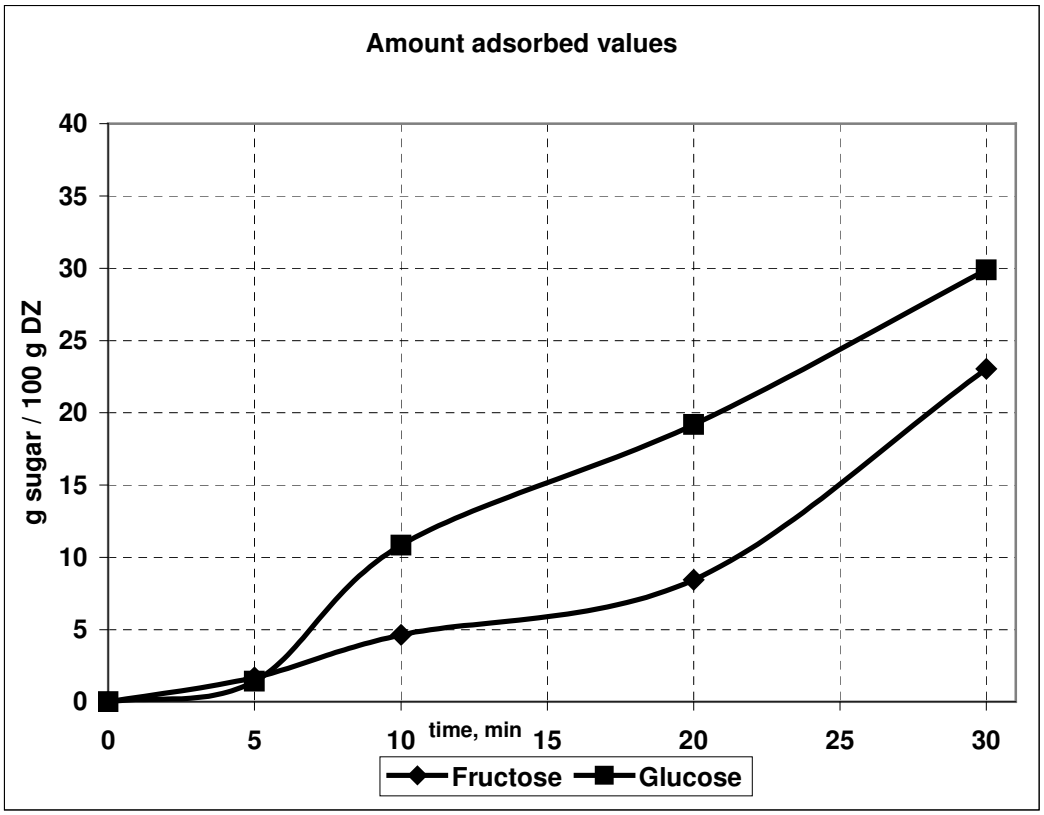

Figure 3.14 Adsorption Kinetics of Sugar Solutions (35% w/v F + 25% w/v G) on H-Y zeolite

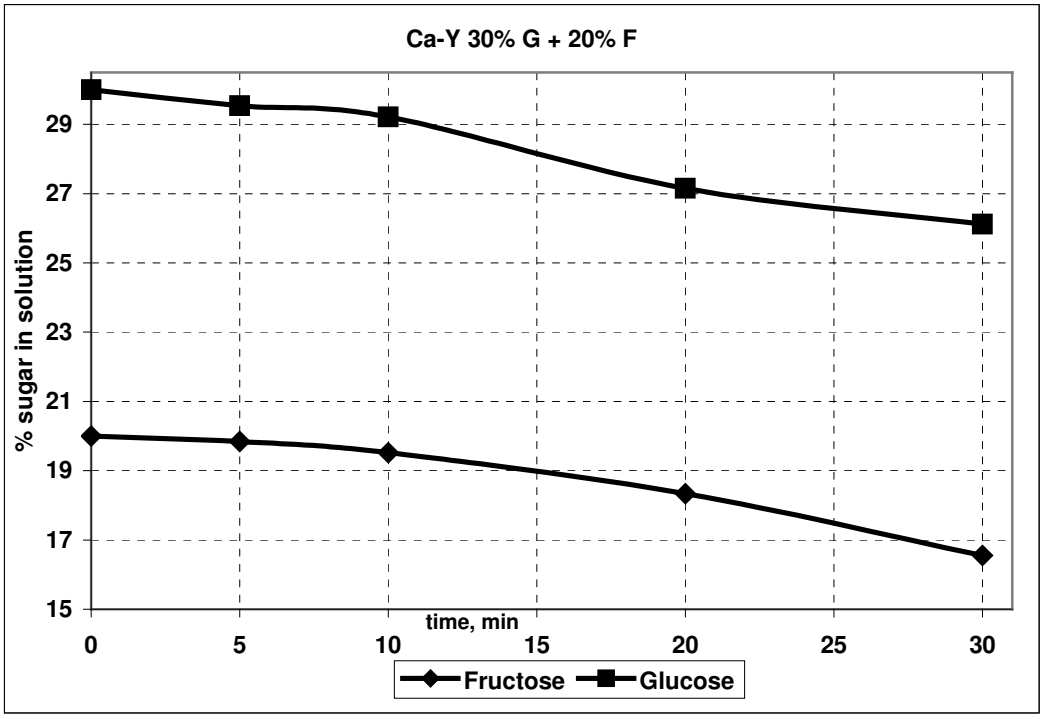

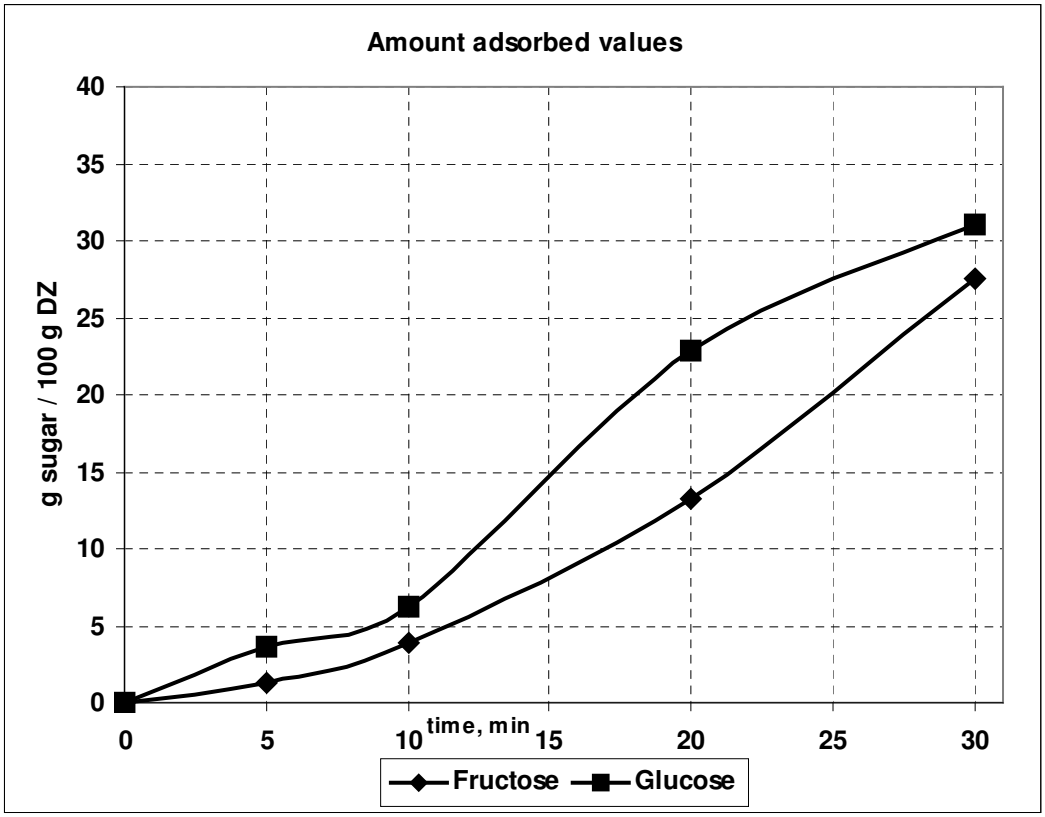

Figure 3.15 Adsorption Kinetics of Sugar Solutions (20% w/v F + 30% w/v G) on Ca-Y zeolite

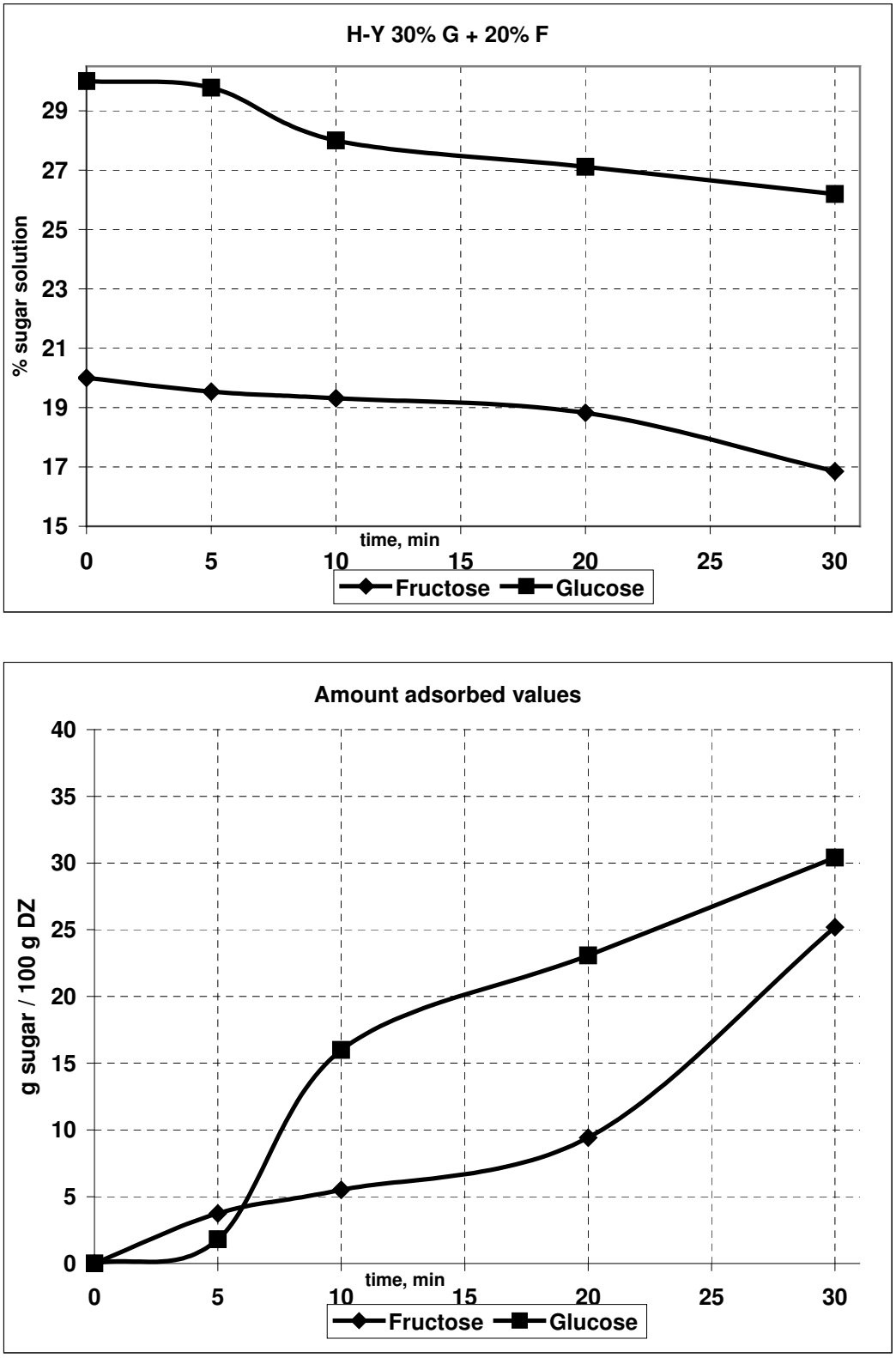

Figure 3.16 Adsorption Kinetics of Sugar Solutions (20% w/v F + 30% w/v G) on H-Y zeolite

30 % w/v fructose and 20 % w/v glucose solutions did not demonstrate acceptable separations on Ca-Y and H-Y zeolites. On Ca-Y zeolite, the adsorption rates of either fructose or glucose processed parallel, keeping the difference between their adsorption rates. The situation changed at minute 25 when fructose adsorption rate started to increase. This did not show a desired separation profile, as shown on Figure 3.17.

The adsorption rates of the solution 30% w/v fructose and 20% w/v glucose were also parallel to each other during their process. There was almost no separation in spite of the increasing adsorption rates for both glucose and fructose. Figure 3.18 shows the amount-adsorbed values of the solution on H-Y zeolite.

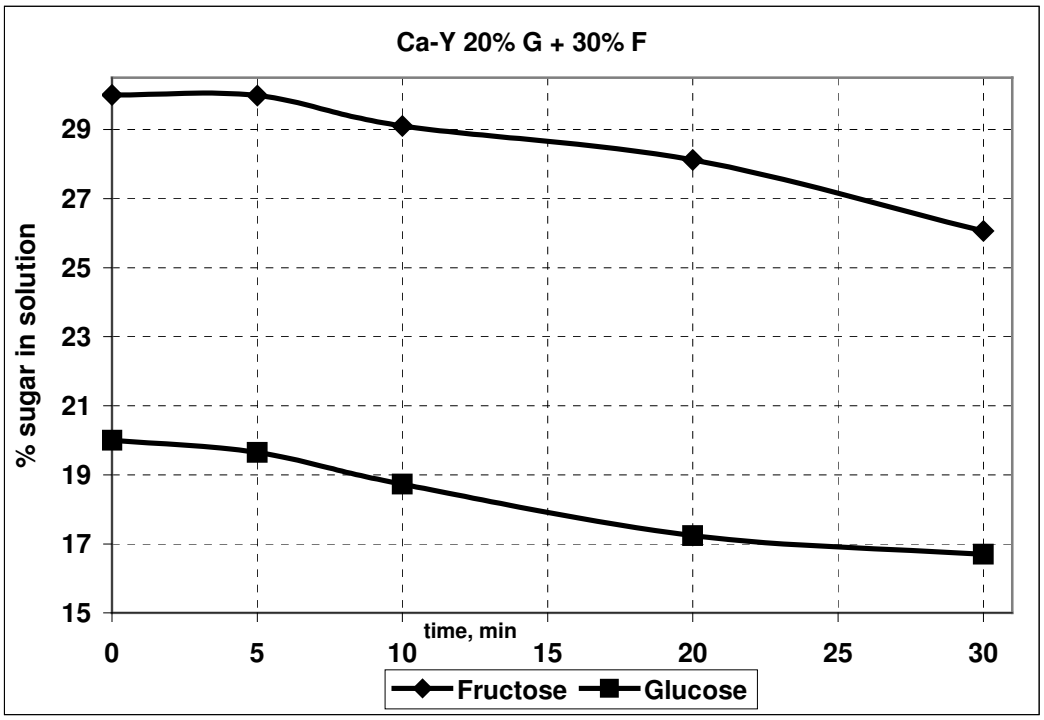

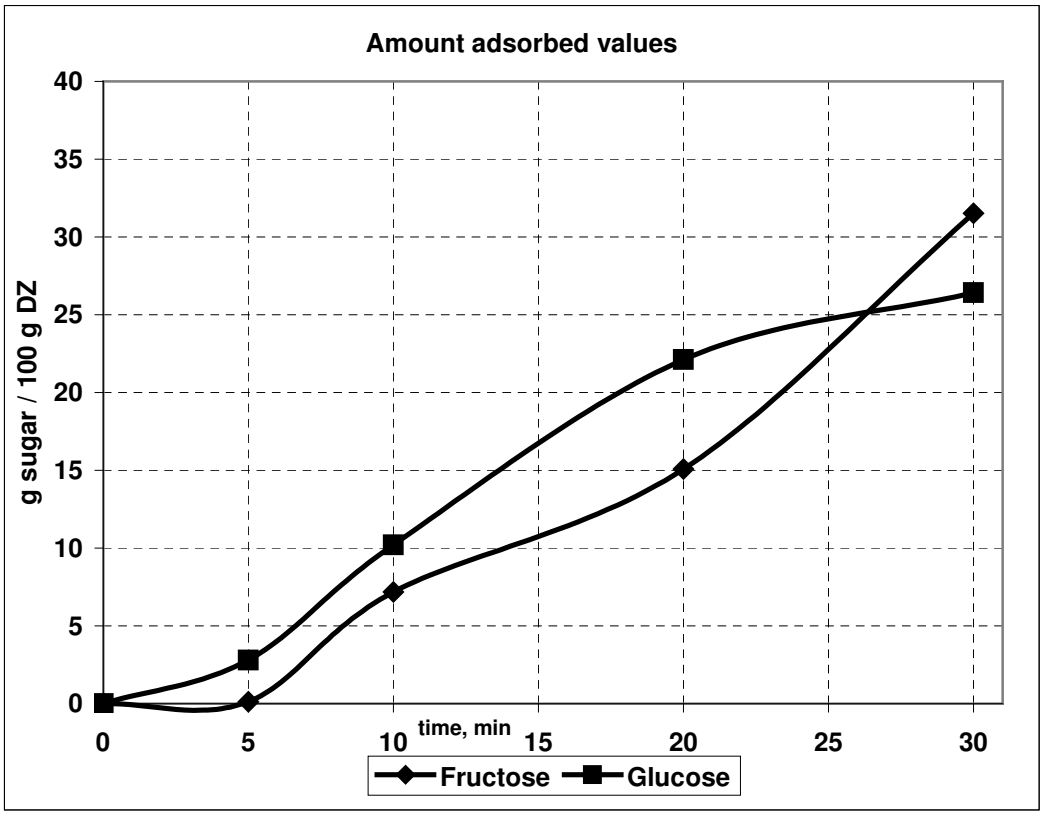

Figure 3.17 Adsorption Kinetics of Sugar Solutions (30% w/v F + 20% w/v G) on Ca-Y zeolite

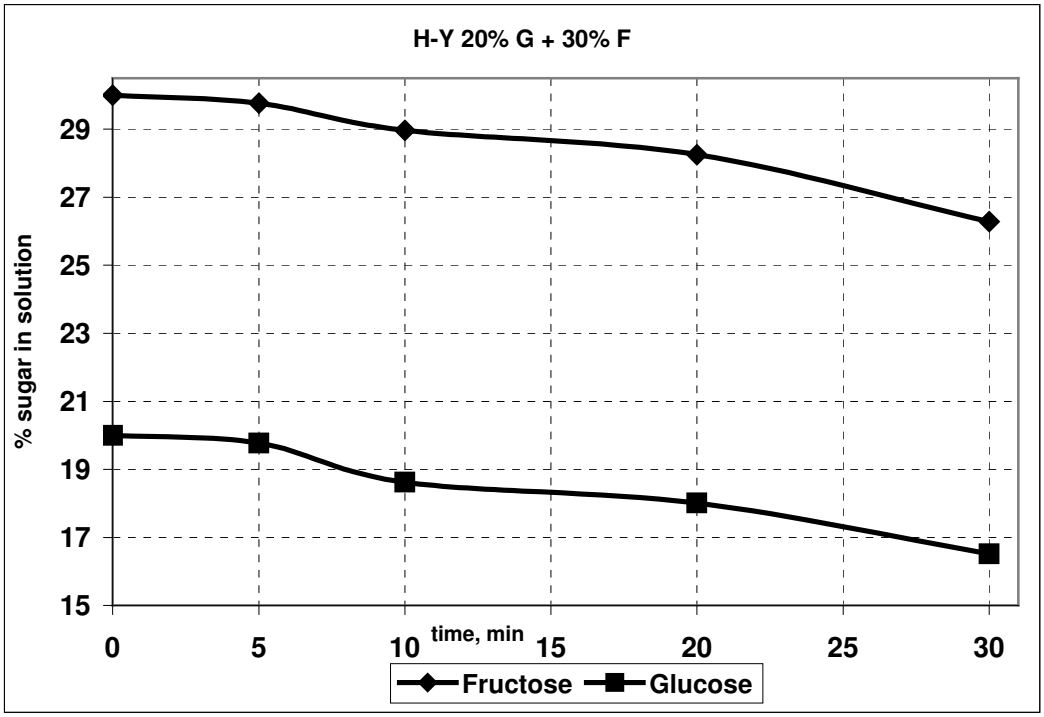

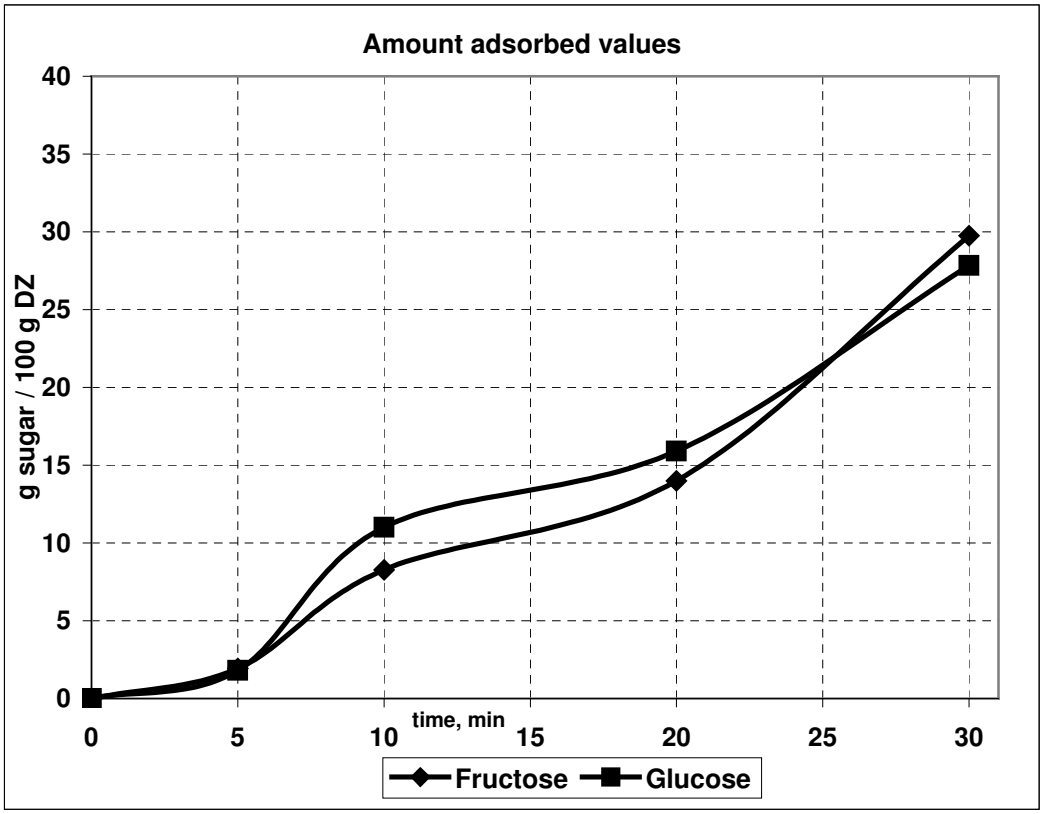

Figure 3.18 Adsorption Kinetics of Sugar Solutions (30% w/v F + 20% w/v G) on H-Y zeolite

The common thing seen on the results was the fast adsorption of glucose on both zeolites and for almost all solutions, except the mixtures which did not show any difference between glucose and fructose rate of adsorption values. Adsorption of fructose was slow, compared to glucose and followed a linear trend for both zeolites and almost all solutions.

The adsorption rates of the solutions at 30^{th} and 60^{th} minutes of the experiments were plotted for comparison. The results were analyzed according to the glucose and fructose amount-adsorbed values for both of the zeolites. The equimolar mixtures of 12.5 %, 20 %, 25 %, 30 % and 35 % w/v solutions were taken on the graphs. It was clear on the graphs that amount adsorbed values were increasing in the first 20 minutes and then started decreasing or stayed linear; except for the fructose rate of adsorption at 60^{th} minute, which had a continuously increasing curve even at the concentrations of 35 % w/v solutions.

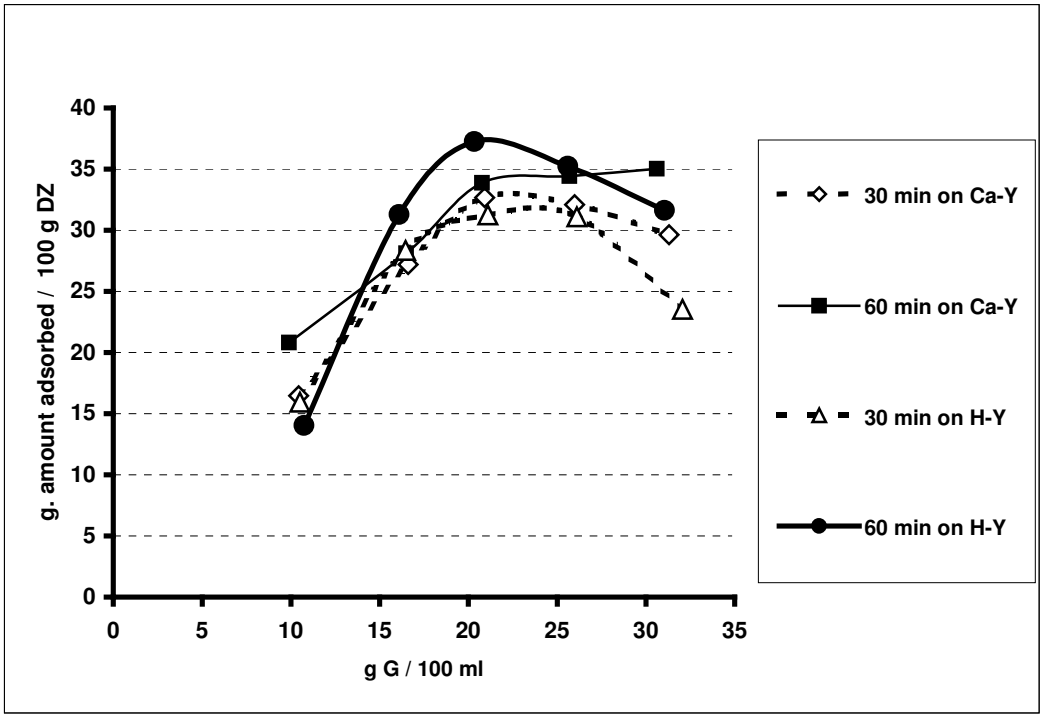

Figure 3.19 Glucose adsorption graphs at 30th and 60th minutes with the equal initial concentration mixtures.

As seen in Figure 3.19, the adsorption rate of glucose for minute 30 was favorable, but curve went downward after 25 % w/v mixture solution, which had 20.91 % w/v glucose in it. Increasing the concentration amounts decreased the amount-adsorbed values for the solutions, which had initial glucose concentrations of 30 and 35 % w/v. The adsorption rates of the same solutions were different for 60th minute on the same zeolites. 25% w/v glucose and fructose mixture, had 20.77 % w/v glucose concentration at minute 60 and the adsorption rate did not decreased; instead increased up to 35 grams of glucose per 100 grams of dry zeolite. The increased values of rate of adsorption could be mentioned after 60 minutes of treatment and the best values found for the Ca-Y zeolite were the glucose and fructose mixtures, having initially 25 % w/v concentrations.

The same solutions had a different tendency towards H-Y zeolite. The adsorption rate results plotted as parabolic curves with the peak values for 25 % w/v initial amount concentrations for glucose. Increasing the concentration decreased the adsorption of glucose after an extent. Also, for 25 % and 30 % initial concentration solutions, at the minute 30, the amount-adsorbed values were very close. Increasing the duration of treatment with zeolite did not change the adsorption behavior, which showed, higher concentrations did not show better adsorptions than 25% w/v initial concentration mixtures.

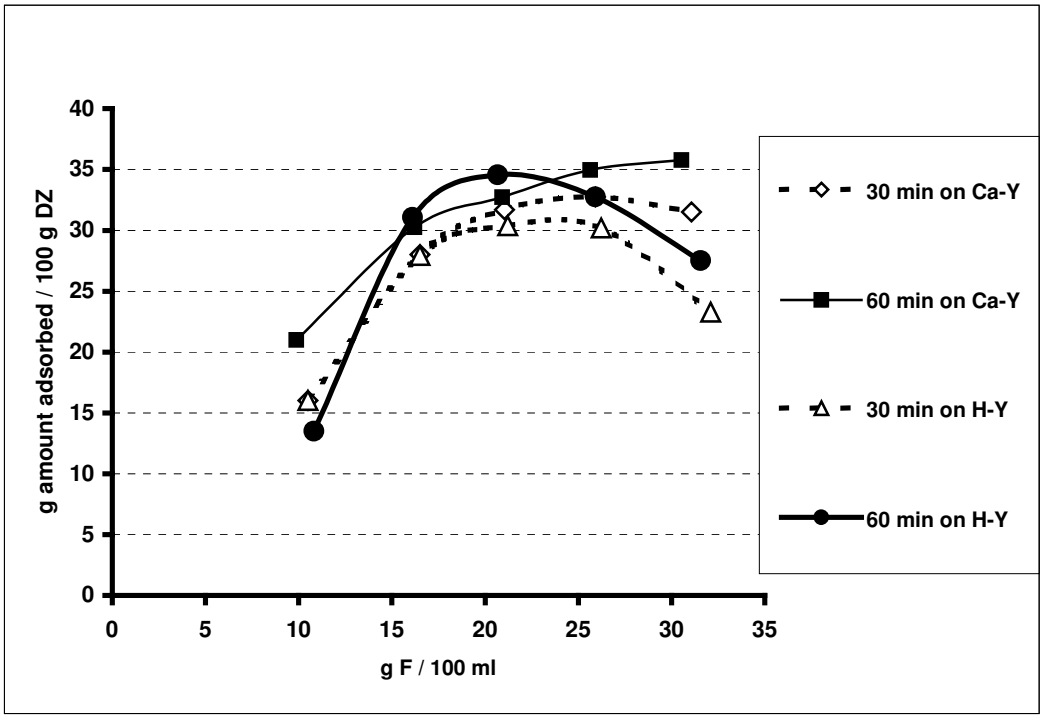

Figure 3.20 Fructose adsorption graphs at 30th and 60th minutes with the equal initial concentration mixtures.

Fructose adsorption rates were similar to adsorption rates of glucose on Ca-Y zeolite. On Figure 3.20, adsorption rates of equimolar mixtures were plotted. The results were

acceptable compared to glucose adsorption rates, which were increasing with the increasing fructose concentrations of the mixtures.

Rate of adsorption graphs for H-Y zeolite were parabolic. The highest values were the initially 25% w/v concentration mixture values. A breaking point was seen afterwards. The solid phase was adsorbed due to the H bonding. More sugar molecules were getting interacted with each other and the newly added sugar took off the adsorbed sugar. Considering all the isotherms, the best adsorption rate curve was for glucose adsorption on Ca-Y zeolite for 30 and 60 minutes and also on the fructose side, fructose adsorption on Ca-Y zeolite. This showed us that Ca-Y zeolite had an acceptable adsorption profile compared to H-Y zeolite. H-Y zeolite showed parabolic rate of adsorption profiles.

The curve fitting was not performed on those adsorption graphs; the graphs were decreasing with increasing concentrations due to the sugar-sugar interactions with each other. It is possible to continue the experiments after diluting the mixtures

The rate of adsorption data of the solutions including the non-equimolar sugar concentrations were plotted for Ca-Y and H-Y zeolites as Figure 3.21 for 30^{th} minute, Figure 3.22 for 60^{th} minute, Figure 3.23 for 30^{th} minute, Figure 3.24 for 60^{th} minute,

The common thing was the similar dispersion of non-equimolar solutions with the equimolar mixtures; if there was a breaking point or equilibrium, both equimolar and non-equimolar mixtures had the same trends, as seen on the Figures 3.21, 3.22, 3.23, and 3.24.

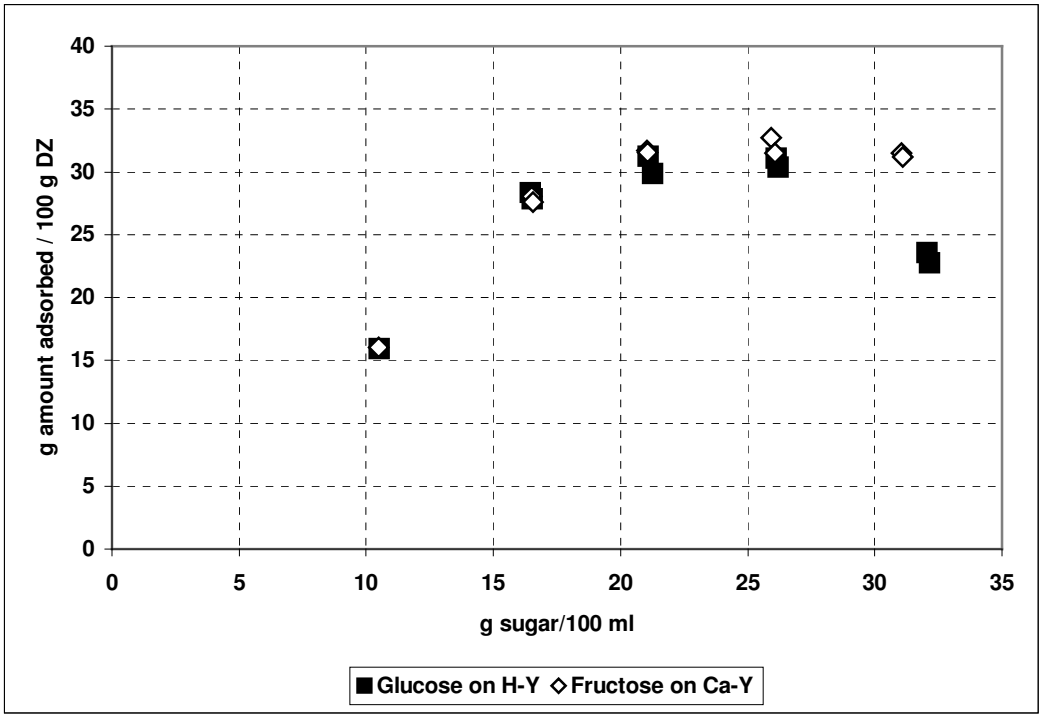

Figure 3.21 Adsorptions of all solutions at 30th minute on Ca-Y zeolite.

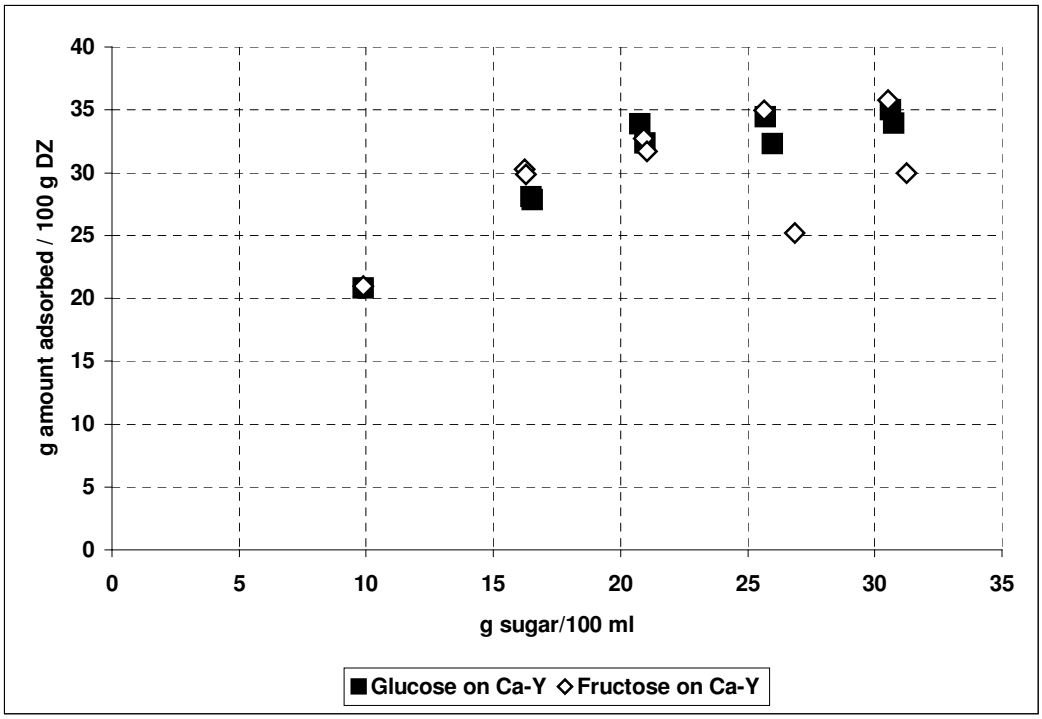

Figure 3.22 Adsorptions of all solutions at 60th minute on Ca-Y zeolite

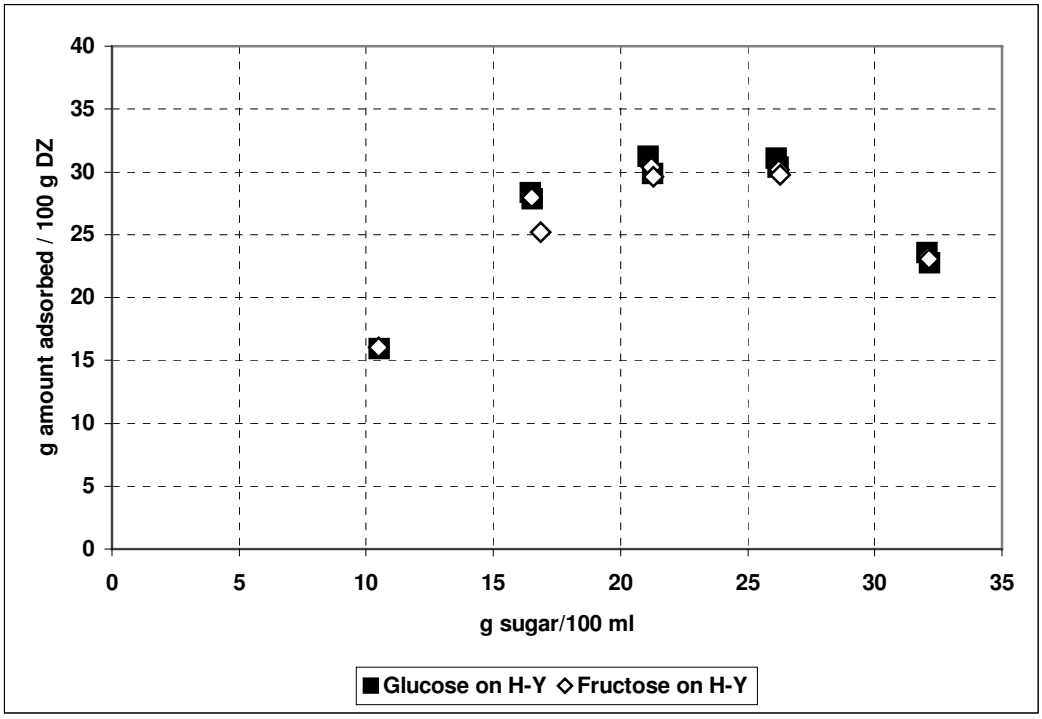

Figure 3.23 Adsorptions of all solutions at 30th minute on H-Y zeolite.

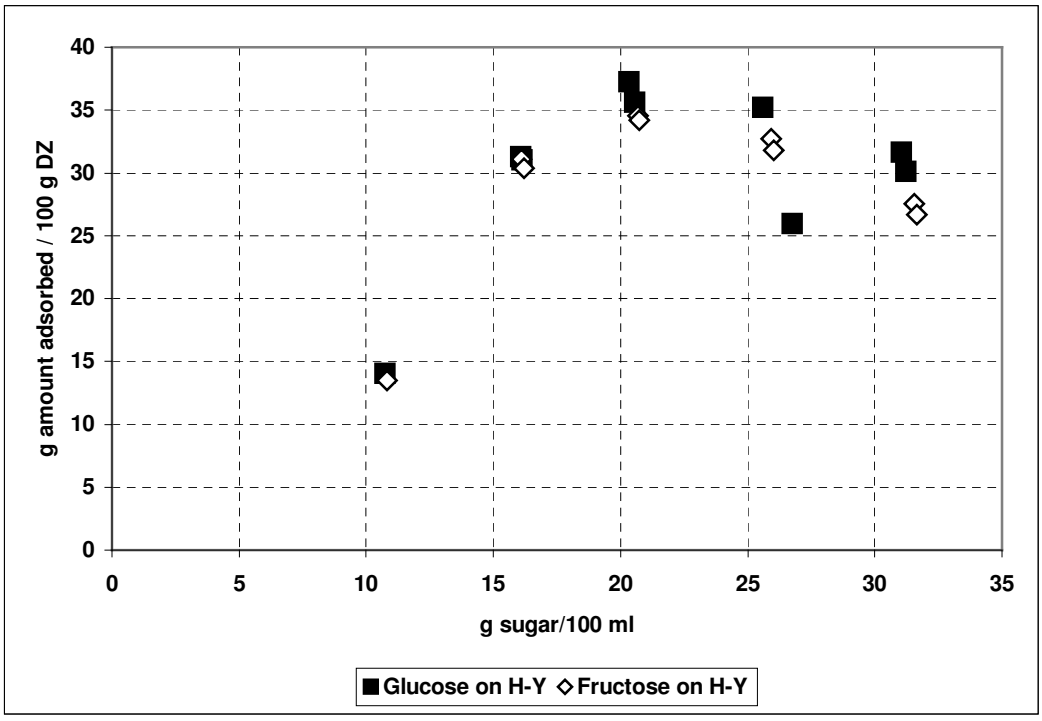

Figure 3.24 Adsorptions of all solutions at 60th minute on H-Y zeolite.

After the adsorption graphs, Ca-Y and H-Y zeolites were observed for glucose versus fructose amount adsorbed values, as 50 % and 60 % sugar mixtures. 25 % w/v G+25 % w/v F, 20 % w/v G+30 % w/v F w/v and 30 % w/v G+20 % w/v F w/v mixtures were observed for 50 % total sugar concentration and 30 % w/v G+30 % w/v F, 25 % w/v G+35 % w/v F, and 35 % w/v G+25 % w/v F mixtures were observed for 60 % total sugar concentrations.

Figure 3.25 and 3.26 depicts the 50 % sugar concentrations for the zeolites.

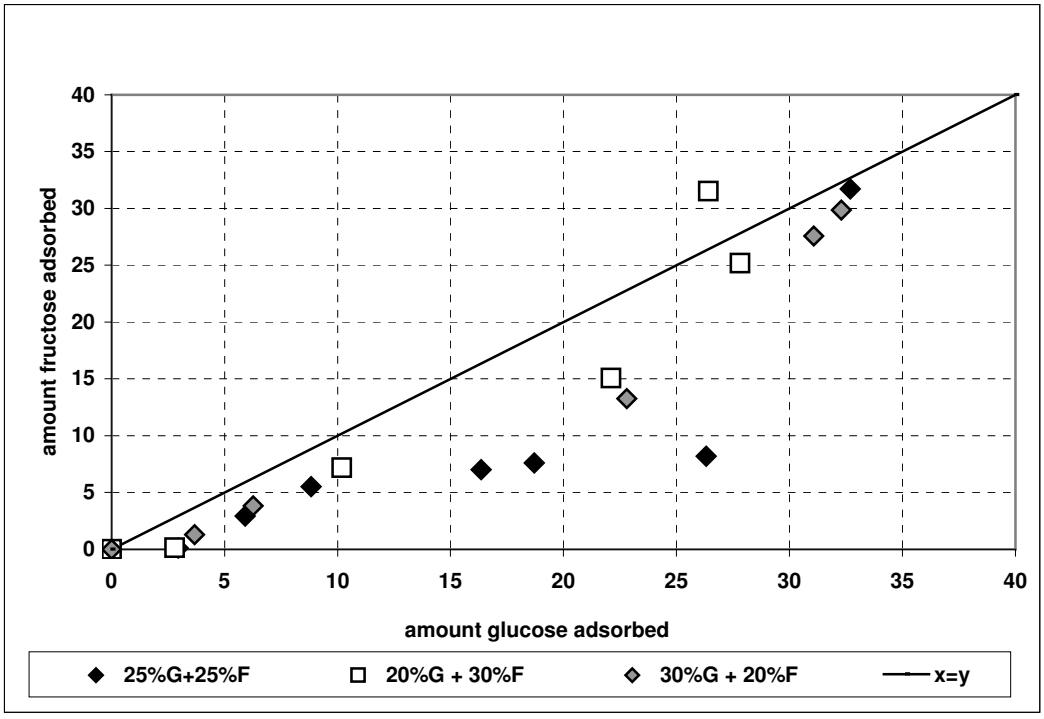

Figure 3.25 Amount adsorbed values of glucose versus fructose on Ca-Y zeolite in 50% total sugar solutions

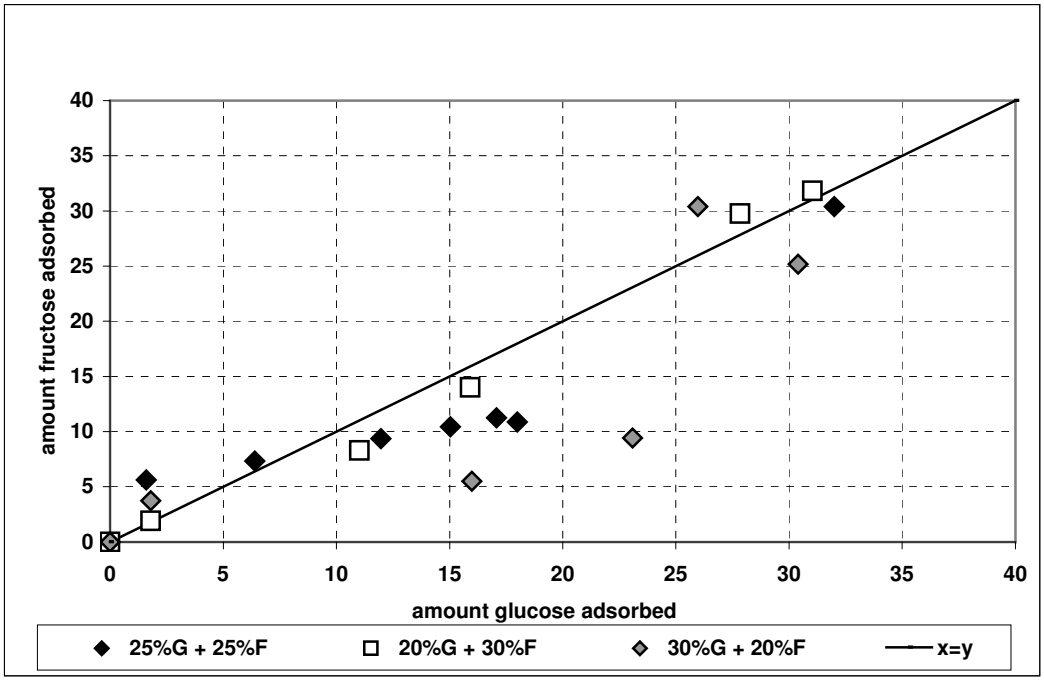

Figure 3.26 Amount adsorbed values of glucose versus fructose on H-Y zeolite in 50% total sugar solutions

The data, which were at the glucose side for 50 % mixture, were seen with a few points at the lag time and between 25th and 30th minutes on fructose side. This showed that glucose was adsorbed more than fructose on for 50% total sugar concentrations.

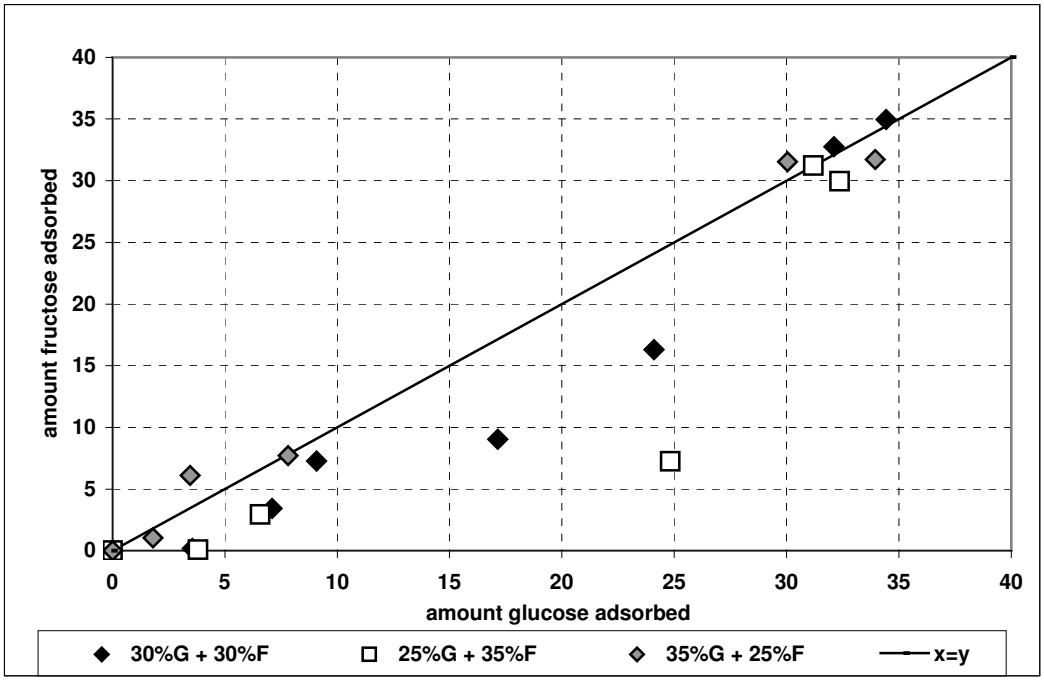

Figure 3.27 Amount adsorbed values of glucose versus fructose on Ca-Y zeolite in 60% total sugar solutions

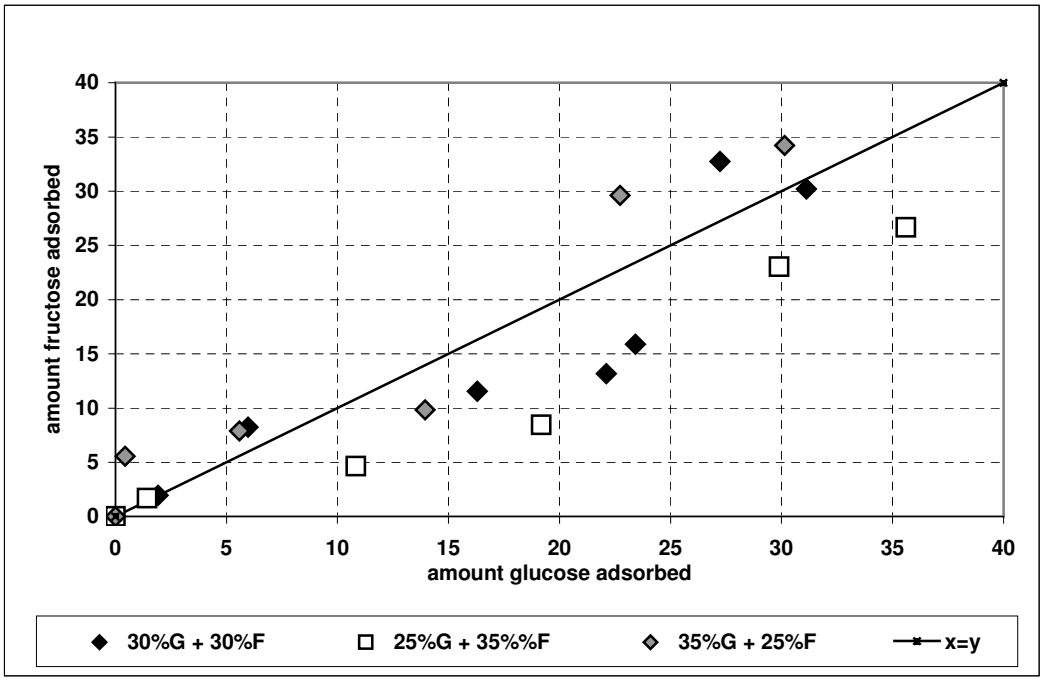

Figure 3.28 Amount adsorbed values of glucose versus fructose on H-Y zeolite in 60% total sugar solutions

As seen on Figure 3.27 and Figure 3.28, glucose adsorption rate was again greater but there were more points passing to the fructose side. This showed that, after a certain concentration like 60%, fructose started to be adsorbed more than glucose. Changing the glucose concentrations from 25 % to 30 % and then to 35 %, there occurred a grouping between each other, which decreased glucose adsorption and switched the points to the fructose side.

For Ca-Y zeolite, glucose trend was towards the higher glucose concentrations, on the contrary of H-Y zeolite, which had a trend towards the lower glucose concentration in the solutions.

More calculations were performed for indication of separation. Table 3.1 shows the times when the separation started, when there was the maximum separation and when the separation ended. Table 3.2 shows the separation amounts in the given periods.

Table 3.1 Beginning time, maximum time and end time of separation

	Ca-Y ZEOLITE		
type of solution	separation point(min)	max separation(min)	end of separation(min)
12:5F+12.5G	10	20	30
25F+25G	10	20	30
35F+35G*	0	5	10
20F+20G	7	15	30
30F+30G	10	15	30
25F+35G*	10	20	30
35F+25G	10	20	30
20F+30G	10	20	30
30F+20G	0	20	27
	H-Y ZEOLITE		
type of solution	separation point(min)	max separation(min)	end of separation(min)
12:5F+12.5G	7	20	30
25F+25G	7	15	30
35F+35G*	7	20	30
20F+20G	7	15	30
30F+30G	7	15	30
25F+35G*	0	12	25
35F+25G	5	20	30
20F+30G	7	20	30
30F+20G	5	10	25

Table 3.2 Separation amounts for the given times in Table 3.1
[amount glucose adsorbed-amount fructose adsorbed]

	Ca-Y ZEOLITE		
type of solution	separation point(min)	max separation(min)	end of separation(min)
12:5F+12.5G	0.38	9.15	0.44
25F+25G	3.32	18.13	0.98
35F+35G*	0	2.35	0.01
20F+20G	0.64	12.70	-0.82
30F+30G	1.79	8.10	7.81
25F+35G*	-2.67	0.1	-1.51
35F+25G	3.63	17.57	-0.01
20F+30G	2.44	9.54	3.51
30F+20G	0	7.03	-5.11
	H-Y ZEOLITE		
type of solution	separation point(min)	max separation(min)	end of separation(min)
12:5F+12.5G	-0.38	5.81	-0.09
25F+25G	-0.94	7.12	1.61
35F+35G*	2.34	5.53	0.27
20F+20G	-0.50	6.97	0.42
30F+30G	-2.27	8.94	0.92
25F+35G*	0	-2.40	-6.91
35F+25G	-0.25	10.75	6.86
20F+30G	-1.94	13.65	5.22
30F+20G	-0.12	2.74	1.91

Despite some solutions which showed no or very small separation on the amount adsorbed graphs (35 % w/v G + 35 % w/v F, 35 % w/v G + 25 % w/v F on Figures 3.5, 3.6, 3.11 and 3.12 respectively), most solutions had a separation zone; i.e. the zone where the difference between amount-adsorbed values was the biggest.

To understand which solutions had better separations on Ca-Y zeolite under the same conditions, differences between the amount-adsorbed values were graphed against the adsorption differences between glucose and fructose, as shown in Figure 3.29. If the total sugar concentration was not under consideration for comparison, 25 % w/v G + F mixture seemed to give the best separation. But, when the total sugar concentrations were divided to the total adsorption differences for comparison among concentrations as dimensionless values; 12.5 % w/v G + F solution gave the biggest constant, which was followed by 25 % w/v G + F solution. This comparison was given in Figure 3.30.

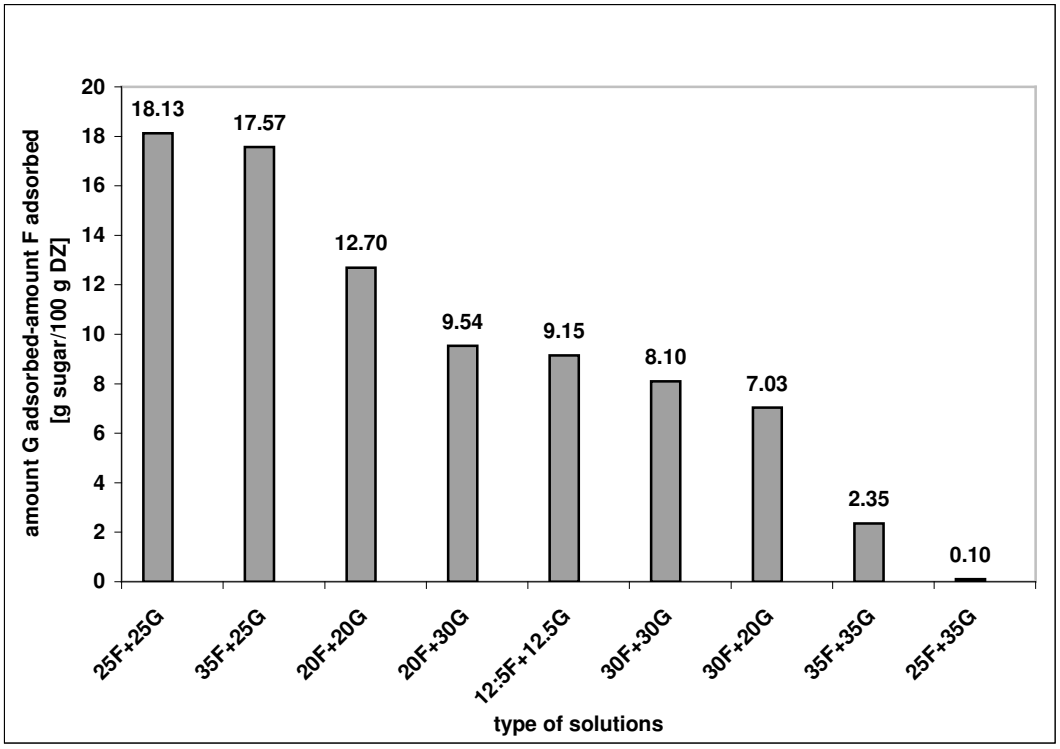

Figure 3.29 Data of separation amounts given in Table 3.2 for the given solution types at the maximum separation point on Ca-Y zeolite

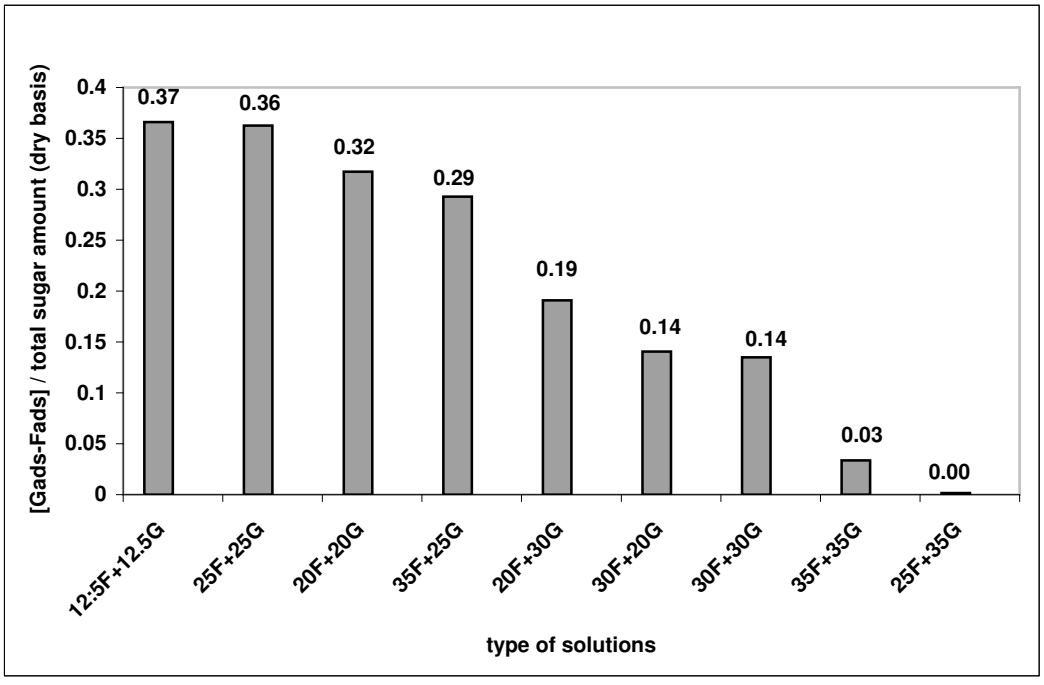

Figure 3.30 Data of experimental separation amounts, given in Table 3.1, divided by initial total sugar amounts in the mixture, on Ca-Y zeolite

As shown in the Figure 3.29, the biggest separation was between 25 % w/v glucose-fructose mixture, with an 18.13 g sugar / 100 g dry zeolite difference and the smallest one was between 35 % w/v glucose – 25 % w/v fructose mixture. Figure 3.30 shows the solutions, which were divided by their total initial sugar concentrations in the mixtures. 12.5 % w/v glucose-fructose mixture had the biggest amount-adsorbed difference value in Figure 3.30

For another comparison; the minimum and maximum separation points, calculated from the difference of the amount adsorbed values of glucose and fructose, were plotted for each solution to see their adsorption differences. As seen on Figure 3.31, there was no strict separation region at a certain time for the mixtures. The separations started early and lasted long with very low adsorption differences, which caused poor separations. Ca-Y had bigger adsorption differences mostly around minute 20, as seen in Figure 3.32

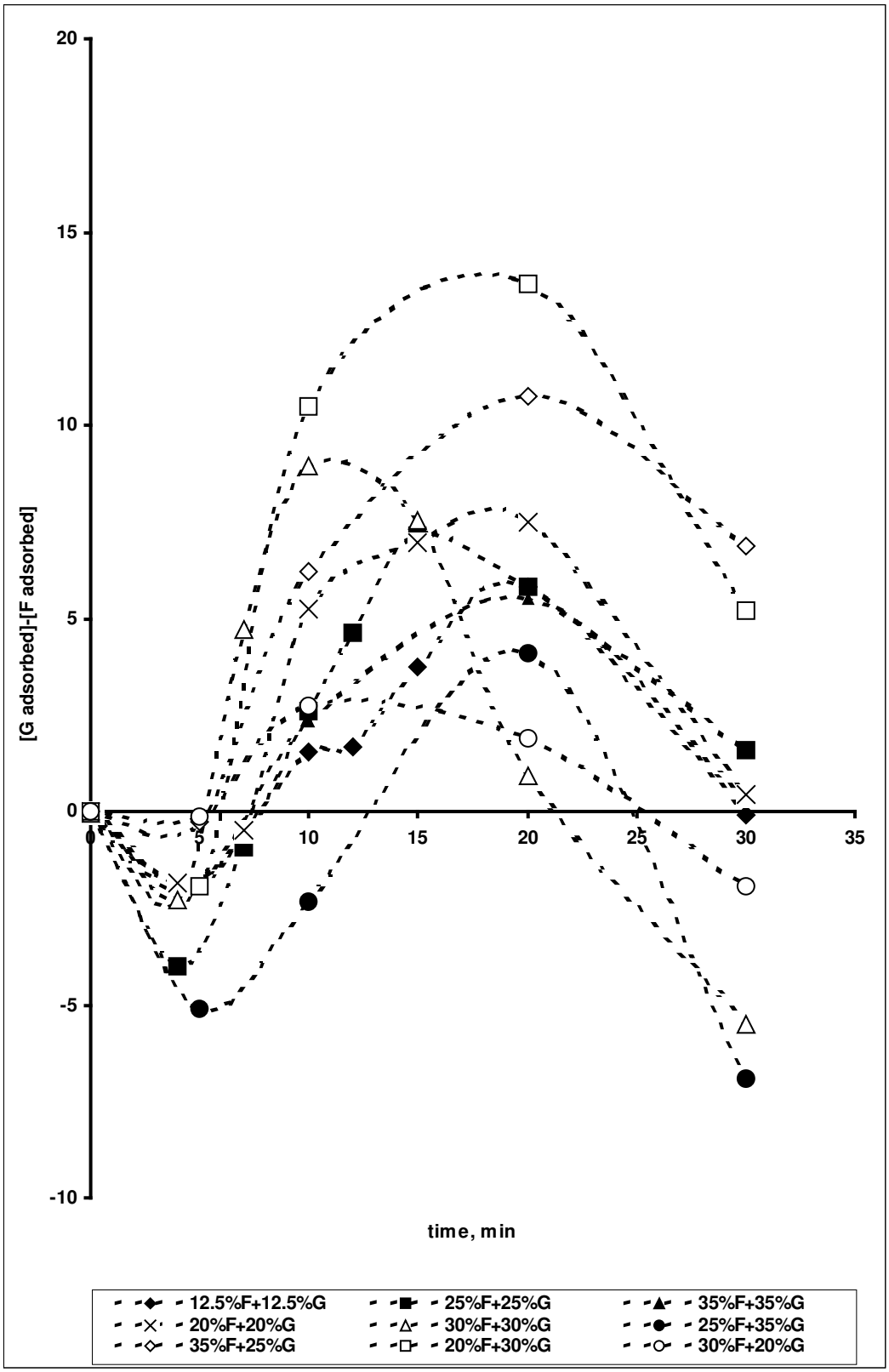

Figure 3.31 The adsorption behaviors of the mixtures on H-Y zeolite, experimental results

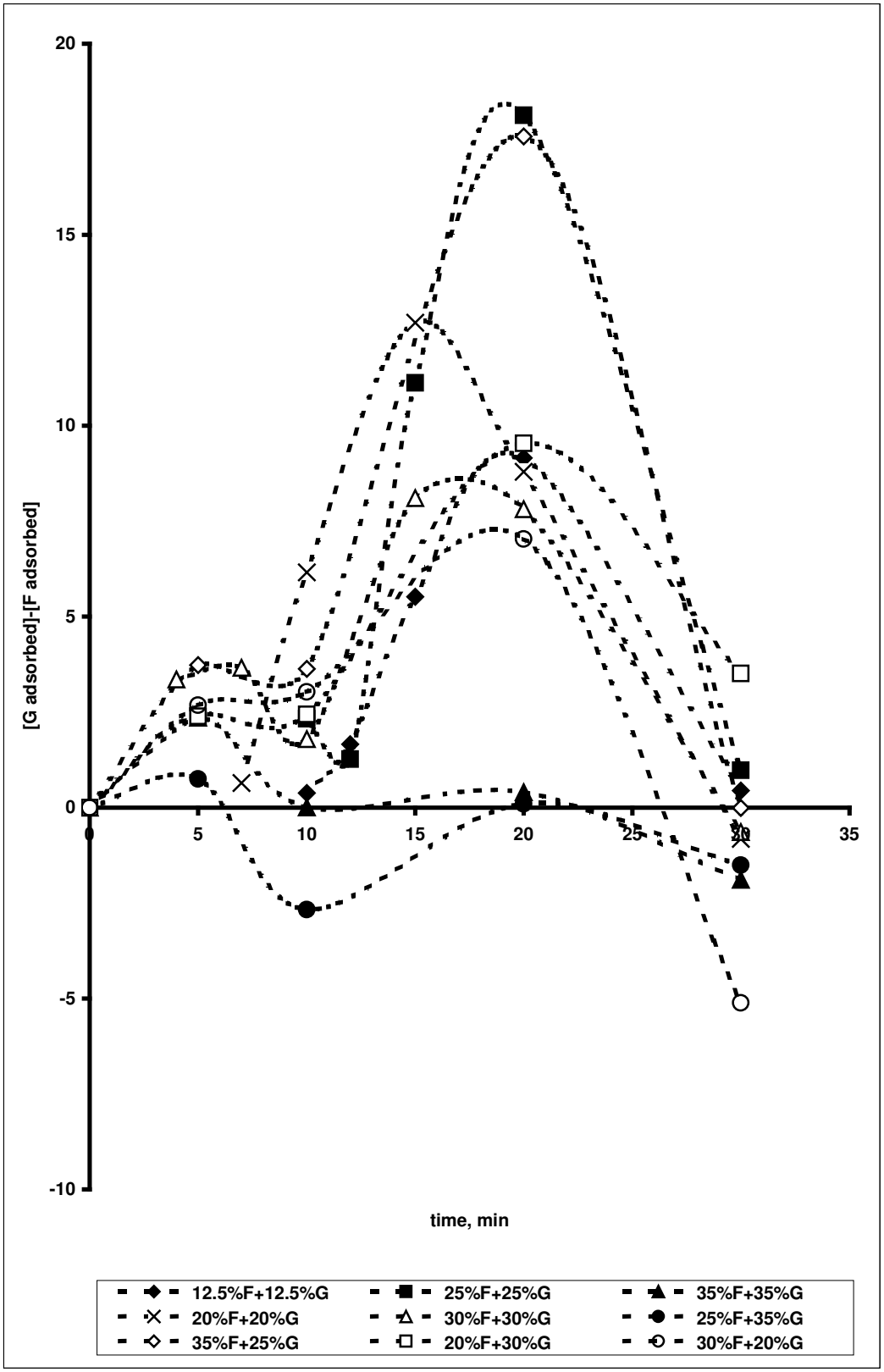

Figure 3.32 The adsorption behaviors of the mixtures on Ca-Y zeolite, experimental results

The graphs depict that, mixtures treated with Ca-Y zeolite had better separation profiles; the separation zones were much determined with the peaks, as seen on Figure 3.32. But, treated with H-Y zeolites, their amount-adsorbed differences did not make big peaks that showed a rather poor separation, compared to Ca-Y zeolite, as seen on Figure 3.31.

Figure 3.33 and 3.34 shows the best fitting curves fitted for each separation behaviors. The equation and their correlation factors were given in Appendix F. For an effective comparison, the maximum points were found. Finally, the significance of the regressions was analyzed with the F-test to see weather the x variable of the polynomials explained by Y variable or not.

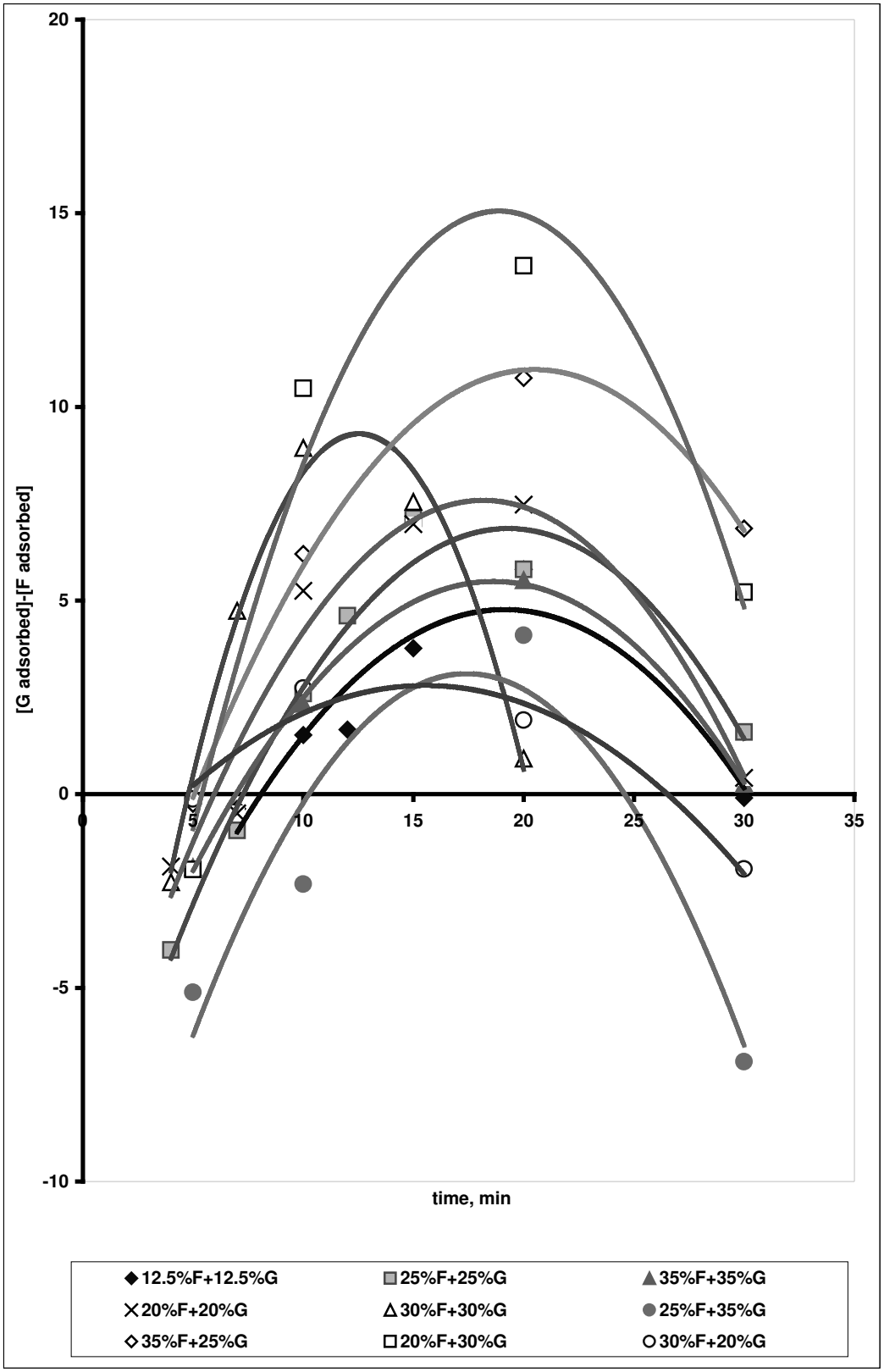

Figure 3.33 The adsorption behaviors of the mixtures on H-Y zeolite, fitted results

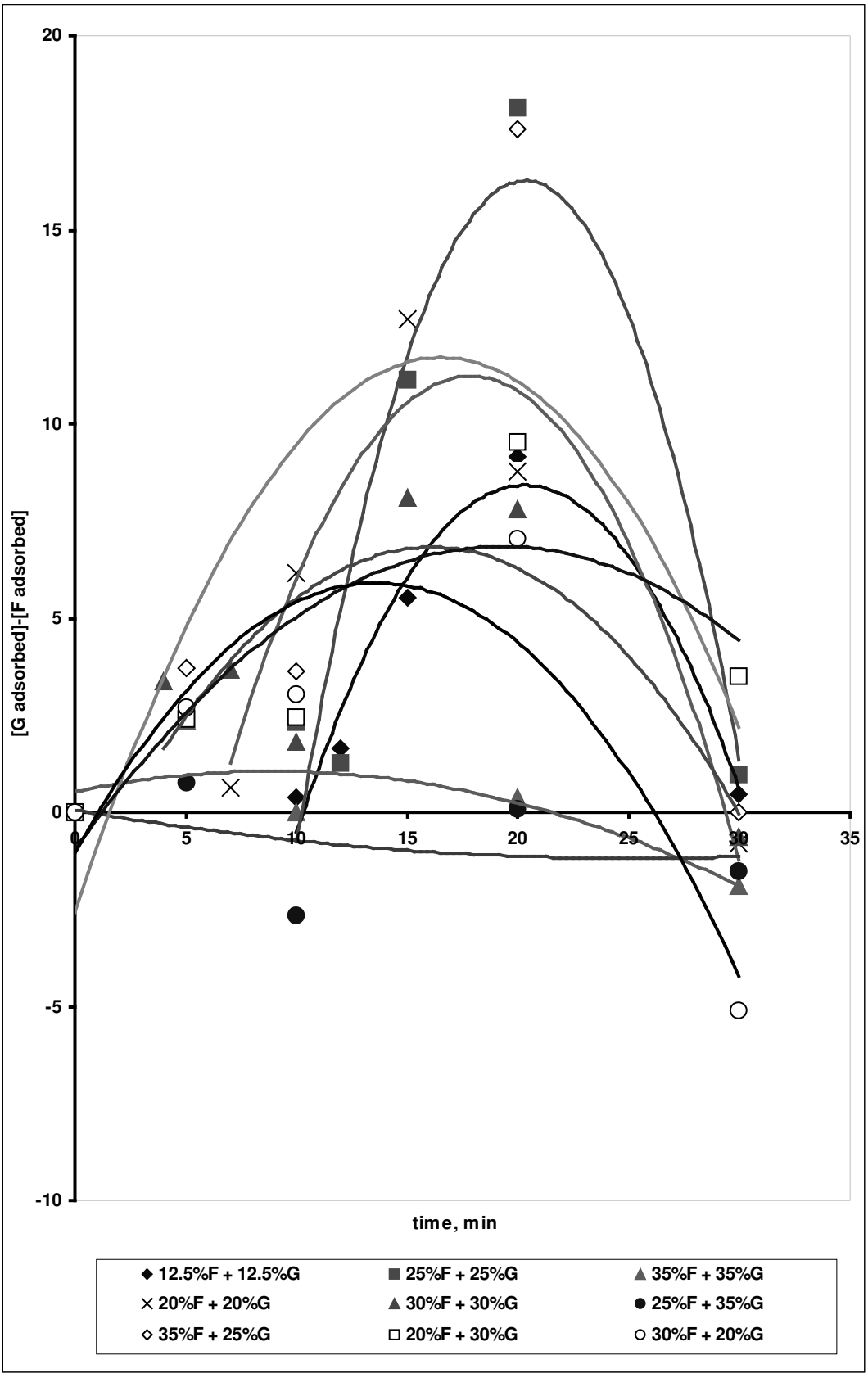

Figure 3.34 The adsorption behaviors of the mixtures on Ca-Y zeolite, fitted results

Figure 3.35 shows the differences of amount adsorbed values between glucose and fructose, plotted from the maximum point data, obtained by the best fitting equations to the separation curves.

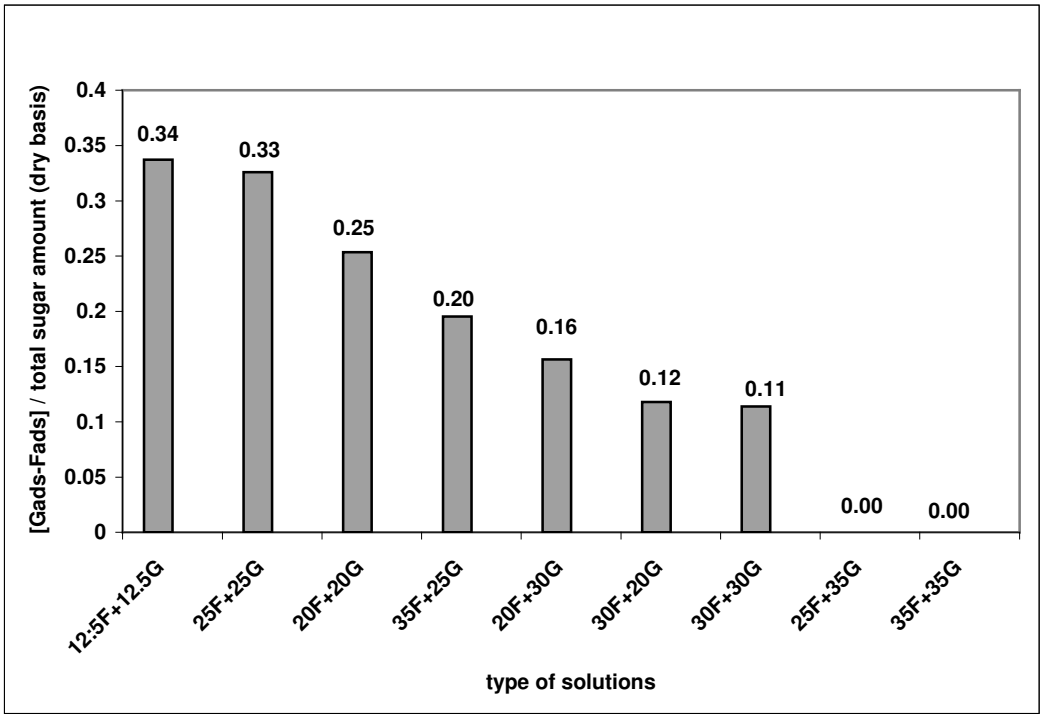

Figure 3.35 Data of separation amounts divided by initial total sugar amounts in the mixture, on Ca-Y zeolite, fitted results

The graphs, plotted on Figure 3.31 and Figure 3.32 were fitted to the equations, given in Appendix F. The correlation factors were as high as 0.99 levels for 35% w/v glucose and fructose mixtures, treated on H-Y zeolites, which was plotted best with "$y = -0.0402x^2 + 1.4979x - 8.4603$" equation. This function had a maximum point for the interval of 18^{th} and 19^{th} minutes, (18'63") and a maximum value of 5.49 g glucose and fructose difference per 100 g DZ. This data was tested for significance and in spite of the very high correlation factor, the regression was not found to be

significant, the probability of getting this sample evidence, X and Y input data, was not that low.

With the same method, all the equations were tested according to F test, and the correlation factors and F test results are given in Appendix F.

The bars shown in Figure 3.35 are almost similar to the bars shown in Figure 3.30, considering their order with magnitude. The maximum points of the curve fitting results were calculated and the theoretical results had the same orders with the real values.

Except 30% w/v and 35% w/v glucose and fructose, 25% w/v glucose-35% w/v fructose, 35% w/v fructose-25% w/v glucose, 30% glucose-20% w/v fructose mixtures treated on Ca-Y zeolite, all the curve fittings had correlation factors higher than 0.8.

Grabka [9] studied the effect of the distribution in the tautomeric forms of glucose and fructose, and found that they may interact with the zeolite surface in various ways. In one of the studies, the effect of Ca^{2+} ions was investigated. The results of the studies with $CaCl_2$ addition are given in Figure 3.35. There should be 1 mol of Ca interacting with 1 mol of fructose so as to form a complex, which was the subject of investigation. The equimolar 12.5% and 25% w/v glucose and fructose solutions were analyzed considering this complex formation.

The adsorption behavior from aqueous glucose and fructose mixture was strongly affected towards higher selectivity side. Grabka found in his studies that Ca^{2+} ions are making complexes with fructose but not with glucose. Since fructose

was kept in the solution as calcium-fructose complex, the fructose adsorption in the zeolite slowed down and glucose adsorption stayed unaffected, the rate difference between glucose and fructose adsorptions increased, resulting in better separation.

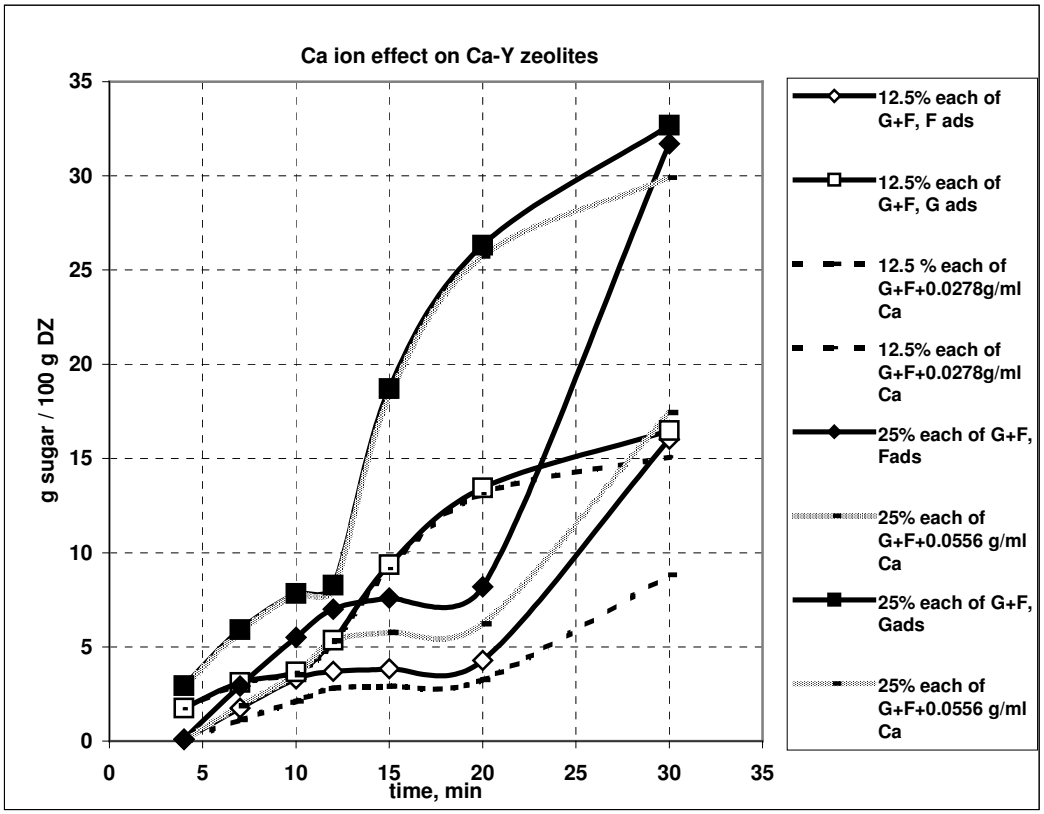

Figure 3.36 Adsorption kinetics of sugar solutions 12.5% w/v G+F and 25% w/v G+F on Ca-Y with addition of 1 mol $CaCl_2$ for one mol of fructose

The adsorption behavior from aqueous glucose and fructose mixture was strongly affected in the direction of higher selectivity. Additions of $CaCl_2$ were shown in Figure 3.36, which showed the glucose adsorption behavior was not affected, while the adsorption of fructose slowed down significantly.

The analyzed zeolites had their effects in the first half hour of the treatments. Considering the adsorption rates for glucose, the effect from the zeolites started after the first ten minutes, while fructose adsorption started after first 20 minutes, and for

most of the trials; the rate of adsorption values were very close to each other. Cockman [11] mentioned about the transformation of β-fructopyranose into α-fructofuranose in the first 10-15 minutes, followed by a slower change over the next 10-15 min. to reach the equilibrium composition. Fructose in the samples, however, showed an unexpected, characteristic rate profile. For some of the treatments, there were non-adsorbing values. Besides, for some of the trials, no separation took place, as the values of adsorption rates were almost equal.

Tautomeric distributions played a role in the fructose profile. Mutarotations may occur depending on various reasons like temperature changes, cation addition [9], pH changes and alcoholic environments [11]. It is a fact that, mutarotations change the fructose-glucose profile with the adsorption effect of the zeolites. Heper [27] also found the improved adsorption difference between glucose and fructose in Ca-Y zeolite after Ca^{+2} additions.

The presence of Ca^{+2} ions in solutions of glucose and fructose is known [9] to affect the relative distribution of their tautomeric forms, which may interact with the zeolite surface, in different ways. The Ca^{+2} ions in Ca-Y zeolite may have affects on the adsorption profiles. Since the mutarotation shifts the equilibrium to the less adsorbing pyranose from, the glucose adsorption was slow in this range, causing a rate difference between fructose and leading to a good separation.

It might be summarized as; additions of Ca^{2+} ions to the medium increased the time to reach equilibrium for glucose, and lowered fructose adsorption by a shift due to the tautomeric change that has occurred as a result of present Ca^{2+}.

3.2 Fitting Results

The next step was fitting the data from the data gathered. The "Response Surface Methodology" was used. Response was found from the input variables that influence the response, which are also called independent variables and the response function was created from the analytical function, which is used to approximate the response.

Various approaches were tested to get a suitable model from the results. The trials were made by LAB Fit Curve Fitting Software–V 7.2.31–(1999–2005) by Wilton and Cleide P. Silva–DF / CCT / UFPB. The idea was getting a perfect adsorption surface model from the instantaneous sugar concentrations. Various models like "$Y_{X(t)} = A * X_{1\,(t)} + B * X_{2\,(t)} + C$" / "$Y_{X(t)} = A * X_{1\,(t)} * X_{2\,(t)} + B$" / "$Y_{X(t)} = A * (X_{1\,(t)} + X_{2\,(t)}) + B * (X_{1\,(t)} * X_{2\,(t)}) + C$" and "$Y_{X(t)} = A * X_{1\,(t)} + B * X_{2\,(t)} + C * (X_{1\,(t)} * X_{2\,(t)}) + D$" were tried. Response graphs are given in Appendices G, H, J and I. The models, which have given best fits and high correlation factors, are given in Table 3.3. Checking the R^2 values tested the closeness to real values. Depending on the models, some of the R^2 values were as high as 88%, which demonstrated a very high correlation to the dat

Table 3.3 Curve fitting results of the adsorption models

Y=A*(X1+X2) + B*(X1*X2) + C		minute	A	B	C	D	R²
Ca-Y zeolite	Glucose ads.	30	1.31	-0.04914	4.314		**0.801**
	Fructose ads.	30	1.292	-0.04616	4.518		**0.867**
Y=A*X1 + B*X2 + C*X1*X2 + D		**minute**	**A**	**B**	**C**	**D**	**R²**
Ca-Y zeolite	Glucose ads.	30	1.39	1.228	-0.04911	4.289	**0.814**
	Fructose ads.	30	1.202	1.385	0.0462	4.546	**0.882**

* A, B, C, and D are constants of the models.

The model "$Y_{X(t)} = A^* (X_{1\,(t)} + X_{2\,(t)}) + B^* (X_{1\,(t)} * X_{2\,(t)}) + C$", is the adsorption of either glucose or fructose versus the sum and multiplication of the sugar concentrations at time *t*. Fructose showed a good correlation to the model, i.e. fructose adsorption on Ca-Y zeolite at minute 30 fit to the model at 87% correlation. The R^2 value is 0.867.

"$Y_{X(t)} = A^* X_{1\,(t)} + B^* X_{2\,(t)} + C^* (X_{1\,(t)} * X_{2\,(t)}) + D$" model was analyzed on the data; the adsorption of either sugars versus sum and multiplication of sugar concentrations at time *t.* The results were the most fitted ones among other results, especially on Ca-Y zeolite. Glucose adsorption at 30th minute fitted the model at 81% correlation and fructose adsorption at 30th minute as high as 88% correlation.

Considering the rate of adsorptions, some logarithmic models were tried. One of the models was "$x = x_i - e^{At+B*Xtotal}$", the concentrations of all the solutions against glucose and fructose adsorptions on Ca-Y and H-Y zeolite. The correlation factors were around 0.65 for all the models, as shown in Table 3.4. The non-linear regressions according to the model were shown in Appendix K. The model relates the instantaneous concentration at time "*t*" to the initial concentration and total sugar concentrations with a lag time period.

Table 3.4 Curve fitting to the model $x = x_i - e^{At+B*Xtotal}$

$x = x_i - e^{At+B*Xtotal}$		A	B	R^2
Ca-Y	Glucose	0.0622	-0.01299	0.657
	Fructose	0.06332	-0.01872	0.637
H-Y	Glucose	0.04115	-0.001549	0.663
	Fructose	0.0487	-0.01075	0.641

Another model **"$x=x_i-e^{-A*t}$"** was also graphed with all the data in the first half hour of the trials. This model fit the data better, and had correlation factors as high as 0.795. The results of the model were shown in Table 3.5 and plotted on Figure 3.37 and Figure 3.38

Table 3.5 Curve fitting to the model $x=x_i-e^{-A*t}$

$x=x_i-e^{-A*t}$		Best fit equation	R^2
Ca-Y	Glucose	$y=1.2964 * \ln(x) - 6.9022$ / $y=115.13 * e^{0.6129 * t}$	0.795
	Fructose	$y=2.1706 * \ln(x) - 9.7833$ / $y=52.792 * e^{0.8868 * t}$	0.729
H-Y	Glucose	$y=1.5471 * \ln(x) - 7.5868$ / $y=80.613 * e^{0.5075 * t}$	0.785
	Fructose	$y=1.0347 * \ln(x) - 6.3626$ / $y=177.31 * e^{0.7085 * t}$	0.733

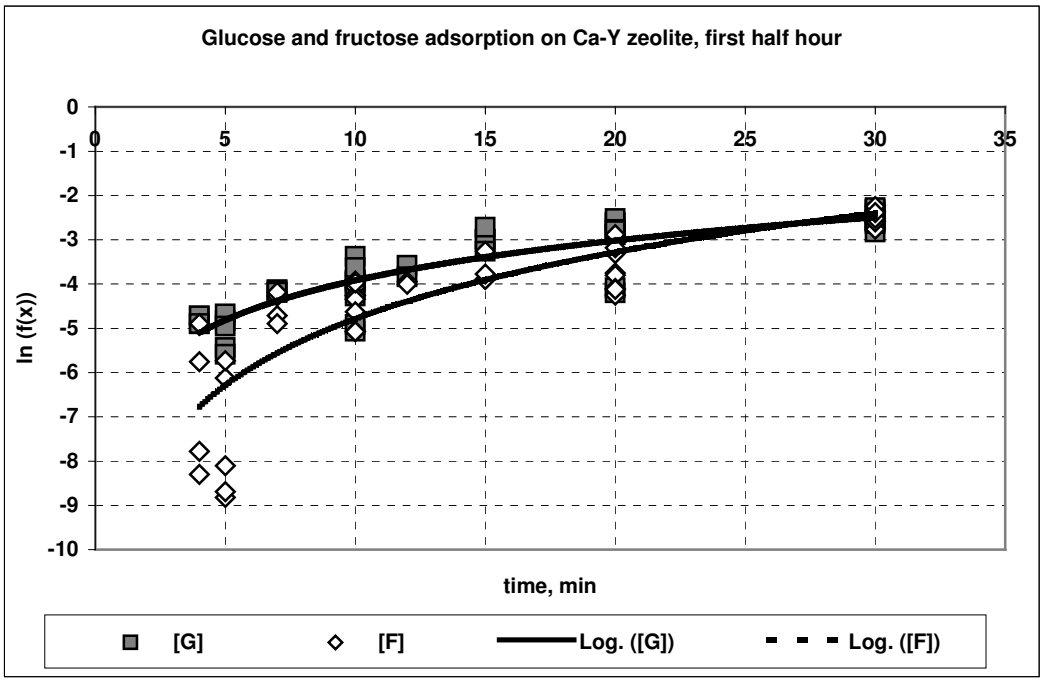

Figure 3.37 Glucose and fructose adsorption on Ca-Y zeolite, all data at the first half hour of trials.

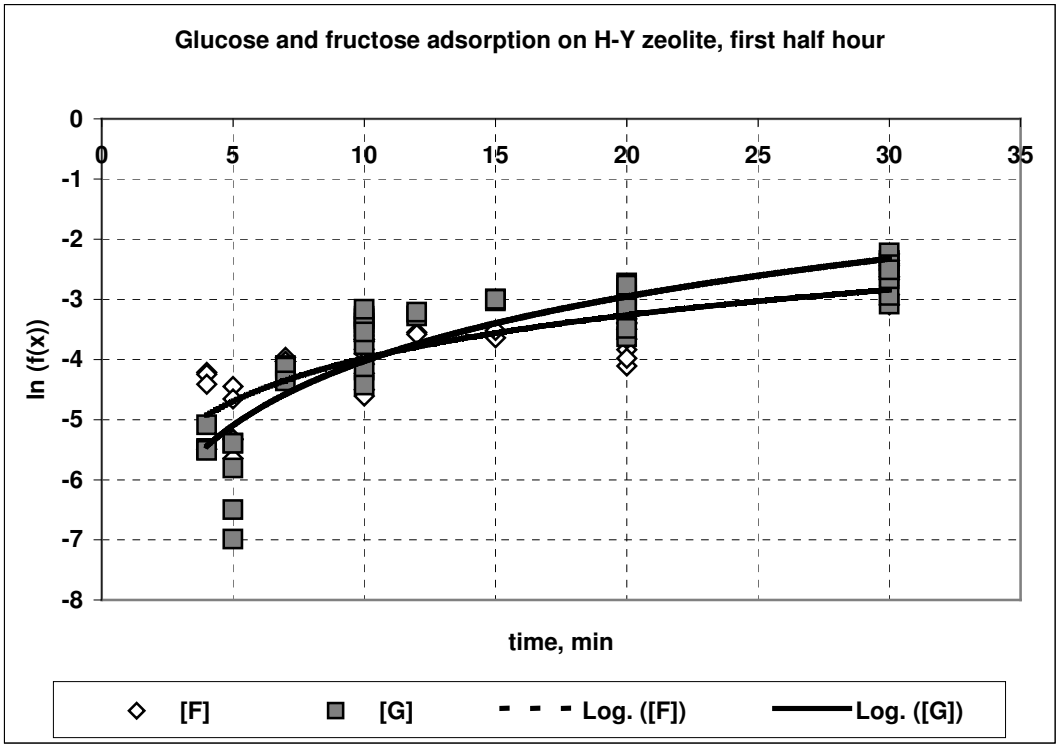

Figure 3.38 Glucose and fructose adsorption on H-Y zeolite, all data at the first half hour of trials.

The model "$x=x_i-e^{-A*t}$" better fit the data. The convergence values of both glucose and fructose were very close to each other for both zeolites that made the model acceptable.

CHAPTER 4

CONCLUSION

In this study, the kinetics and equilibrium of the adsorption of Ca- and H-forms of zeolite Y from the aqueous solutions containing 12.5 % w/v, 20 % w/v, 25 % w/v, 30 % w/v, 35 % w/v of equimolar mixtures of glucose and fructose; and 25 % w/v + 35 % w/v, 35 % w/v +25 %, 20 % w/v + 30 % w/v and 30 % w/v + 20 % w/v glucose-fructose mixtures were studied batch wise at 50°C.

The analyses were done by the analytical methods of "Cystein-carbazole" and "Lane& Eynon's" methods instead of using HPLC.

On the observations, Ca-Y zeolite showed vast differences on adsorption profiles. Glucose adsorption was fast on both zeolites for almost all solutions, except the ones that did not show any adsorption difference. Fructose adsorption was slow, compared to glucose and showed a linear trend for both zeolites and at most of the solutions. Using the same solutions under the same conditions compared Ca-Y and H-Y zeolites, and Ca-Y zeolite was shown to have the better separation capacity.

The separation behaviors of the mixtures were observed on both zeolites; the peaks found on the curves verified the best separations around or at minute 20.

The mixtures were also observed on adsorption rate graphs plotted at 30^{th} and 60^{th} minutes. Due to the competition between sugar molecules, more molecules were getting into interaction with each other; the adsorbed molecules were pulling newly added ones.

Addition of $CaCl_2$ to the mixture of Ca-Y and aqueous solutions of glucose and fructose enhanced the difference between the amount-adsorbed values, which caused a positive effect on separation.

Very high concentrations like 35 % w/v of equimolar mixture of glucose and fructose showed almost no separation; better results could be obtained by dilution.

The fittings made by "Response Surface Method" had high correlations to the model "$Y_{(t)} = A^* (X_{1\,(t)} + X_{2\,(t)}) + B^* (X_{1\,(t)} * X_{2\,(t)}) + C$" for Ca-Y zeolite, around 80 % for glucose adsorption and 87 % for fructose adsorption at minute 30. The model "$Y_{(t)} = A^* X_{1\,(t)} + B^* X_{2\,(t)} + C^* (X_{1\,(t)} * X_{2\,(t)}) + D$" for Ca-Y zeolite around 81 % for glucose and 88 % for fructose adsorptions.

The time dependent mathematical models, which consider the lag phase at the beginning of the adsorption profiles, were also used to fit the data. All data in the first half hour of treatments were treated with models "$x=x_i-e^{At+B*Xtotal}$" and "$x=x_i-e^{-A*t}$" with correlations as high as 66.3% and 79.5% respectively.

REFERENCES

[1] Austin, T.G., Shreve's Chemical Process Industries, 5th Ed., 1984

[2] Howling, D., Birch, G. G., Parker, K. J., Sugar: Science and Technology, Applied Science, Publishers, London, p260, 1979

[3] Vuilleumier, S. Worldwide production of high-fructose syrup and crystalline fructose, American Journal of Clinical Nutrition, vol. 58, no.5, p 733S-736S, 1993

[4] Grant, M. H., Kirk and Othmer Encyclopedia of Chemical Technology, 4th Ed., Vol. 23, p 4-6, 1997

[5] Grant, M. H., 1997, Kirk and Othmer Encyclopedia of Chemical Technology, 4th Ed., Vol. 23, p 25-31, 1997

[6] Schenck, F. W., Hebeda, R. E., Starch Hydrolysis Products: Worldwide Technology, Production and Applications, VCH Publishers, Inc., 1992.

[7] Blanchard, P. H., Geiger, E. O., Sugar Technology, Rev. 11, 1-94, 1984

[8] Elvers. B., Ulmann's Encyclopedia of Industrial Chemistry, 5th ed., Vol 12, pp 510-550, 1989

[9] Grabka, S.J., A ^{13}C NMR study of glucose, fructose and sucrose interactions with calcium hydroxide, Zuckerind., Vol 118, pp 369-374, 1993

[10] Shallenberger, R.S., Birch, G.G., Sugar Technology, AVI. Publ. Co. Inc., Wesport Connecticut, USA, 1975

[11] Cokman, M., Kubler, D.G., The mutarotation of fructose and the invertase hydrolysis of sucrose, J. Carbohydrate Chemistry, Vol 6, Iss 2, pp.181-201, 1987

[12] Perry, R.H., Green. D., Chemical engineers' handbook, Mc Graw Hill, pp 16.02-16.29, 1999

[13] Elvers, B., "Ulmann's Encyclopedia of Industrial Chemistry", 5th ed., Vol 12, pp 457-476.

[14] Grant, M.H., "Kirk and Othmer Encyclopedia of Chemical Technology", 4th Ed., Vol 23, pp 15-19, 1997

[15] Tosheva, L. Zeolite Macrostructures, Licentiate thesis in Departmant of Chemical and Metrallurgical Engineering, Lulea Tekniska Universitet, Sweden, 1999

[16] Breck, D.W., Zeolite Molecular Sieves, John Wiley and Sons Inc., New York, 1974

[17] Bekkumn, H. V, Flanigen, E. M., Jansen, J. C., Introduction to Zeolite Science and Practice, Elsevier, Amsterdam, 1991

[18] Hashimoto, K., Adachi, S., Models for the separation of glucose fructose mixture using a simulated moving bed adsorber, J. of Chem. Eng. of Japan, Vol 16, pp 400-406, 1983

[19] Klatt, K. U., Hanisch F., Dünnebier, G. Model-based control of a simulated moving bed chromatographic process for the separation of fructose and glucose, J. of Process Control, Vol 12, pp203-219, 2001

[20] Zhang, Y., Hidajat, K. Ray, A. K., Optimal design and operation of SMB bioreactor: production of high fructose syrup by isomerization of glucose, Biochemical Engineering Journal, vol 21, pp 111-121, 2004

[21] Lee, K. N., Continuous separation of glucose and fructose at high concentration using two-section simulated moving bed process, Korean J. Chem. Eng., 20(3), pp 532-537, 2002

[22] Ching, C.B., Ho,C., Hidajat,K., "Comparison of resin and zeolite adsorbents for fructose –glucose separation at high concentrations", Chem. Eng Sci., Vol 42, pp 2547-2555, 1987

[23] Buttersack, C., Wach, W., Adsorption of glucose and fructose containing disaccharides on different fujasides, Zeolites and related microporous materials: state of art, Weitkamp, J. H., Ed., Elsevier Science, 1994

[24] Buttersack, C., Wach, W., Buchholz, K., Specific adsorption of saccharides by dealuminated Y zeolites", J. Phys. Chem., Vol 97, pp 11861-11864, 1993

[25] Schöllner, R., Einicke, W. D., Glaser, B., Liquid-phase adsorption of monosaccharide-water mixtures on X and Y zeolites, J. Chem. Soc. Faraday Trans., Vol 89, pp1871-1876, 1993

[26] Atalay, B.D., Adsorption of fructose and glucose on zeolites sodium X and sodium, calcium, and decationated forms of Y, M.S.Thesis in Ch. E., M.E.T.U., Ankara, 1999

[27] Heper, M. Sodium, calcium, ammonium, magnesium and hydrogen forms of zeolite Y for the adsorption of glucose and fructose from aqueous solutions, Department of Biotechnology, M.E.T.U, 2002

[28] Hirota, T., Continuous Chromatographic Separation of Fructose/Glucose, Sugar y Azucar, 99 245-247, January 1980

[29] Dishe, Z, Borenfreund, E., A new spectrophotometric method for the detection and determination of keto sugars and trioses, Department of Ophthalmology, College of Physicians and Surgeons, Columbia University, New York, pp. 583-587, February 14, 1951.

[30] Box, G.E.P. and Draper N.R., Empirical Model - Building and Response Surfaces, John Wiley & Sons, New York.1987

[31] Myers, R.H. and Montgomery, D.C., Response Surface Methodology, Process and Product Optimization Using Designed Experiments, Second Edition, John Wiley & Sons, New York, 2002

[32] Box, G.E.P. and Wilson, K.B., On the Experimental Attainment of Optimum Conditions, Journal of the Royal Statistical Society, Volume 13, pp. 1-45, 1951.

[33] Hoerl, A.E., 'Optimum Solution of Many Variables Equations, Chemical Engineering Progress, vol.55, No.11, pp 69-78, 1959

[34] Ryu, D. Y., Chung, S. H., Katoh, K., Performance of continuous glucose isomerase reactor system for the production of fructose syrup, J. Biotechnology and Bioengineering, Vol. 19, pp 159-184, 1977

[35] Lane, J. H. and Eynon, L., Determination of reducing sugars by means of Fehling's solution with methylene blue as internal indicator. J. Soc. Chem. Ind. 42, 32T, 1923

APPENDIX A

CALIBRATIONS FOR CYSTEIN-CARBAZOLE, LANE-EYNON METHODS AND ACCU-CHEK DEVICE

A.1 The "Cystein-Carbazole" Method

This method detects even the trace amounts of fructose in the samples. This method was updated and a calibration curve was created to apply this old method to our samples.

Samples containing only fructose were prepared as concentrations of 0.02 g/l to 0.1 g/l and the method was applied to the samples. Before the experiments were started, the proper wavelength to study was chosen. One of the samples and the blank solution absorbance values were observed for varying wavelengths. In Table A.1, the wavelengths and absorbance values for the sample, and in Table A.2, the values of the blank solution were shown.

Table A.1 The wavelengths and absorbance values for the sample solution

Wavelength	Absorbance
283.2	0.3571
395.2	0.1982
483.6	0.3263
542.4	1.0006
568.4	1.0048
560.8	1.0576
560	1.0611

Table A.2 The wavelengths and absorbance values for the blank solution

Wavelength	Absorbance
284	2.9311
364	0.8382
372	1.4903
380	0.4795
388	0.2399
484	0.1379
560.4	0.0984

The curves were drawn for both data, and as seen on the Figure A.1, the highest value for the sample and least value for the blank is at 560 nm wavelengths. So, 560 nm was selected as the working wavelength.

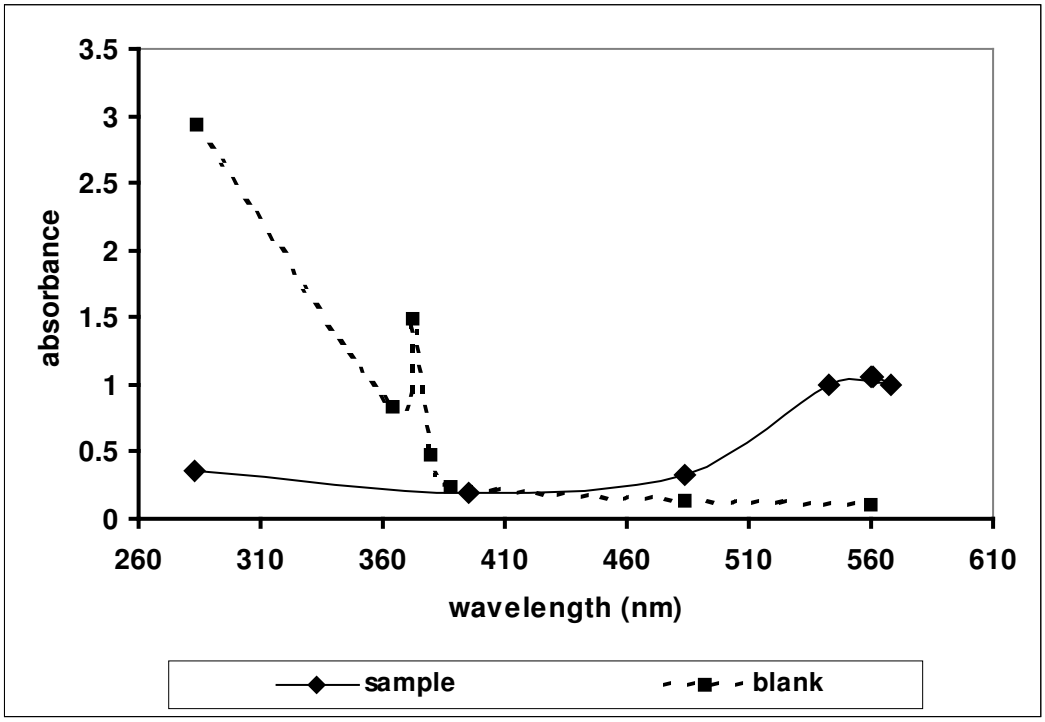

Figure A.1 Wavelength and absorbance values of sample and blank solutions

After selecting the proper wavelengths, the samples for fructose were prepared and a curve was fitted, that is Figure A.2.

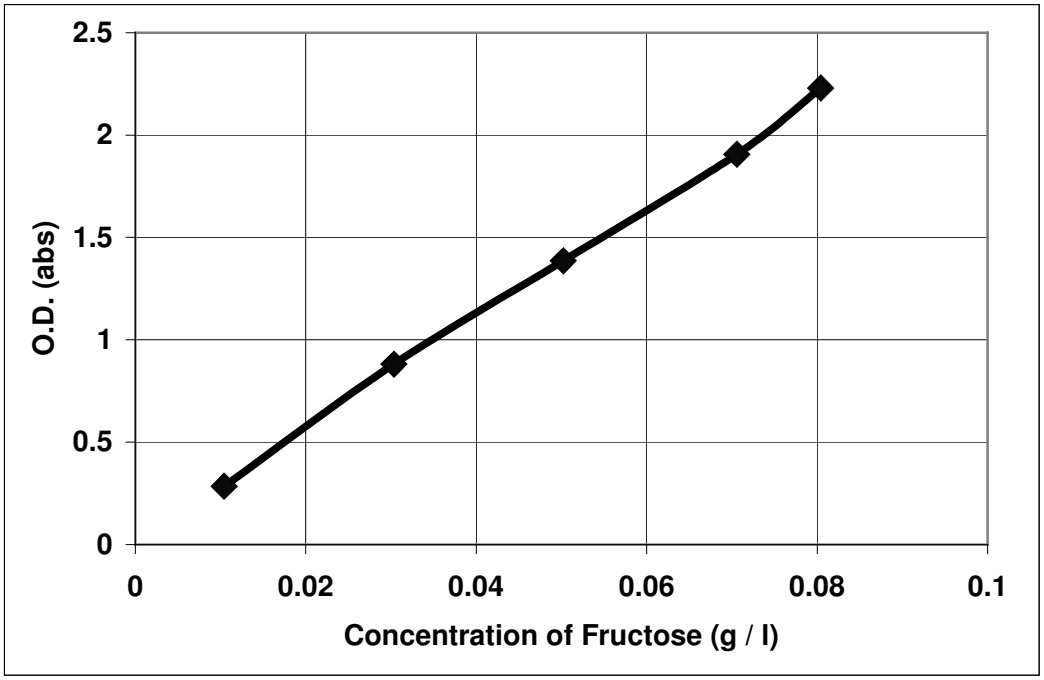

Figure A.2 Fructose concentrations versus absorbance values

It was clear from the graph that the results had a linear trend. Next step was observing the effect of glucose on the detection of fructose. To observe the effect of equal and two-fold amounts of glucose, various concentrations with equimolar glucose and fructose concentrations and one fructose to double glucose concentrations were prepared, and analyzed. The results are seen on Figure A.3 and Figure A.4, sequentially.

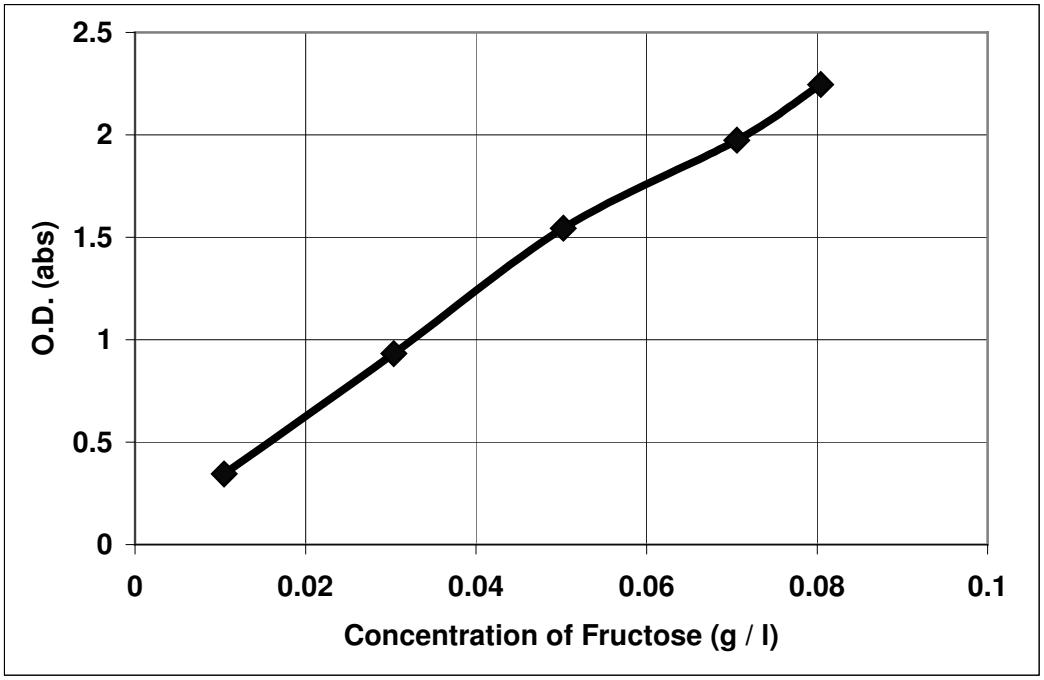

Figure A.3 Fructose concentrations with the presence of equimolar amounts of glucose versus absorbance values

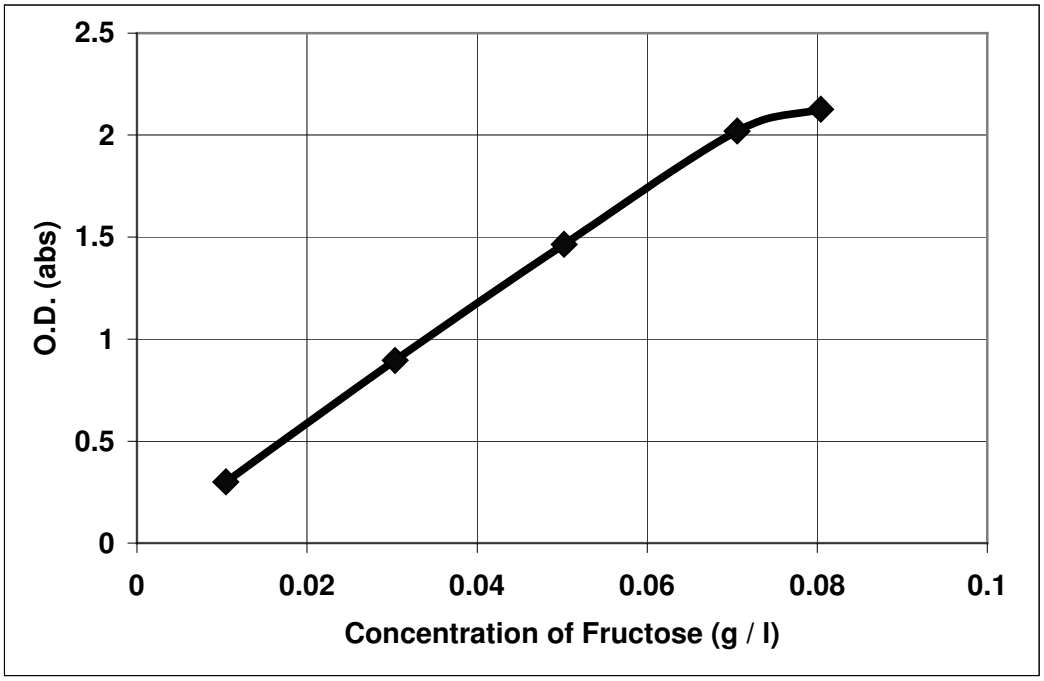

Figure A.4 Fructose concentrations with the presence double amount of glucose versus absorbance values

After glucose samples were analyzed according to the method, the absorbance results were plotted with the fructose analysis results, as seen in Figure A.5. The results showed that this method was not appropriate to analyze glucose in the samples.

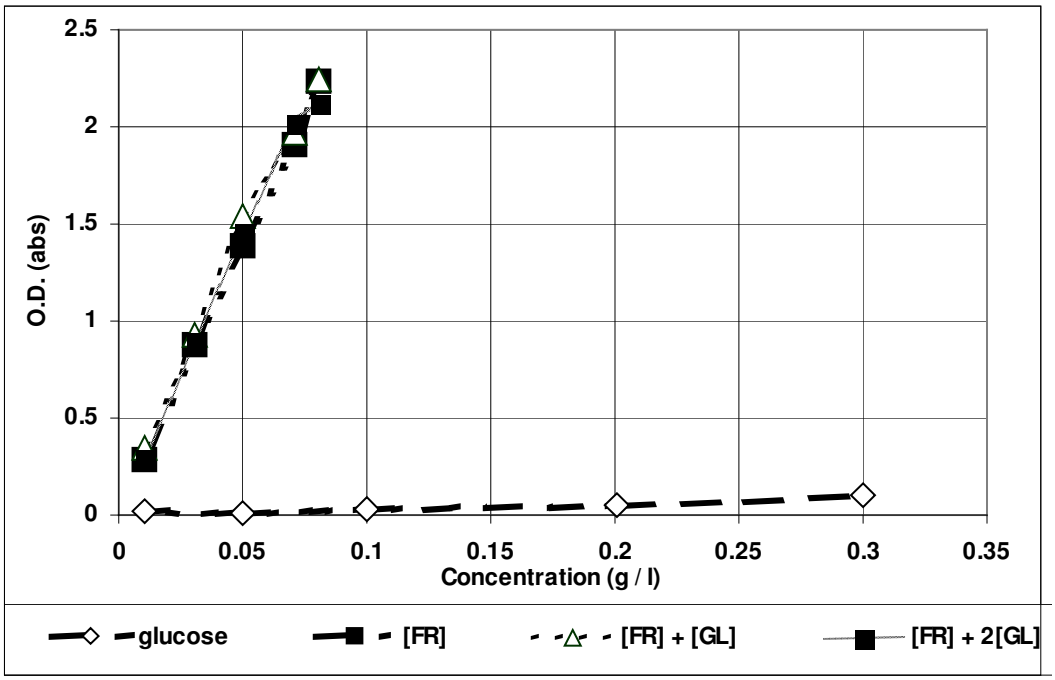

Figure A.5 All data, combined on the same graph

Though this method seemed to detect concentrations up to 0.1 (g/l) concentrations, the absorbance values exceed the limit of reading limit, 1. So, working on the 0 – 0.04 g/l concentration range for fructose was proper, and the experiments were repeated with new samples. Starting from the fructose samples only, glucose was added and its amount was increased up to ten fold. No affect of glucose was observed on detection of fructose. Figure A6 shows the results of new fructose samples.

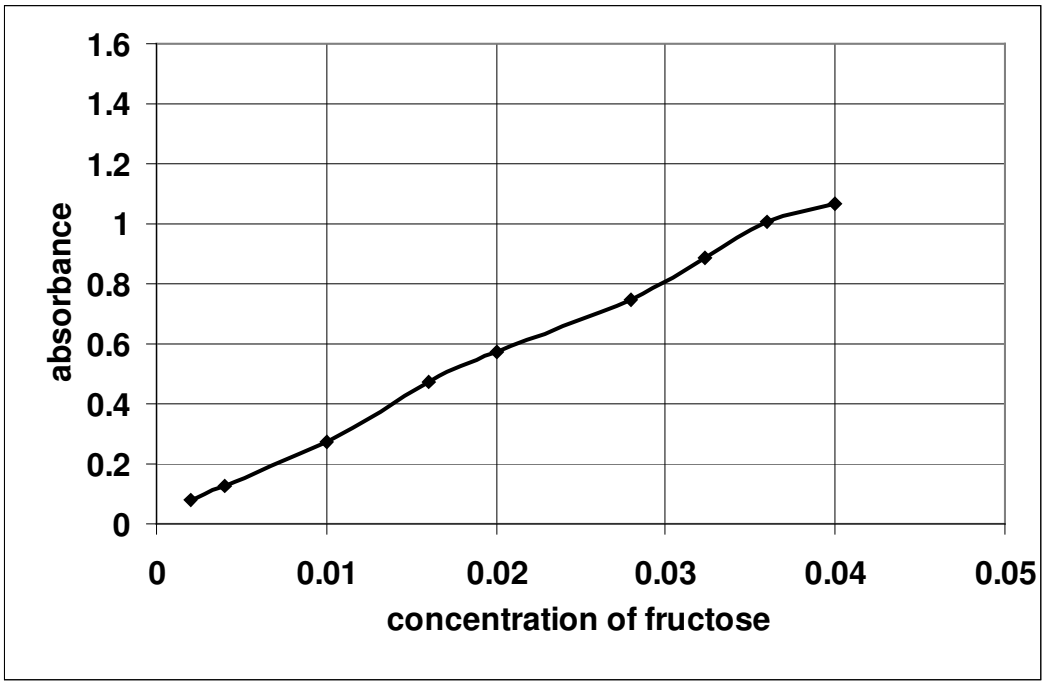

Figure A.6 Fructose concentrations versus absorbance

Again, glucose was added to the solutions at the same amounts of fructose, and samples were detected.

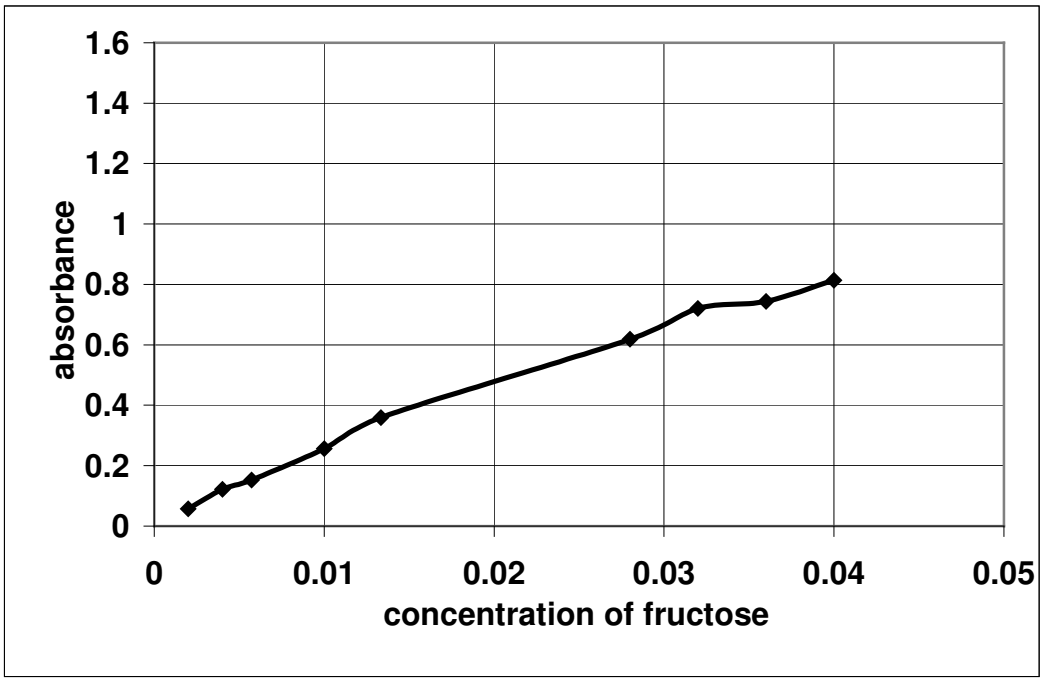

Figure A.7 Fructose and same amounts of glucose, versus absorbance

The next step was detecting the samples according to their shell lives. New solutions were prepared in 3 sets; one set for freshly prepared samples, one set for 24-hour before the analysis prepared ones and another group which were kept in freezer for 24 hours before the analysis. The results were shown on Figure A.8

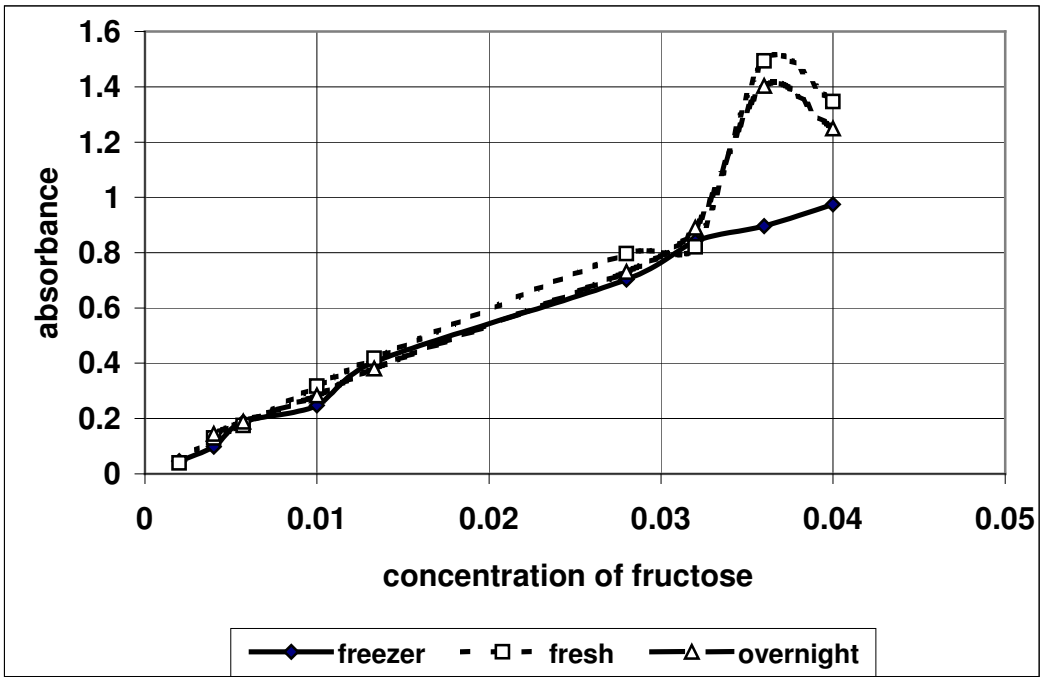

Figure A.8 Fructose and twice amounts of glucose, versus absorbance

Finally, the glucose amounts were increased from two-fold to ten-fold of the fructose in the same solutions and there were no significant effects observed on the detection of fructose, as shown in Figure A.9.

To create a calibration curve, the average of absorbance values were calculated and the calibration curve was drawn as shown by Figure A.10

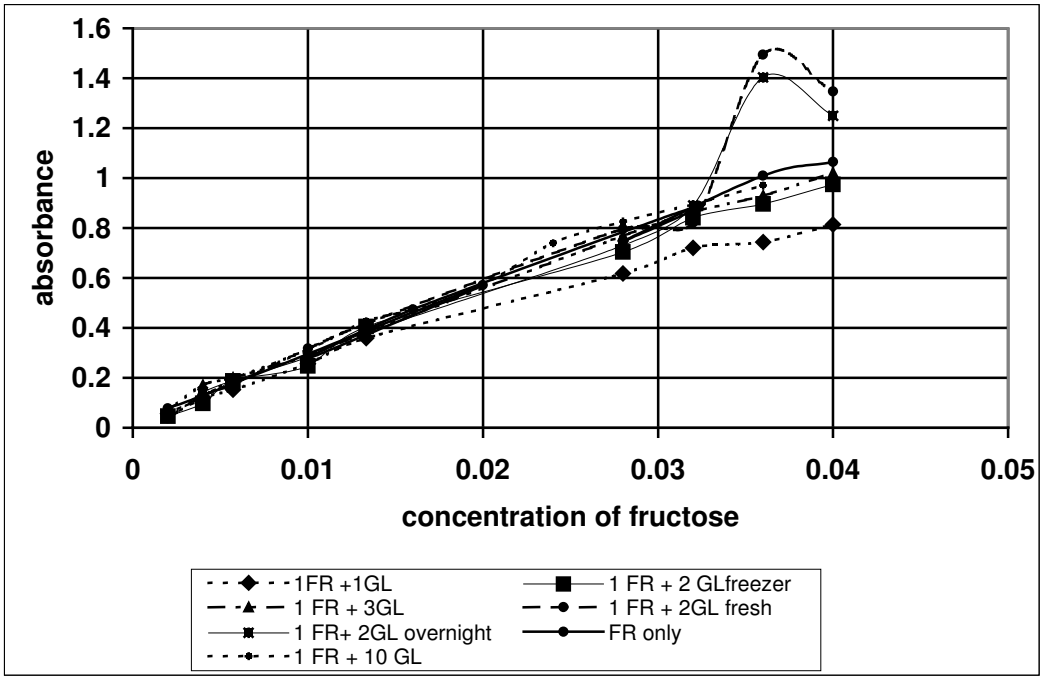

Figure A.9 Fructose and various amounts of glucose concentrations versus absorbance

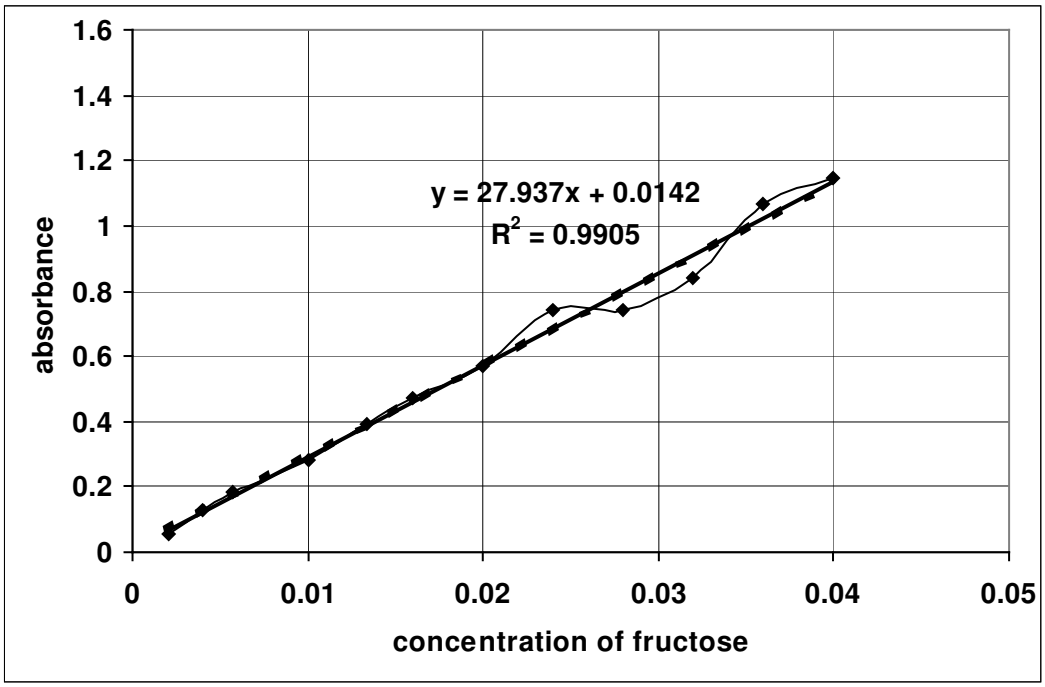

Figure A.10 Average of all fructose samples, with and without glucose, the trend line is the calibration line, with the function y = 27.937x + 0.0142 and the correlation factor,R^2, of 0.9905

The calibration curve as shown on Figure A.10 was fitted as "y=27.937x + 0.0142" with the correlation factor of 0.9905..

A.2 The "Lane-Eynon's Copper Titration Method" Method

This method determines the reducing sugars by titration, using the Fehling's solution and with the help of the tables indicating the amounts of invert sugar, dextrose, fructose, maltose or lactose equivalent to volumes for reduced Fehling's solution. In the experiments, total sugar analyses were done by the Soxhlet modification of Lane and Eynon titration. If the method was applied to a single type of reducing sugar, glucose or fructose in the experiments, the factor was found from the table directly equivalent to the titrate amount. When the method was applied to the mixture of glucose and fructose, a correction factor was added to the calculations after the equivalent to invert sugar amount was found from the table for the amount titrated.

For the reducing sugars, sugar in 100 mL of solution was found from the Equation A1.

Reducing sugar amount (mg / 100 mL) = (Factor * 100) / Titration (mL)……..…….(A.1)

If the fructose and glucose were together in the solution, Equation A.2 was also used, which was calibrated due to the ratio of the invert sugars.

Percent invert sugar * 0.95 = Percent sucrose……..…(A.2)

In the analysis of total reducing sugar amounts in the solutions, a correction factor of 0.95 was used.

The experiments of various glucose and fructose concentration volumetric calculations by the correction factors, as seen on Table A.3, and various mixture concentration calculations, with the correction factor calculations, as seen on Table A.4, were successful and this method was accepted as a calibrated methodology and decided to be used.

Table A.3 Glucose and fructose solutions detected

Glucose trials	Fructose Trials
0.2 % Glucose solution	0.1 % Fructose solution
0.3 % Glucose solution	0.15 % Fructose solution
0.4 % Glucose solution	0.2 % Fructose solution
0.5 % Glucose solution	0.3 % Fructose solution
0.6 % Glucose solution	0.4 % Fructose solution
0.7 % Glucose solution	0.5 % Fructose solution
	0.6 % Fructose solution
	0.7 % Fructose solution
	0.8 % Fructose solution

Table A.4 Fructose and glucose mixtures detected

The sample used	The result of the sample's analysis
0.05 % F + 0.05 % G (0.1 % G+F)	% 0.106
0.1 % F + 0.1 % G (0.2 % G+F)	% 0.197
0.15 % F + 0.15 % G (0.3 % G+F)	% 0.296
0.2 % F + 0.2 % G (0.4 % G+F)	% 0.404
0.3 % F + 0.3 % G (0.6 % G+F)	% 0.580
0.4 % F + 0.4 % G (0.8 % G+F)	% 0.790
0.05 % F + 0.1 % G (0.15 % G+F)	% 0.150
0.2 % F + 0.3 % G (0.5 % G+F)	% 0.500
0.1 % F + 0.3 % G (0.4 % G+F)	% 0.400
0.1 % F + 0.4 % G (0.5 % G+F)	% 0.500
0.2 % F + 0.4 % G (0.6 % G+F)	% 0.590

In table A.5, the factors required for treatment with 10 mL of Fehling's solution and in Table A.6, the factors required for 25mL of Fehling's solution was given.

Table A.5 Factors for Lane and Eynon's Process, using 10 mL of Fehling's solution

Titer	*Invert sugar No sucrose*	*Invert sugar + 1 g Sucrose per 100 ml*	*Invert sugar + 5 g Sucrose per 100 ml*	*Invert sugar + 10 g Sucrose per 100 ml*	*Invert sugar + 25 g Sucrose per 100 ml*	*Dextrose (Glucose)*	*Laevulose (Fructose)*
15	50.5	49.9	47.6	46.1	43.4	49.1	52.2
16	50.6	50	47.6	46.1	43.4	49.2	52.3
17	50.7	50.1	47.6	46.1	43.4	49.3	52.3
18	50.8	50.1	47.6	46.1	43.3	49.3	52.4
19	50.8	50.2	47.6	46.1	43.3	49.4	52.5
20	50.9	50.2	47.6	46.1	43.2	49.5	52.5
21	51	50.2	47.6	46.1	43.2	49.5	52.6
22	51	50.3	47.6	46.1	43.1	49.6	52.7
23	51.1	50.3	47.6	46.1	43	49.7	52.7
24	51.2	50.3	47.6	46.1	42.9	49.8	52.8
25	51.2	50.4	47.6	46	42.8	49.8	52.8
26	51.3	50.4	47.6	46	42.8	49.6	52.9
27	51.4	50.4	47.6	46	42.7	49.9	52.9
28	51.4	50.5	47.7	46	42.7	50	53
29	51.5	50.5	47.7	46	42.6	50	53.1
30	51.5	50.5	47.7	46	42.5	50.1	53.2
31	51.6	50.6	47.7	45.9	42.5	50.2	53.2
32	51.6	50.6	47.7	45.9	42.4	50.2	53.3
33	51.7	50.6	47.7	45.9	42.3	50.3	53.3
34	51.7	50.6	47.7	45.8	42.2	50.3	53.4
35	51.8	50.7	47.7	45.8	42.2	50.4	53.4
36	51.8	50.7	47.7	45.8	42.1	50.4	53.5
37	51.9	50.7	47.7	45.7	42	50.5	53.5
38	51.9	50.7	47.7	45.7	42	50.5	53.6
39	52	50.8	47.7	45.7	41.9	50.6	53.6
40	52	50.8	47.7	45.6	41.8	50.6	53.6
41	52.1	50.8	47.7	45.6	41.8	50.7	53.7
42	52.1	50.8	47.7	45.6	41.7	50.7	53.7
43	52.2	50.8	47.7	45.5	41.6	50.8	53.8
44	52.2	50.9	47.7	45.5	41.5	50.8	53.8
45	52.3	50.9	47.7	45.4	41.4	50.9	53.9
46	52.3	50.9	47.7	45.4	41.4	50.9	53.9
47	52.4	50.9	47.7	45.3	41.3	51	53.9
48	52.4	50.9	47.7	45.3	41.2	51	54
49	52.5	51	47.7	45.2	41.1	51	54
50	52.5	51	47.7	45.2	41	51.1	54

Table A. 6 Factors for Lane and Eynon's Process, using 25 mL of Fehling's solution

Titer	*Invert sugar No sucrose*	*Invert sugar + 1 g Sucrose per 100 ml*	*Dextrose (Glucose)*	*Laevulose (Fructose)*
15	123.6	122.6	120.2	127.4
16	123.6	122.7	120.2	127.4
17	123.6	122.7	120.2	127.5
18	123.7	122.7	120.2	127.5
19	123.7	122.8	120.3	127.6
20	123.8	122.8	120.3	127.6
21	123.8	122.8	120.3	127.7
22	123.9	122.9	120.4	127.7
23	123.9	122.9	120.4	127.8
24	124	122.9	120.5	127.8
25	124	123	120.5	127.9
26	124.1	123	120.6	127.9
27	124.1	123	120.6	128
28	124.2	123.1	120.7	128
29	124.2	123.1	120.7	128.1
30	124.3	123.1	120.8	128.1
31	124.3	123.2	120.8	128.1
32	124.4	123.2	120.8	128.2
33	124.4	123.2	120.9	128.2
34	124.5	123.3	120.9	128.3
35	124.5	123.3	121	128.3
36	124.6	123.3	121	128.4
37	124.6	123.4	121.1	128.4
38	124.7	123.4	121.2	128.5
39	124.7	123.4	121.2	128.5
40	124.8	123.4	121.2	128.6
41	124.8	123.5	121.3	128.6
42	124.9	123.5	121.4	128.6
43	124.9	123.5	121.4	128.7
44	125	123.6	121.5	128.7
45	125	123.6	121.5	128.8
46	125.1	123.6	121.6	128.8
47	125.1	123.7	121.6	128.9
48	125.2	123.7	121.7	128.9
49	125.2	123.7	121.7	129
50	125.3	123.8	121.8	129

A.3 Glucose analysis by Roche Accu-Chek® Active Glucose Meter

A blood glucose-meter, Accu-Chek® Active, was supplied from Roche and used for detection of glucose amounts in the samples. This device is originally developed for whom suffering from diabetics. It detects the amount of glucose in a drop of blood. When the blood is slipped on the strip, the device starts an enzymatic reaction and visual changes occur on the face of the strip, that indicate the amount of the glucose concentration in the blood in units of mg/dl.

Concentrations as high as 100 mg / dl are considered to be normal for an healthy person, and levels between 100 and 126 mg/dl are referred as impaired fasting glucose or pre-diabetes. Diabetes is typically diagnosed when fasting blood glucose levels are 126 mg/dl or higher. The calibrations of the device were done by various concentrations around 50 and 150 mg / dl.

The trials were started from 50 mg / dl glucose solutions up to 120 mg / dl. Solutions detected by the glucose meter, but the results did not show any change even the amounts were increasing, as shown by Figure A.11.

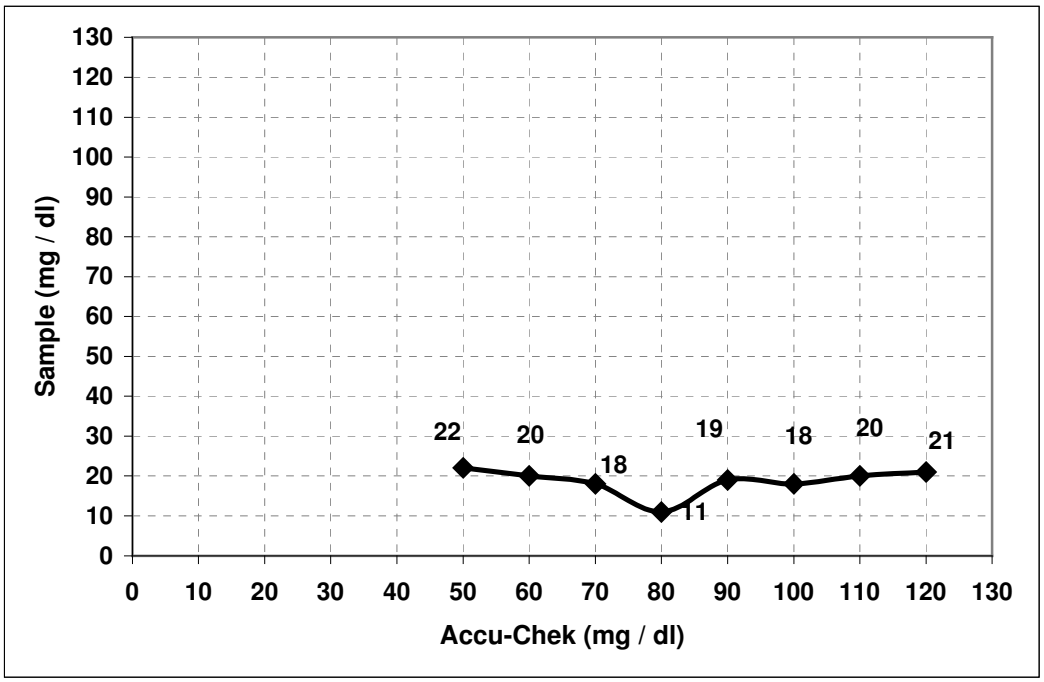

Figure A.11 Experimental versus Accu-Chek® results

The range of the concentration of samples was changed when the above graph was obtained. Figure A.12 shows the results after changing the range of samples. But, there were still conflicts, so the sample concentration range was completed and a new calibration curve was obtained, as seen on Figure A.13. Finally, the glucose-meter analysis method was skipped totally, referring to the calibration curves.

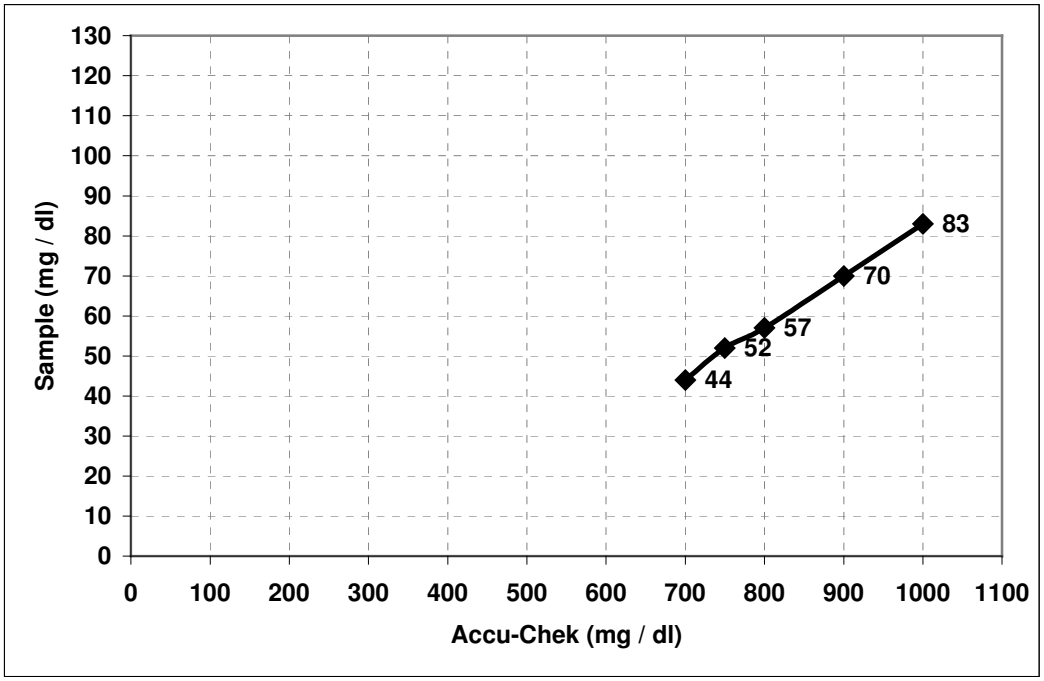

Figure A.12 The calibration curve of samples for the higher levels of glucose concentration

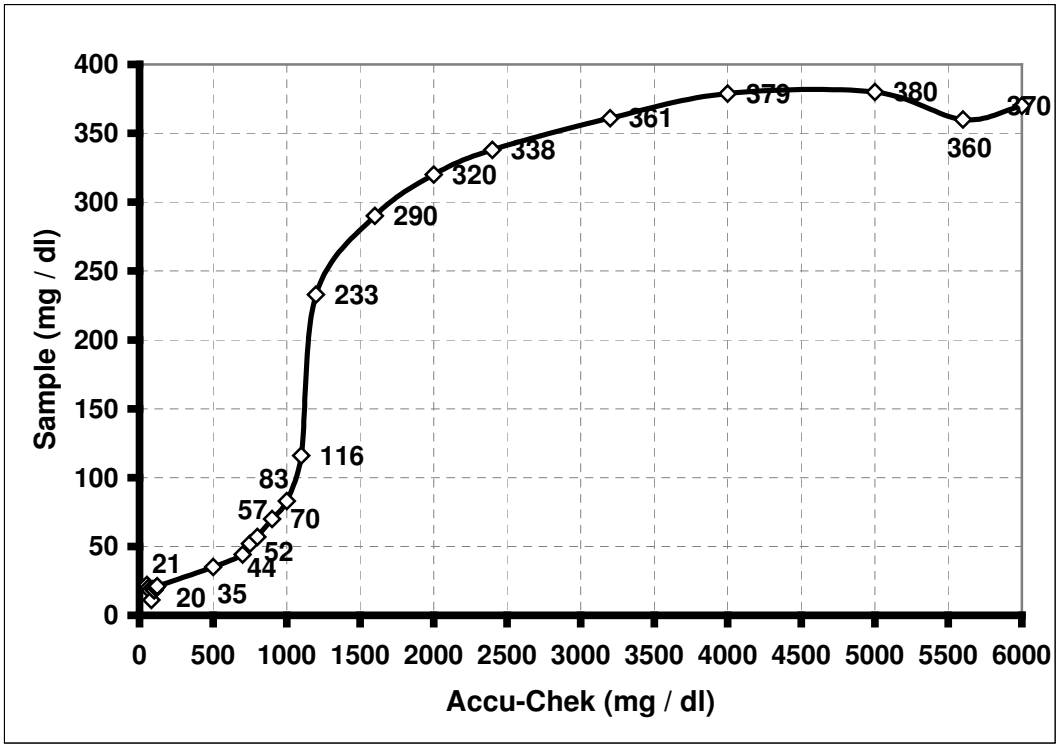

Figure A.13 Calibration curve of Roche Accu-Chek® Glucose-Meter

APPENDIX B

CALCULATION AND RAW DATA FOR SOLUTION CONCENTRATIONS

As the experiments were carried out, it was needed to determine the amount of sugars in the final solutions. The sample measurement had two steps. The prepared solutions were brought into two different concentrations by dilution, one for cystein-carbazole analysis, which was more diluted, and another for Lane and Eynon's method. After calculating the total reducing sugar in the solution, by Lane and Eynon's procedure; diluted sample was used for fructose detection by cystein-carbazole method. The difference between the results gave the glucose concentration in the solution.

First, diluted sample was analyzed; absorbance value was read by UV spectrophotometer and concentration of the fructose was found from the curve, seen on Figure A.10

Other sample was analyzed for total sugar concentration. Required amount of Fehling's solution was poured and the "Lane & Eynon's" method was applied. Total reducing sugar amount was found.

Table B.1 Final solution concentrations of glucose and fructose mixtures on Ca-Y zeolite at 50ºC, Values as % sugar (w/v), 12.5% (w/v) G+F as initial concentrations, focused on the first half hour.

Ca-Y		
time(min)	G from mix	F from mix
0	12.50	12.50
4	12.28	12.49
7	12.11	12.28
10	12.04	12.09
12	11.83	12.04
15	11.33	12.02
20	10.82	11.96
30	10.44	10.50

Table B.2 Final solution concentrations of glucose and fructose mixtures on H-Y zeolite at 50ºC, Values as % sugar (w/v), 12.5% (w/v) G+F as initial concentrations, focused on the first half hour.

H-Y		
time(min)	G from mix	F from mix
0	12.50	12.50
4	12.40	12.14
7	12.12	12.07
10	11.71	11.9
12	11.62	11.83
15	11.34	11.81
20	11.02	11.74
30	10.51	10.50

Table B.3 Final solution concentrations of glucose and fructose mixtures on Ca-Y zeolite at 50ºC, Values as % sugar (w/v), 25 % (w/v) G+F as initial concentrations, focused on the first half hour.

Ca-Y		
time(min)	G from mix	F from mix
0	25.00	25.00
4	24.63	24.99
7	24.26	24.63
10	24.02	24.31
12	23.97	24.12
15	22.66	24.05
20	21.71	23.98
30	20.91	21.04

Table B.4 Final solution concentrations of glucose and fructose mixtures on H-Y zeolite at 50ºC, Values as % sugar (w/v), 25 % (w/v) G+F as initial concentrations, focused on the first half hour.

H-Y		
time(min)	G from mix	F from mix
0	25.00	25.00
4	24.80	24.30
7	24.20	24.08
10	23.50	23.83
12	23.12	23.70
15	22.75	23.64
20	22.87	23.59
30	21.00	21.20

Table B.5 Final solution concentrations of glucose and fructose mixtures on Ca-Y zeolite at 50ºC, Values as % sugar (w/v), 35 % (w/v) G+F as initial concentrations, focused on the first hour.

Ca-Y		
time(min)	G from mix	F from mix
0	35.00	35.00
5	34.70	34.99
10	34.56	34.56
20	33.98	34.03
30	31.30	31.06
60	30.62	30.53

Table B.6 Final solution concentrations of glucose and fructose mixtures on H-Y zeolite at 50ºC, Values as % sugar (w/v), 35 % (w/v) G+F as initial concentrations, focused on the first hour.

H-Y		
time(min)	G from mix	F from mix
0	35.00	35.00
5	34.90	34.66
10	33.95	34.24
20	33.21	33.90
30	32.06	32.09
60	31.05	31.56

Table B.7 Final solution concentrations of glucose and fructose mixtures on Ca-Y zeolite at 50ºC, Values as % sugar (w/v), 20 % (w/v) G+F as initial concentrations, focused on the first hour.

Ca-Y		
time(min)	G from mix	F from mix
0	20.00	20.00
4	19.65	19.88
7	19.38	19.46
10	18.69	19.46
15	17.57	19.16
20	17.16	18.26
30	16.60	16.50
60	16.49	16.22

Table B.8 Final solution concentrations of glucose and fructose mixtures on H-Y zeolite at 50ºC, Values as % sugar (w/v), 20 % (w/v) G+F as initial concentrations, focused on the first hour.

H-Y		
time(min)	G from mix	F from mix
0	20.00	20.00
4	19.76	19.52
7	19.38	19.31
10	18.58	19.24
15	18.15	19.02
20	17.82	18.76
30	16.46	16.51
60	16.09	16.12

Table B.9 Final solution concentrations of glucose and fructose mixtures on Ca-Y zeolite at 50ºC Values as % sugar (w/v), 30 % (w/v) G+F as initial concentrations, focused on the first hour.

Ca-Y		
time(min)	G from mix	F from mix
0	30.00	30.00
4	29.56	29.98
7	29.11	29.57
10	28.87	29.09
15	27.86	28.87
20	26.99	27.96
30	25.99	25.91
60	25.67	25.63

Table B.10 Final solution concentrations of glucose and fructose mixtures on H-Y zeolite at 50ºC, Values as % sugar (w/v), 30 % (w/v) G+F as initial concentrations, focused on the first hour.

H-Y		
time(min)	G from mix	F from mix
0	30.00	30.00
4	29.76	29.76
7	29.25	28.97
10	27.96	28.56
15	27.24	28.35
20	27.07	28.02
30	26.11	26.23
60	26.60	25.91

Table B.11 Final solution concentrations of glucose and fructose mixtures on Ca-Y zeolite at 50ºC, Values as % sugar (w/v), 35 % (w/v) G + 25 % (w/v) F as initial concentrations, focused on the first hour.

Ca-Y		
time(min)	G from mix	F from mix
0	35.00	25.00
5	34.78	24.87
10	34.57	24.24
20	34.02	24.04
30	31.25	21.06
60	30.76	21.04

Table B.12 Final solution concentrations of glucose and fructose mixtures on H-Y zeolite at 50ºC, Values as % sugar (w/v), 35 % (w/v) G + 25 % (w/v) F as initial concentrations, focused on the first hour.

H-Y		
time(min)	G from mix	F from mix
0	35.00	25.00
5	34.95	24.31
10	34.30	24.01
20	33.26	23.77
30	32.16	21.30
60	31.23	20.72

Table B.13 Final solution concentrations of glucose and fructose mixtures on Ca-Y zeolite at 50ºC, Values as % sugar (w/v), 25 % (w/v) G + 35 % (w/v) F as initial concentrations, focused on the first hour.

Ca-Y		
time(min)	G from mix	F from mix
0	25.00	35.00
5	24.52	34.99
10	24.18	34.63
20	21.90	34.09
30	21.10	31.10
60	20.96	31.26

Table B.14 Final solution concentrations of glucose and fructose mixtures on H-Y zeolite at 50ºC, Values as % sugar (w/v), 25 % (w/v) G + 35 % (w/v) F as initial concentrations, focused on the first hour.

H-Y		
time(min)	G from mix	F from mix
0	25.00	35.00
5	24.82	34.79
10	23.65	34.42
20	22.60	33.95
30	21.26	32.12
60	20.55	31.67

Table B.15 Final solution concentrations of glucose and fructose mixtures on Ca-Y zeolite at 50ºC, Values as % sugar (w/v), 30 % (w/v) G + 20 % (w/v) F as initial concentrations, focused on the first hour.

Ca-Y		
time(min)	G from mix	F from mix
0	30.00	20.00
5	29.54	19.84
10	29.22	19.52
20	27.15	18.34
30	26.12	16.55
60	25.96	16.27

Table B.16 Final solution concentrations of glucose and fructose mixtures on H-Y zeolite at 50ºC, Values as % sugar (w/v), 30 % (w/v) G + 20 % (w/v) F as initial concentrations, focused on the first hour.

H-Y		
time(min)	G from mix	F from mix
0	30.00	20.00
5	29.78	19.53
10	28.00	19.31
20	27.12	18.82
30	26.20	16.85
60	26.75	16.20

Table B.17 Final solution concentrations of glucose and fructose mixtures on Ca-Y zeolite at 50ºC, Values as % sugar (w/v), 20 % (w/v) G + 30 % (w/v) F as initial concentrations, focused on the first hour.

Ca-Y		
time(min)	G from mix	F from mix
0	20.00	30.00
5	19.65	29.99
10	18.73	29.10
20	17.23	28.12
30	16.69	26.06
60	16.52	26.85

Table B.18 Final solution concentrations of glucose and fructose mixtures on H-Y zeolite at 50ºC, Values as % sugar (w/v), 20 % (w/v) G + 30 % (w/v) F as initial concentrations, focused on the first hour.

H-Y		
time(min)	G from mix	F from mix
0	20.00	30.00
5	19.78	29.76
10	18.62	28.97
20	18.01	28.25
30	16.52	26.28
60	16.12	26.02

APPENDIX C

CALCULATION AND RAW DATA FOR ADSORPTION VALUES

The adsorption values were required to compare the adsorption capacities of the zeolites. The data obtained as percent values were converted to g adsorbed per 100g dry zeolite values.

$$\text{Amount sugar adsorbed per 100 g dry zeolite} = \frac{Wi - Wf}{Wz} * 100$$

Where;

Wi = Weight of sugar in the beginning solution, g

Wf = Weight of sugar in the final solution, g

Wz = Weight of dry zeolite (zeolite is in equilibrium with air at 30%, contains 25% moisture), g

A sample calculation is carried out for the data given in table C.1 by using data given in table B.1.for adsorption of glucose on Ca-Y at 0.5^{th} hour (50ºC).

Initial glucose concentration was 12.5%, final concentration was % 10.44078, solution volume is 6 mL, amount of dry zeolite is 0.75g (1 g zeolite with 25% moisture)

$Wi: \frac{12.5\,g\ glu\cos e}{100\,ml\ solution} * 6\,ml\ solution = 0.75$ g glucose in the initial solution

Wf: $\frac{10.44078\,g\,glu\cos e}{100\,ml\,solution} * 6\,ml\ solution =$ 0.6264468 g glucose in the final solution

Wz: 0.75 g DZ

Amount of glucose adsorbed = $\frac{0.75 - 0.6264468}{0.75} * 100 =$ 16.47376g glucose in 100g DZ Adsorption values are given in Tables C.1-C.18

Table C.1 Adsorption values of glucose and fructose mixtures on Ca-Y zeolite (g adsorbed * 100 g DZ) at 50ºC, Values as % sugar (w/v), 12.5% (w/v) G+F as initial concentrations, focused on the first half hour.

Ca-Y		
time(min)	G from mix	F from mix
0	0	0
4	1.75	0.08
7	3.12	1.75
10	3.67	3.29
12	5.35	3.70
15	9.36	3.84
20	13.43	4.28
30	16.47	16.03

Table C.2 Adsorption values of glucose and fructose mixtures on H-Y zeolite (g adsorbed * 100 g DZ) at 50ºC, Values as % sugar (w/v), 12.5% (w/v) G+F as initial concentrations, focused on the first half hour.

H-Y		
time(min)	G from mix	F from mix
0	0	0
4	0.82	2.90
7	3.06	3.43
10	6.35	4.82
12	7.06	5.39
15	9.25	5.49
20	11.86	6.05
30	15.94	16.03

Table C.3 Adsorption values of glucose and fructose mixtures on Ca-Y zeolite (g adsorbed * 100 g DZ) at 50ºC, Values as % sugar (w/v), 25 % (w/v) G+F as initial concentrations, focused on the first half hour.

Ca-Y		
time(min)	G from mix	F from mix
0	0	0
4	2.95	0.10
7	5.91	2.93
10	8.83	5.50
12	16.35	7.06
15	18.71	7.59
20	26.32	8.19
30	32.69	31.71

Table C.4 Adsorption values of glucose and fructose mixtures on H-Y zeolite (g adsorbed * 100 g DZ) at 50ºC, Values as % sugar (w/v), 25 % (w/v) G+F as initial concentrations, focused on the first half hour.

H-Y		
time(min)	G from mix	F from mix
0	0	0
4	1.60	2
7	6.39	7.36
10	11.96	9.39
12	15.03	10.42
15	17.99	10.87
20	17.06	11.26
30	32.00	30.39

Table C.5 Adsorption values of glucose and fructose mixtures on Ca-Y zeolite (g adsorbed * 100 g DZ) at 50ºC, Values as % sugar (w/v), 35 % (w/v) G+F as initial concentrations, focused on the first hour.

Ca-Y		
time(min)	G from mix	F from mix
0	0	0
5	2.44	0.08
10	3.49	3.49
20	8.16	7.76
30	29.63	31.52
60	35.03	35.77

Table C.6 Adsorption values of glucose and fructose mixtures on H-Y zeolite (g adsorbed * 100 g DZ) at 50ºC, Values as % sugar (w/v), 35 % (w/v) G+F as initial concentrations, focused on the first hour.

H-Y		
time(min)	G from mix	F from mix
0	0	0
5	0.84	2.73
10	8.37	6.04
20	14.35	8.83
30	23.55	23.28
60	31.64	27.51

Table C.7 Adsorption values of glucose and fructose mixtures on Ca-Y zeolite (g adsorbed * 100 g DZ) at 50ºC, Values as % sugar (w/v), 20 % (w/v) G+F as initial concentrations, focused on the first hour.

Ca-Y		
time(min)	G from mix	F from mix
0	0	0
4	2.82	1.00
7	4.98	4.34
10	10.45	4.29
15	19.45	6.75
20	22.69	13.89
30	27.20	28.02
60	28.11	30.26

Table C.8 Adsorption values of glucose and fructose mixtures on H-Y zeolite (g adsorbed * 100 g DZ) at 50ºC, Values as % sugar (w/v), 20 % (w/v) G+F as initial concentrations, focused on the first hour.

H-Y		
time(min)	G from mix	F from mix
0	0	0
4	1.94	3.81
7	4.99	5.48
10	11.36	6.11
15	14.78	7.81
20	17.43	9.95
30	28.35	27.93
60	31.28	31.07

Table C.9 Adsorption values of glucose and fructose mixtures on Ca-Y zeolite (g adsorbed * 100 g DZ) at 50ºC, Values as % sugar (w/v), 30 % (w/v) G+F as initial concentrations, focused on the first hour.

Ca-Y		
time(min)	G from mix	F from mix
0	0	0
4	3.55	0.19
7	7.10	3.44
10	9.08	7.28
15	17.14	9.04
20	24.10	16.29
30	32.10	32.75
60	34.44	34.96

Table C.10 Adsorption values of glucose and fructose mixtures on H-Y zeolite (g adsorbed * 100 g DZ) at 50ºC, Values as % sugar (w/v), 30 % (w/v) G+F as initial concentrations, focused on the first hour.

H-Y		
time(min)	G from mix	F from mix
0	0	0
4	1.92	1.96
7	5.97	8.24
10	16.29	11.56
15	22.11	13.17
20	23.42	15.88
30	31.12	30.19
60	27.23	32.74

Table C.11 Adsorption values of glucose and fructose mixtures on Ca-Y zeolite (g adsorbed * 100 g DZ) at 50ºC, Values as % sugar (w/v), 35 % (w/v) G + 25 % (w/v) F as initial concentrations, focused on the first hour.

Ca-Y		
time(min)	G from mix	F from mix
0	0	0
5	1.79	1.04
10	3.44	6.11
20	7.81	7.71
30	30.04	31.54
60	33.95	31.71

Table C.12 Final solution concentrations of glucose and fructose mixtures on H-Y zeolite at 50ºC, Values as % sugar (w/v), 35 % (w/v) G + 25 % (w/v) F as initial concentrations, focused on the first hour.

H-Y		
time(min)	G from mix	F from mix
0	0	0
5	0.44	5.55
10	5.58	7.90
20	13.95	9.84
30	22.72	29.63
60	30.14	34.21

Table C.13 Adsorption values of glucose and fructose mixtures on Ca-Y zeolite (g adsorbed * 100 g DZ) at 50ºC, Values as % sugar (w/v), 25 % (w/v) G + 35 % (w/v) F as initial concentrations, focused on the first hour.

Ca-Y		
time(min)	G from mix	F from mix
0	0	0
5	3.81	0.08
10	6.57	2.94
20	24.83	7.25
30	31.20	31.21
60	32.37	29.95

Table C.14 Adsorption values of glucose and fructose mixtures on H-Y zeolite (g adsorbed * 100 g DZ) at 50ºC, Values as % sugar (w/v), 25 % (w/v) G + 35 % (w/v) F as initial concentrations, focused on the first hour.

H-Y		
time(min)	G from mix	F from mix
0	0	0
5	1.43	1.68
10	10.84	4.63
20	19.18	8.44
30	29.89	23.03
60	35.60	26.68

Table C.15 Adsorption values of glucose and fructose mixtures on Ca-Y zeolite (g adsorbed * 100 g DZ) at 50ºC, Values as % sugar (w/v), 30 % (w/v) G + 20 % (w/v) F as initial concentrations, focused on the first hour.

Ca-Y		
time(min)	G from mix	F from mix
0	0	0
5	3.67	1.28
10	6.27	3.83
20	22.80	13.26
30	31.08	27.57
60	32.29	29.85

Table C.16 Adsorption values of glucose and fructose mixtures on H-Y zeolite (g adsorbed * 100 g DZ) at 50ºC, Values as % sugar (w/v), 30 % (w/v) G + 20 % (w/v) F as initial concentrations, focused on the first hour.

H-Y		
time(min)	G from mix	F from mix
0	0	0
5	1.80	3.74
10	15.98	5.50
20	23.08	9.43
30	30.40	25.19
60	25.97	30.38

Table C.17 Adsorption values of glucose and fructose mixtures on Ca-Y zeolite (g adsorbed * 100 g DZ) at 50ºC Values as % sugar (w/v), 20 % (w/v) G + 30 % (w/v) F as initial concentrations, focused on the first hour.

Ca-Y		
time(min)	G from mix	F from mix
0	0	0
5	2.80	0.12
10	10.20	7.17
20	22.11	15.07
30	26.41	31.53
60	27.82	25.18

Table C.18 Adsorption values of glucose and fructose mixtures on H-Y zeolite (g adsorbed * 100 g DZ) at 50ºC, Values as % sugar (w/v), 20 % (w/v) G + 30 % (w/v) F as initial concentrations, focused on the first hour.

H-Y		
time(min)	G from mix	F from mix
0	0	0
5	1.80	1.92
10	11.02	8.28
20	15.91	14.00
30	27.83	29.76
60	31.04	31.82

APPENDIX D

ADSORPTION DATA

The adsorptions of the samples for the 30th and 60th minutes were calculated for the solutions. Adsorption profiles for the specified data were compared for the zeolites Ca-Y and H-Y

Table D.1 Adsorptions of Glucose on Ca-Y zeolite at minutes 30 and 60

Initial concentration in the mixture % w/v	Concentration at minute 30 % w/v	Amount adsorbed at minute 30 % w/v	Concentration at minute 60 % w/v	Amount adsorbed at minute 60 % w/v
12.5	10.44	16.47	9.90	20.81
20	16.60	27.20	16.49	28.11
25	20.91	32.69	20.77	33.88
30	25.99	32.11	25.70	34.44
35	31.30	29.63	30.62	35.03
20G+30F	16.70	26.41	16.52	27.82
30G+20F	26.11	31.08	25.96	32.30
25G+35F	21.10	31.20	20.95	32.37
35G+25F	31.25	30.03	30.76	33.95

Table D.2 Adsorptions of Glucose on H-Y zeolite at minutes 30 and 60

Initial concentration in the mixture % w/v	Concentration at minute 30 % w/v	Amount adsorbed at minute 30 % w/v	Concentration at minute 60 % w/v	Amount adsorbed at minute 60 % w/v
12.5	10.51	15.94	10.74	14.04
20	16.46	28.354	16.09	31.29
25	21.09	31.26	20.34	37.26
30	26.11	31.12	25.60	35.23
35	32.06	23.57	31.05	31.64
20G+30F	16.52	27.83	16.12	31.04
30G+20F	26.20	30.40	26.75	25.97
25G+35F	21.26	29.89	20.55	35.60
35G+25F	32.16	22.72	31.23	30.14

Table D.3 Adsorptions of Fructose on Ca-Y zeolite at minutes 30 and 60

Initial concentration in the mixture % w/v	Concentration at minute 30 % w/v	Amount adsorbed at minute 30 % w/v	Concentration at minute 60 % w/v	Amount adsorbed at minute 60 % w/v
12.5	10.50	16.03	9.88	20.99
20	16.50	28.02	16.22	30.26
25	21.04	31.71	20.91	32.73
30	25.91	32.75	25.63	34.96
35	31.06	31.52	30.53	35.77
20G+30F	26.06	31.53	26.85	25.18
30G+20F	16.55	27.57	16.27	29.85
25G+35F	31.10	31.21	31.26	29.96
35G+25F	21.06	31.54	21.04	31.70

Table D.4 Adsorptions of Fructose on H-Y zeolite at minutes 30 and 60

Initial concentration in the mixture % w/v	Concentration at minute 30 % w/v	Amount adsorbed at minute 30 % w/v	Concentration at minute 60 % w/v	Amount adsorbed at minute 60 % w/v
12,5	10.50	16.03	10.81	13.49
20	16.51	27.93	16.12	31.07
25	21.20	30.39	20.68	34.55
30	26.23	30.19	25.91	32.74
35	32.09	23.28	31.56	27.51
20G+30F	26.28	29.76	26.02	31.82
30G+20F	16.85	25.18	16.20	30.38
25G+35F	32.12	23.03	31.67	26.68
35G+25F	21.30	29.63	20.72	34.21

APPENDIX E

REPRODUCIBILITY GRAPH

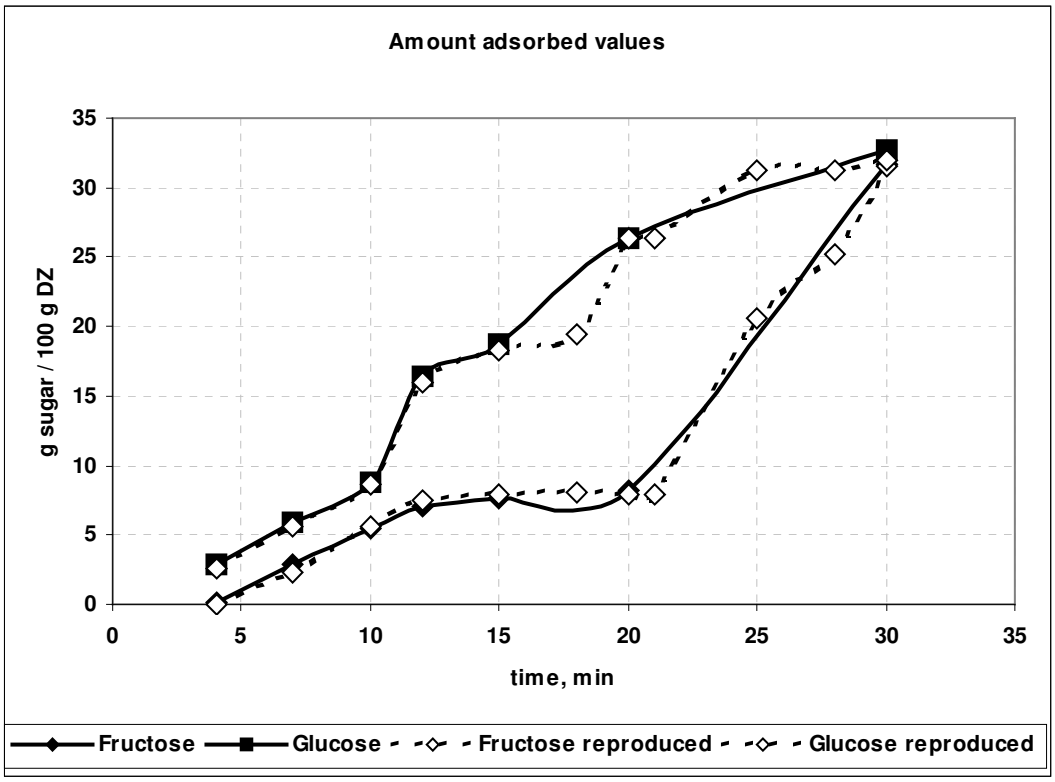

Figure E.1. Reproducibility experiment of adsorption kinetics of 25 % w/v G+F on Ca-Y zeolite

APPENDIX F

SIGNIFICANCE OF THE CURVE FITTINGS

Table F.1 Curve fitting of the separation data, graphed on Figure 3.32 and Figure 3.33; the adsorption behaviors of mixtures on H-Y and Ca-Y zeolites.

			F tabulated			
type of solution	**equation of adsorption difference**	**F computed**	**0.1 % CI**	**0.5 % CI**	**0.01 % CI**	**R2**
Ca-Y zeolite						
12.5 % F+12.5% G	$y = -0.0837x^2 + 3.4035x - 26.171$ max (20.33,8.43)	0.00	5.54	10.13	34.12	0.9562
25 % F + 25 % G	$y = -0.1593x^2 + 6.4792x - 49.596$ max (20.34,16.29)	0.00	5.54	10.13	34.12	0.8748
35 % F + 35 % G	$y = 0.0011x^2 - 0.1044x + 1.238$ No maximum	1.70	4.54	7.71	21.20	0.3977
20 % F + 20 % G	$y = -0.0636x^2 + 2.1518x - 8.0607$ max (16.92,10.14)	0.00	4.06	6.61	16.26	0.8189
30 % F + 30 % G	$y = -0.0354x^2 + 1.1411x - 2.3578$ max (16.12,6.84)	0.14	4.54	7.71	21.20	0.6355
25 % F + 35 % G	$y = 0.0025x^2 - 0.1142x + 0.1109$ max (22.84, -1.19)	1.45	5.54	10.13	34.12	0.547
35 % F + 25 % G	$y = -0.0524x^2 + 1.7315x - 2.5918$ max (16.52, 11.71)	0.17	5.54	10.13	34.12	0.5792
20 % F + 30 % G	$y = -0.0335x^2 + 1.2901x - 4.5777$ max (13.36, 7.82)	0.31	8.53	18.51	98.50	0.6741
30 % F + 20 % G	$y = -0.0377x^2 + 1.0253x - 1.0693$ max (13.60, 5.90)	0.33	5.54	10.13	34.12	0.8138
H-Y zeolite						
12.5 % F+12.5% G	$y = -0.0325x^2 + 1.2238x - 7.1641$ max (18.83,4.36)	0.77	4.06	6.61	16.26	0.8967
25 % F + 25 % G	$y = -0.0474x^2 + 1.8308x - 10.807$ max (19.31, 6.87)	1.35	4.06	6.61	16.26	0.9681
35 % F + 35 % G	$y = -0.0402x^2 + 1.4979x - 8.4603$ max (18.63, 5.49)	0.19	8.53	18.51	98.50	0.9984
20 % F + 20 % G	$y = -0.0509x^2 + 1.8489x - 9.2076$ max (18.16, 7.58)	0.33	4.06	6.61	16.26	0.9433
30 % F + 30 % G	$y = -0.0709x^2 + 2.6977x - 16.523$ max (19.02, 9.14)	0.04	4.06	6.61	16.26	0.9241
25 % F + 35 % G	$y = -0.0606x^2 + 2.1119x - 15.278$ max (17.42, 3.12)	0.00	8.53	18.51	98.50	0.8888
35 % F + 25 % G	$y = -0.046x^2 + 1.8864x - 8.3664$ max (20.50, 10.97)	1.47	4.54	7.71	21.20	0.9972
20 % F + 30 % G	$y = -0.0828x^2 + 3.1262x - 14.462$ max (18.88, 15.05)	0.28	4.54	7.71	21.20	0.9514
30 % F + 20 % G	$y = -0.0233x^2 + 0.723x - 2.8097$ max (15.52, 2.80)	0.68	5.54	10.13	34.12	0.9441

APPENDIX G

RESULTS OF RESPONSE SURFACE METHODOLOGY WITH THE MODEL "$Y = A * X_1 + B * X_2 + C$"

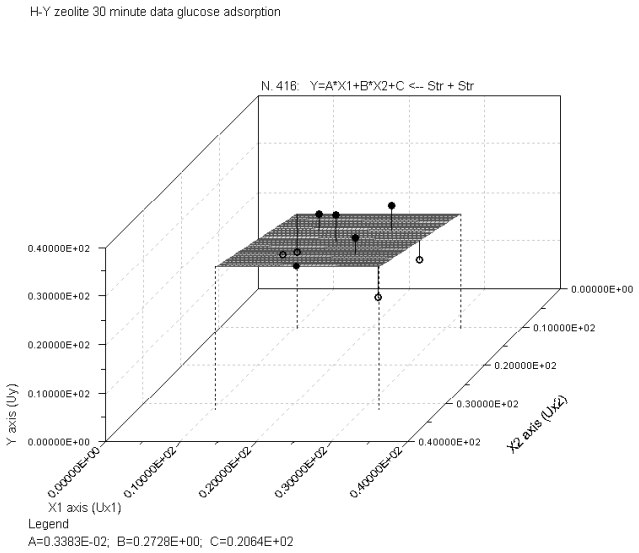

Figure G.1 RSM Analysis for glucose adsorption on H-Y zeolite at minute 30, R^2=0.149

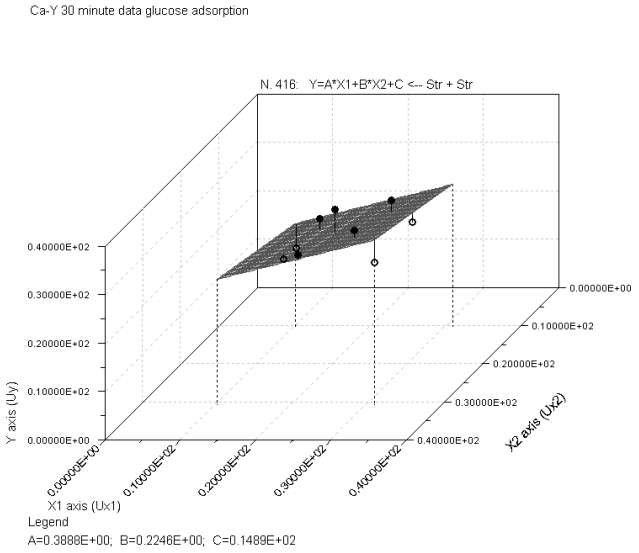

Figure G.2 RSM Analysis for glucose adsorption on Ca-Y zeolite at minute 30, R^2=0.579

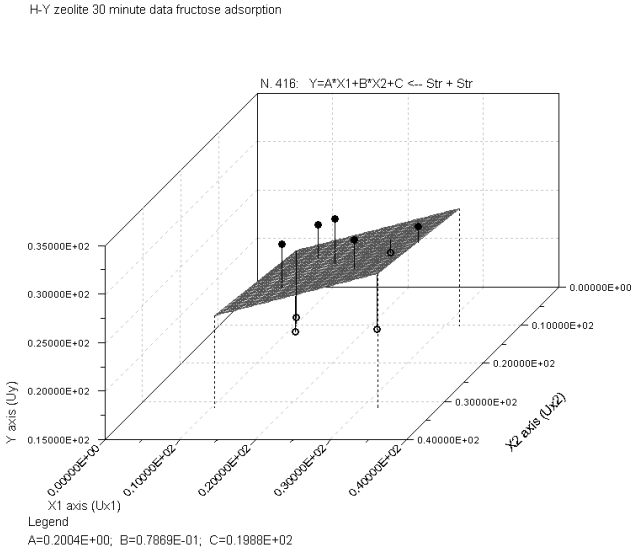

Figure G.3 RSM Analysis for fructose adsorption on H-Y zeolite at minute 30, R^2=0.225

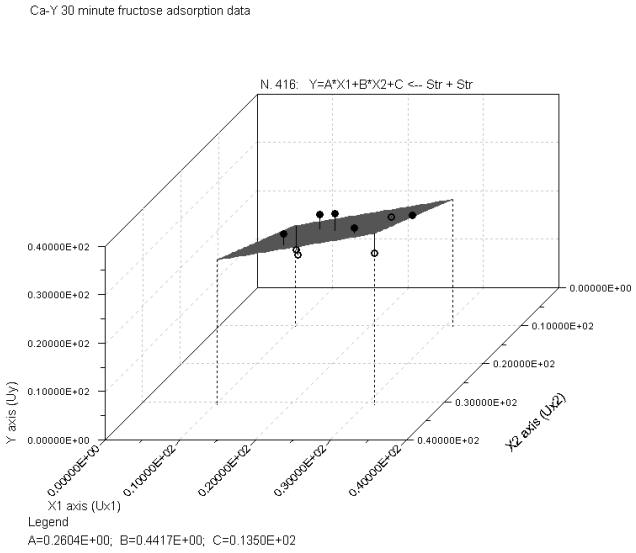

Figure G.4 RSM Analysis for fructose adsorption on Ca-Y zeolite at minute 30, R^2=0.215

APPENDIX H

RESULTS OF RESPONSE SURFACE METHODOLOGY WITH THE MODEL "$Y = A * X_1 * X_2 + B$"

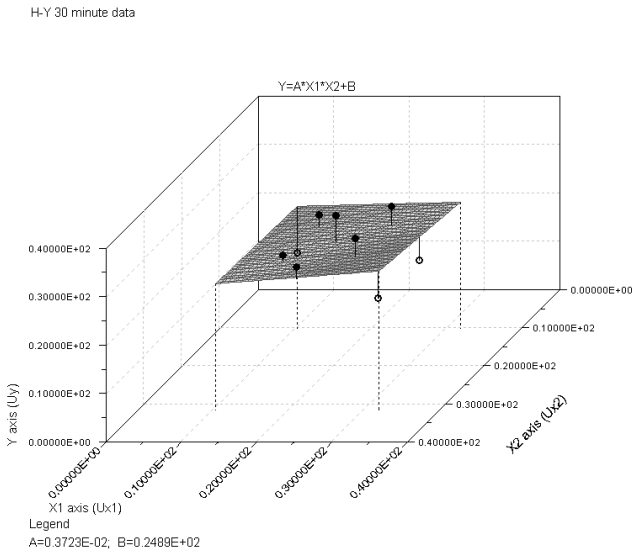

Figure H.1 RSM Analysis for glucose adsorption on H-Y zeolite at minute 30, R^2=0.038

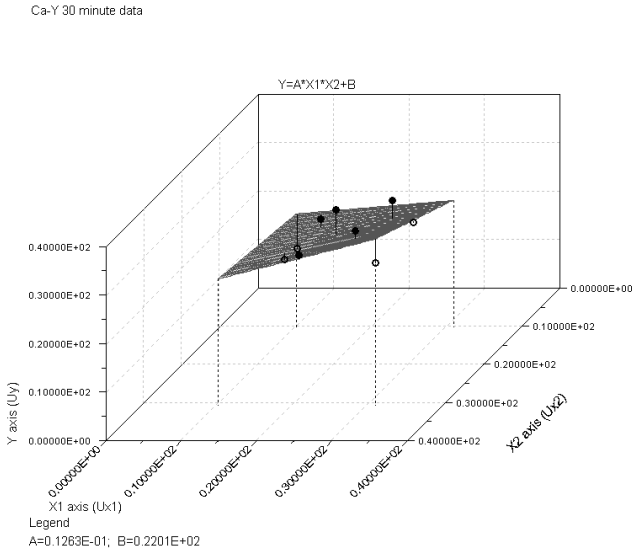

Figure H.2 RSM Analysis for glucose adsorption on Ca-Y zeolite at minute 30, R^2=0.414

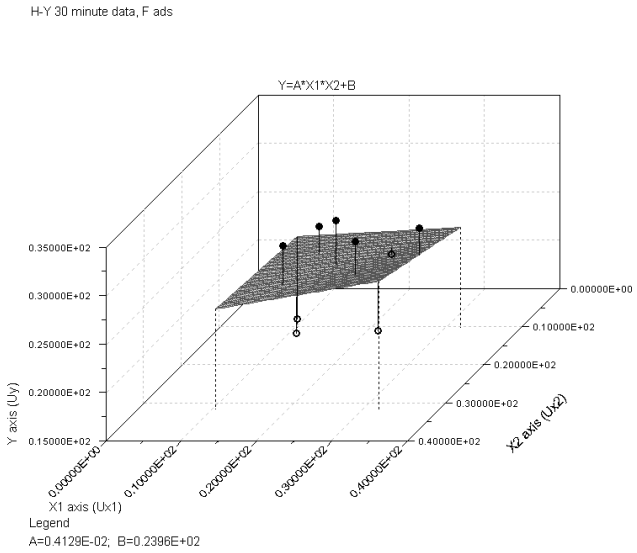

Figure H.3 RSM Analysis for fructose adsorption on H-Y zeolite at minute 30, R^2=0.054

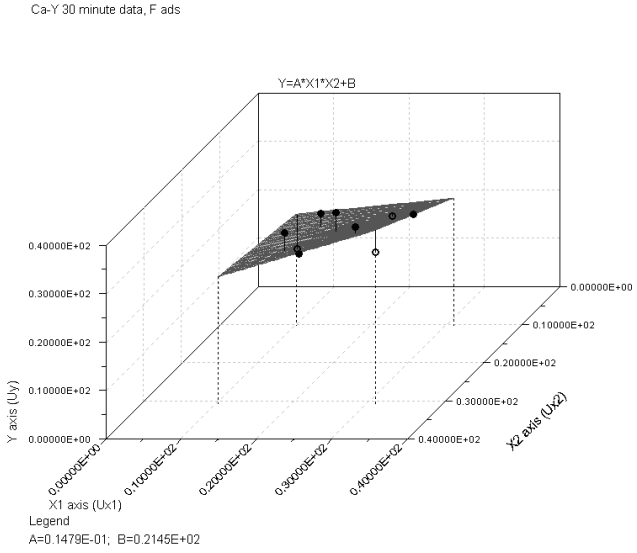

Figure H.4 RSM Analysis for fructose adsorption on H-Y zeolite at minute 30, R^2=0.521

APPENDIX I

RESULTS OF RESPONSE SURFACE METHODOLOGY WITH THE MODEL "$Y = A * (X_1 + X_2) + B * (X_1 * X_2) + C$"

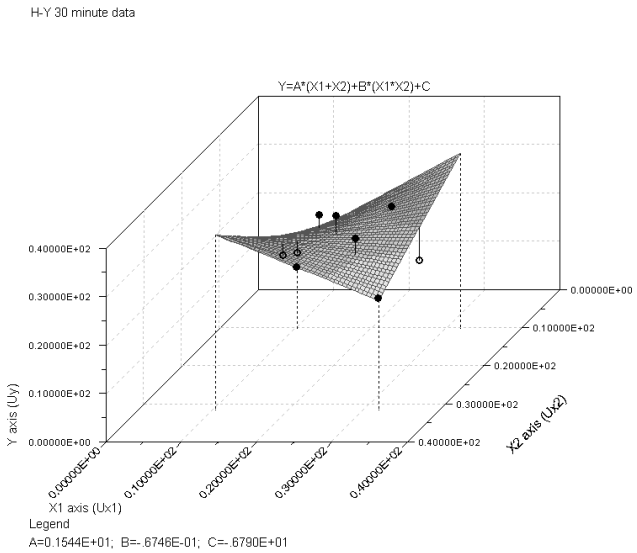

Figure I.1 RSM Analysis for glucose adsorption on H-Y zeolite at minute 30, R^2=0.594

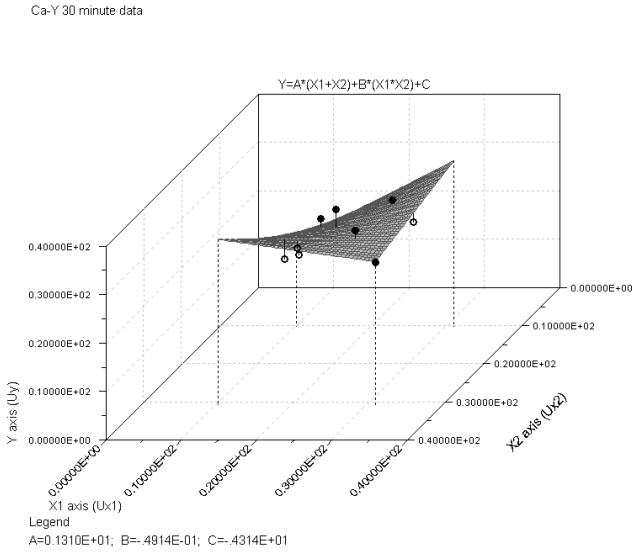

Figure I.2 RSM Analysis for glucose adsorption on Ca-Y zeolite at minute 30, R^2=0.801

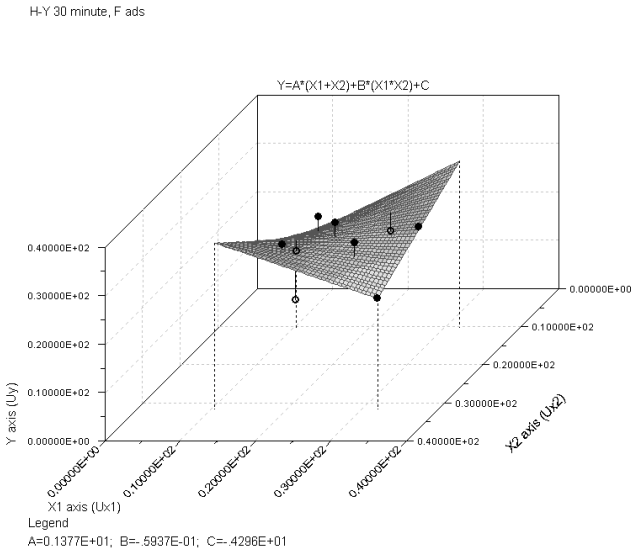

Figure I.3 RSM Analysis for fructose adsorption on H-Y zeolite at minute 30, R^2=0.576

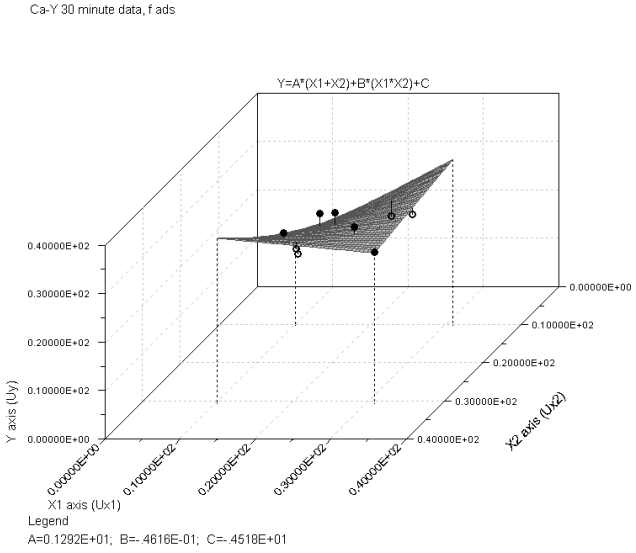

Figure I.4 RSM Analysis for fructose adsorption on Ca-Y zeolite at minute 30, R^2=0.867

APPENDIX J

RESULTS OF RESPONSE SURFACE METHODOLOGY WITH THE MODEL "$Y = A * X_1 + B* X_2 + C * X_1 * X_2 + D$"

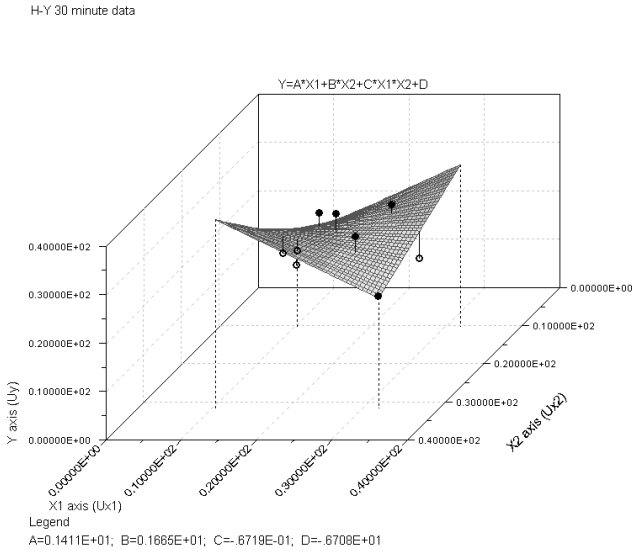

Figure J.1 RSM Analysis for glucose adsorption on H-Y zeolite at minute 30, R^2=0.625

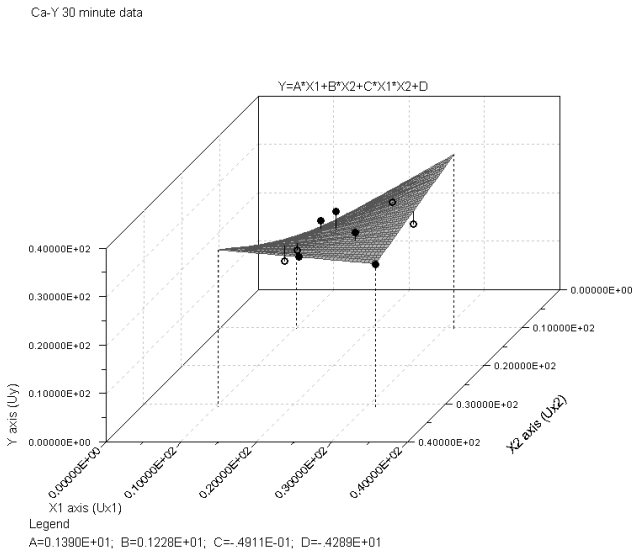

Figure J.2 RSM Analysis for glucose adsorption on Ca-Y zeolite at minute 30, R^2=0.815

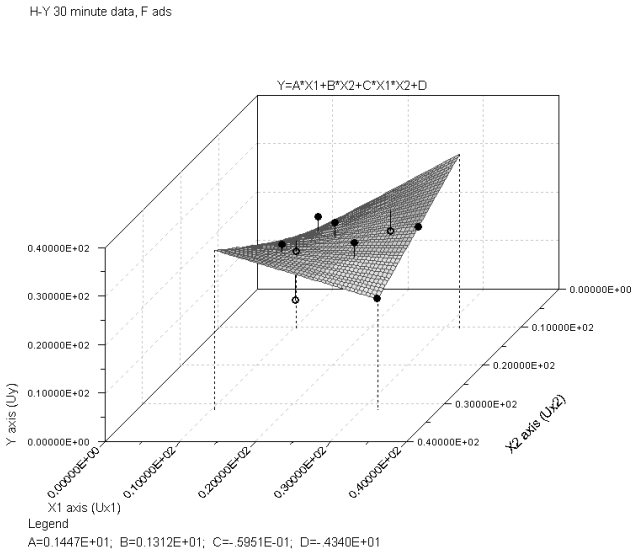

Figure J.3 RSM Analysis for fructose adsorption on H-Y zeolite at minute 30, R^2=0.587

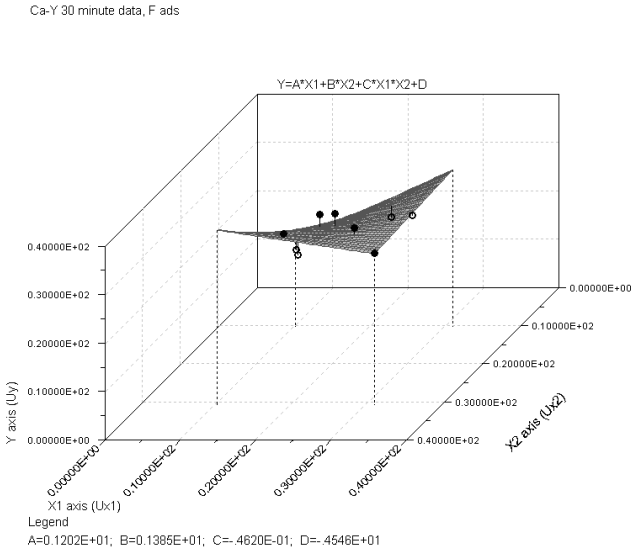

Figure J.4 RSM Analysis for fructose adsorption on Ca-Y zeolite at minute 30, R^2=0.882

APPENDIX K

RESULTS OF RESPONSE SURFACE METHODOLOGY WITH THE MODEL "$x=x_i-e^{At+B*Xtotal}$"

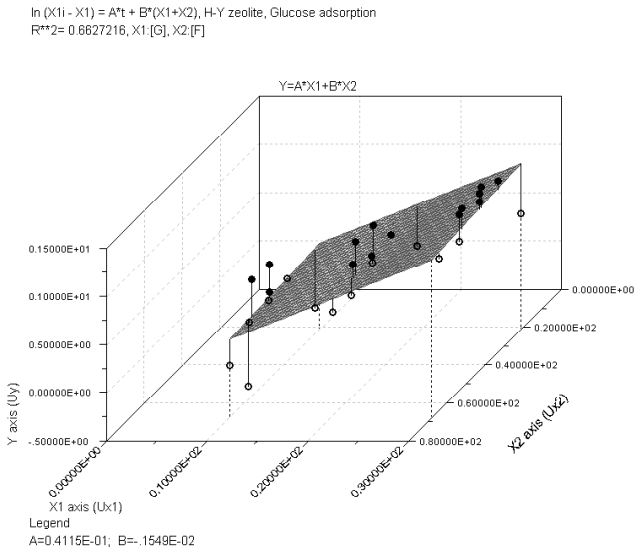

Figure K.1 RSM Analysis for glucose adsorption on H-Y zeolite, R^2=0.663

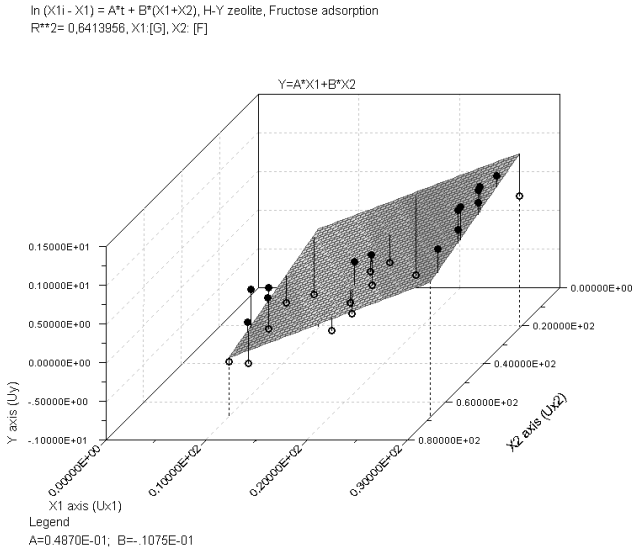

Figure K.2 RSM Analysis for fructose adsorption on H-Y zeolite, R^2=0.641

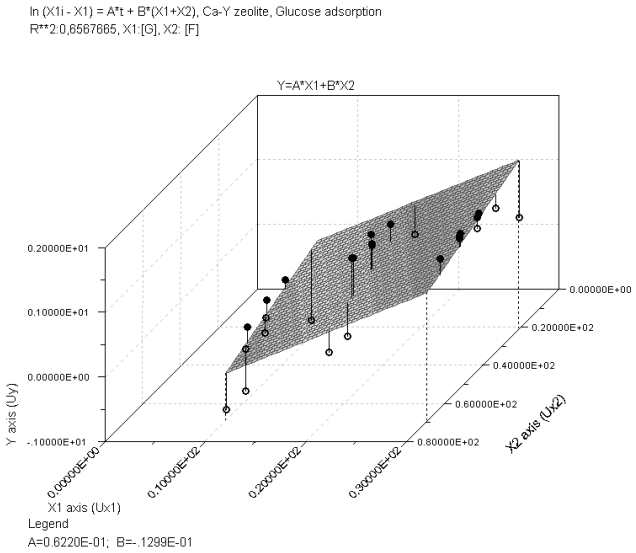

Figure K.3 RSM Analysis for glucose adsorption on Ca-Y zeolite, R^2=0.657

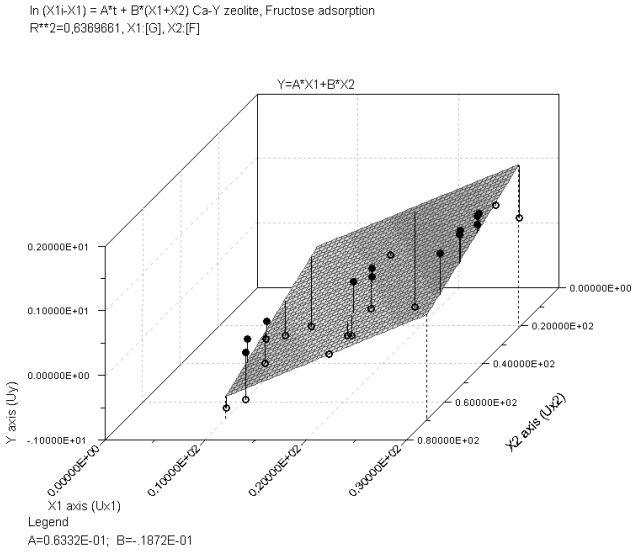

Figure K.4 RSM Analysis for fructose adsorption on Ca-Y zeolite, R^2=0.637